NOTICE

The quality of this microfiche is heavily dependent upon the quality of the original thesis submitted for microfilming. Every effort has been made to ensure the highest quality of reproduction possible.

If pages are missing, contact the university which granted the degree.

Some pages may have indistinct print especially if the original pages were typed with a poor typewriter ribbon or if the university sent us a poor photocopy.

Previously copyrighted materials (journal articles, published tests, etc.) are not filmed.

Reproduction in full or in part of this film is governed by the Canadian Copyright Act, R.S.C. 1970, c. C-30. Please read the authorization forms which accompany this thesis.

THIS DISSERTATION
HAS BEEN MICROFILMED
EXACTLY AS RECEIVED

AVIS

La qualité de cette microfiche dépend grandement de la qualité de la thèse soumise au microfilmage. Nous avons tout fait pour assurer une qualité supérieure de reproduction.

S'il manque des pages, veuillez communiquer avec l'université qui a conféré le grade.

La qualité d'impression de certaines pages peut laisser à désirer, surtout si les pages originales ont été dactylographiées à l'aide d'un ruban usé ou si l'université nous a fait parvenir une photocopie de mauvaise qualité.

Les documents qui font déjà l'objet d'un droit d'auteur (articles de revue, examens publiés, etc.) ne sont pas microfilmés.

La reproduction, même partielle, de ce microfilm est soumise à la Loi canadienne sur le droit d'auteur, SRC 1970, c. C-30. Veuillez prendre connaissance des formules d'autorisation qui accompagnent cette thèse.

LA THÈSE A ÉTÉ
MICROFILMÉE TELLE QUE
NOUS L'AVONS REÇUE

UNIVERSITÉ D'OTTAWA
UNIVERSITY OF OTTAWA

LABORATORY INVESTIGATIONS OF MERCURY KINETICS IN THE OTTAWA RIVER BED SEDIMENTS

by

Helal Ahmed Sayeed

Submitted in partial fulfilment of the requirements for the degree of Master of Applied Science

Department of Civil Engineering
School of Graduate Studies
University of Ottawa
Ottawa, Canada

June 1975

PREFACE

The Ottawa River project is an ongoing multidisciplinary research programme in which a group of engineers, geologists and scientists from the University of Ottawa and National Research Council Laboratories of Canada, are attempting to produce predictive ecological models for part of the Ottawa River system. The river is acting as a receiving body for pollutants from various industries and cities located at points along its shores.

A significant amount of mercury, which is one of the major pollutants, is retained in the bed sediments and, with time, this on-going process has resulted in a contamination problem in the system.

A 4.88 km-long stretch of the river, (1.6 km downstream from the city of Ottawa), was chosen as the study section along which a comprehensive programme of field studies are being performed. As a part of the Ottawa River project this laboratory study was carried out to investigate the relationships between bed sediment characteristics and the distribution and movement of mercury associated with bed load movements.

It has been established (21) that the bulk of mercury contamination in the river resides in the bed sediments. The river bottom consists largely of medium fine sands, in the central (main channel), compacted clay, on the Ontario shore, and agglomerated organic mixtures, largely wood fibres, wood chips, barks and fine sands near the Quebec shore.

Cation exchange capacities of the components of the bed

sediments have been determined to gain information about the proportion of mercury which may be carried adsorbed on stream sediments instead of in solution. Laboratory studies of mercury distribution among various components of the sediment mass lead to predictions of mercury concentrations which closely match observed field values. Sediment components of high organic content, more particularly the wood chips and fines (particles of diameter between 0.45 μm and 38 μm) have associated with them 50 to 100 times the amount of mercury associated with sand particles.

The results emphasize the importance of particle size and material type analysis in studies of pollutant transport by bed sediment movements.

A 9.15 m long laboratory model (flume) was used to study mercury transport by bed sediment movements. Two types of Ottawa River bed sediments, called sand and "woodchip"[1] sediments, were studied. Known amounts of bed sediments were contaminated by adding mercuric chloride labelled with radioactive mercury-203 and were buried in the test section of the study flume. Velocity of mercury transport associated with bed sediments was determined and found to be a function of type of bed sediments as well as mean water velocity.

Mass balance of mercury was also estimated and it was found that over 80 percent of mercury originally associated with bed sediments was transported attached to bed sediment particles being moved downstream. Desorption of mercury from bed sediments to the water phase was comparatively low although suspended-load contained a

[1] Bed sediment consisting of a mixture of wood chips, wood fibres, barks and fine sand obtained from the small CIP (Canadian International paper mill) channel of the study section of the Ottawa River.

significant portion of mercury when bed sediment transport was vigorous. The values of flow parameters (velocities, boundary shear stresses) at the incipient movement of the bed sediment particles were also determined for the two types of sediments mentioned above.

ACKNOWLEDGEMENTS

I wish to express my sincere gratitude and appreciation to my supervisor, Dr. D. R. Townsend, for providing the required laboratory facilities and guidance throughout the project. I am deeply grateful to Dr. Akira Kudo of the National Research Council of Canada for his advice, encouragement, supervision and helping me in conducting the experiments. Thanks are due to Mr. J. L. Earl and Mr. Robert Moore for modifying the laboratory model and building many components of it. I thank Mrs. Marylynne Reardon for her assistance in the experimental work. Facilities provided by the Biological Science Division, National Research Council of Canada are greatly appreciated. I thank Mrs. Wanda Storto for typing this thesis.

This project, funded by the National Research Council of Canada is gratefully acknowledged.

TABLE OF CONTENTS

LIST OF FIGURES

LIST OF TABLES

NOTATIONS

A = Universal Constant (Eq. C.4)

A_* = Universal constant

B = Roughness function

B_* = Universal constant

C_D = Drag coefficient

C_{D_t} = Drag coefficient at terminal fall velocity

C_L = Lift coefficient

$\frac{C}{C_o}$ = Relative concentration (Figures 30, 31, 32 and 33) where C = concentration of mercury at any time t, downstream and C_o = original concentration of mercury at the source

$C_s = \frac{\upsilon_s d}{2(\tau_o)_{cr}}$ = Characteristic sediment coefficient (due to Duboys)

d, d_{50} = Diameter of particle or median diameter of particles in a mixture

D = Depth of flow

Eh = Redox potential measured in volts or millivolts

f = Function of

F_D = Drag force

F_L = Lift force

F_R = Resistant force

g = Gravitational constant

$K(K_{sand}, K_{fines}, K_{wood\ chips})$ = Distribution coefficient (for sand, fines and woodchips)

k_1, k_2, k_3 = Coefficients

L = Lengths of the transects (Fig. 21)

meq = milliequivalent

$\frac{N}{cm^2}$ = Newtons per square centimeter

p = Probability of grain being eroded

pH = Fraction of hydrogen ion (H^+) defined by $pH = \log[1/(H^+)]$

ppm = Parts per million

q = Rate of liquid flow in volume per unit time and unit width

q_s = Bedload rate in weight per unit time and unit width

R_h = Hydraulic radius

R_h' = Hydraulic radius, due to particles

R_* = $\frac{U_* d}{\upsilon}$ = boundary Reynolds number

$(R_*)_{cr}$ = $\frac{(U_*)_{cr} d}{\upsilon}$ = boundary critical Reynolds number

S = Channel slope

S_s = Specific gravity of sand

t = Time

U = Average velocity (of water)

U_o = Local velocity (point velocity) near the bed

$\overline{U}_o$ = Average of the local velocities near the bed

U_{cr} = Mean velocity at incipient motion

U_d = Local velocity at a distance d, above the bed

U_m = Measured point velocity with the help of Preston tube in immediate vicinity of the bed

U_Y = Local velocity at distance Y above the bed

U_* = $\sqrt{\frac{\tau_o}{\rho}}$ = shear velocity

U_*' = Apparent shear velocity (Fig. 52)

$(U_*)_{cr}$ = Shear velocity at critical condition (incipient motion of the bed sediment particles)

υ = Velocity of fluid

υ_s = Velocity of sediment layers (sediment particles)

w = Width of the flume

W_s = Submerged weight of the particle

x = Spatial coordinate

Y = Vertical distance from the bed

γ = Specific weight of water

γ_s = Specific weight of sediment

ρ = Density of water

ρ_s = Density of sediment particles

ϕ = Intensity of bedload

ϕ_* = Intensity of bedload transport for individual grain size

ψ = Flow intensity (intensity of shear on particles)

ψ_* = Intensity of shear on individual grain size

η = Variability factor of lift; distance from reference level

η_o = The standard deviation of η, a universal constant = $\frac{1}{2}$

σ = Standard deviation of sediment particles (Figures 7 and 8)

θ = Angle of repose of the submerged sediment

ω = Terminal fall velocity

μ = Coefficient of viscosity

ν = Kinematic viscosity

$\tau_o = \gamma R_h S$ = Shear stress at boundary

τ_o' = Measured shear stress (Preston tube technique)

$(\tau_o)_{cr}$ = Shear stress at boundary at critical condition (incipient motion of the bed sediment particles)

$\tau_* = \frac{\tau_o}{(\rho_s - \rho)gd}$ = dimensionless shear stress

$(\tau_*)_{cr} = \frac{(\tau_o)_{cr}}{(\rho_s - \rho)gd}$ = dimensionless critical shear stress

CHAPTER 1

INTRODUCTION

1.1 Mercury Pollution in Aquatic System

In recent years, mercury pollution in the aquatic environment has become an issue of great concern in many parts of the world. An evaluation of the fate of mercury in natural watercourses, which are receiving bodies for effluent discharges containing mercury, is of prime importance in any attempt to control such pollutant concentrations below tolerable levels in these systems. Data obtained from such studies can provide an assessment of the probable time factor required for a system to clean itself, assuming polluted discharges to the river are greatly reduced or halted entirely, and can also make possible predictions of the response of the river system to other changes in sources of contamination.

Mercury, which has been naturally or artificially introduced into a dynamic aquatic system such as a river, is initially extracted from the liquid phase and detained by bed sediments (sorption). Some of the detained mercury, both inorganic and organic forms, may subsequently be released (desorption), and some may be stored for an indefinite period of time.

Bed sediments have been regarded as containing substantial amount of mercury in rivers (31), but detailed mass balance studies are rare. In assessing exchange rates across the sediment-water interface, the following seem to be the most applicable transport

mechanisms (34):

(a) sorption by and migration through bed sediments

(b) transport of sediments containing mercury

(c) desorption of mercury from sediments into the water column above the bed.

To study these processes knowledge of the physical, chemical, and mineralogical composition and of macro- and micro-biological conditions of the bed sediments is necessary. It is also important to investigate the influence of hydrodynamic characteristics of the water flowing over contaminated sediments, to determine what fraction of the mercury is being retained in the river system and the pathway and duration of retention.

At present much research on the mechanims governing the movement of pollutants, such as mercury, in rivers is being done - in particular the rate constants and the various environmental factors involved need elucidation (16,25,30,31,32). Although studies have been conducted in the fields of sorption (uptake) (36), migration, and desorption (release) of mercury (37), no comprehensive investigations to date have dealt with the subject of transport of mercury in a river by bed sediment movement. However, various related studies have been published in connection with sediment transport and radioactivity transport in streams (12,24,35,72).

1.2 Ottawa River Project

This study is a part of the "Ottawa River Project". This

project is an ongoing multidisciplinary research programme in which a group of engineers and scientists from the National Research Council Laboratories and the University of Ottawa are attempting to produce predictive ecological models of part of the Ottawa River system.

1.2.1 Description of the River System

The Ottawa River, whose overall length is approximately 1113 km, originates in the drainage area of Lake Temiskaming (in north-eastern Ontario) and eventually joins the St. Lawrence River (at Montreal Island). For about half of its length the river forms the boundary between the Ontario and Quebec provinces. From the headwaters to the City of Ottawa, the river's length is approximately 880 km. The system is extensively used for recreation, water supply, log-driving, and waste disposal from various industries (mainly pulp and paper) and municipalities. The river is seriously polluted downstream from the urban and industrial developments, especially in the Temiskaming, Ottawa-Hull, and Hawkesbury areas (70).

1.2.2 The 4.88 km (3-mile) Study Section of the Ottawa River

A 4.88 km reach of the river has been selected by the investigators for detailed study both to identify the exchange mechanisms and to determine the transport rates contributing to the distribution of mercury within the ecosystem. The study section, which averages 1.5 km in width, begins about 1.6 km downstream from the City of Ottawa and includes Kettle Island and Upper Duck Island (see Fig. 1). This particular reach was chosen specifically for the complicated form and varied environments represented therein. The flows shown in Fig. 1 are the average annual flows.

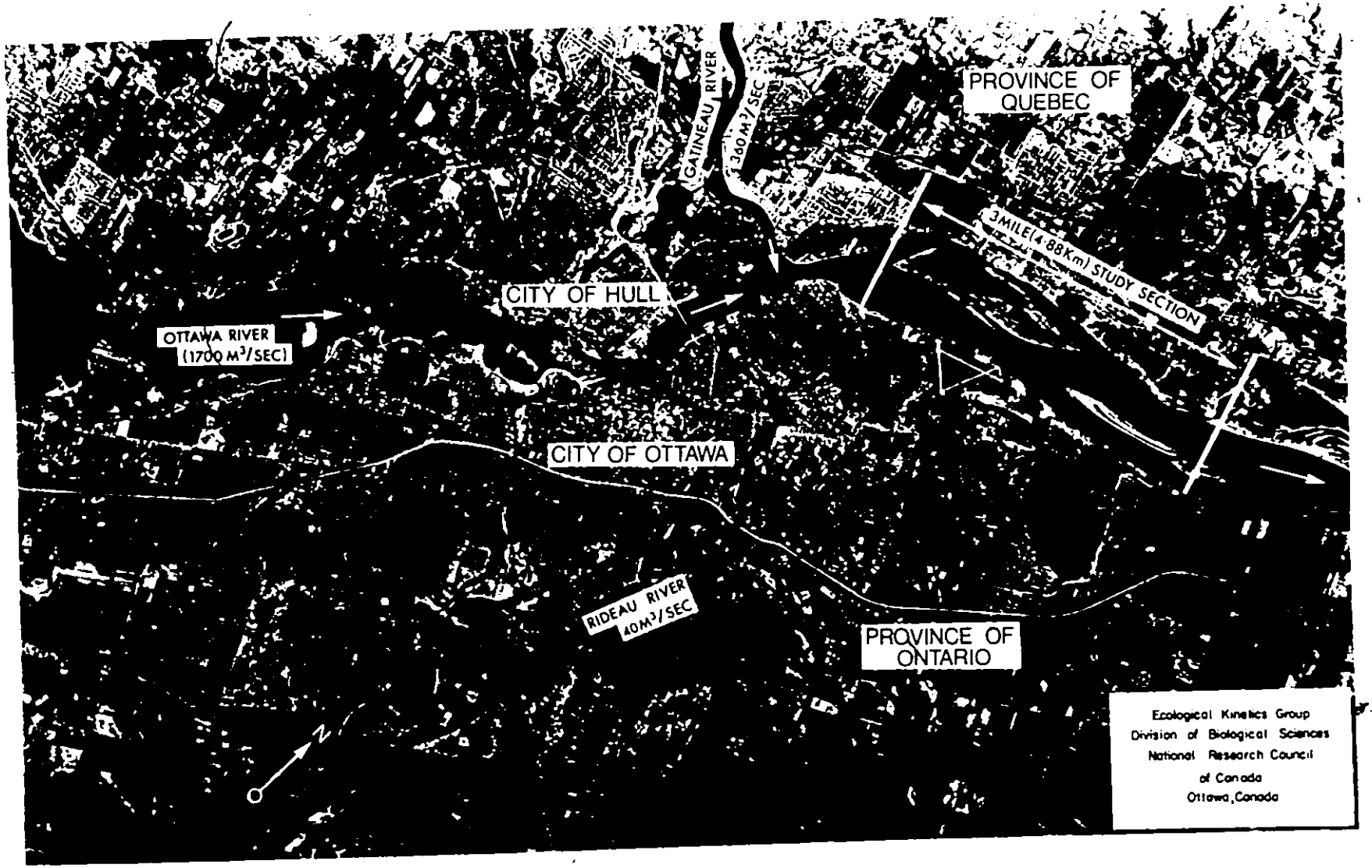

NATIONAL RESEARCH COUNCIL LABORATORIES/UNIVERSITY OF OTTAWA

Fig. 1. - 3 mile (4.88 km) study section of the Ottawa River

In recent years, the mean flow rate has varied from approximately 1,000 m^3/sec (winter low) to 4,000 m^3/sec (spring flood) and the maximum average velocity, corresponding to the latter condition, approaches 2.7 m/sec. Bulk transport of bed sediments is therefore expected to be significant during the brief spring flood period (44).

The river has been receiving waste in the form of wood fragments (fibres, chips, and bark) from adjacent pulp and paper industries for nearly 100 years. Extensive organic deposits are therefore found in the river in the vicinity of such industry and, through the normal transport processes, these materials have become an integral part of the total sediment complex. This feature is an important characteristic of the Ottawa River deposits.

Data obtained in the summer of 1972 (21) showed that the concentration of total mercury ranged from 25.0 ppb to 606.5 ppb (dry weight) in the bed sediments of the study section. The average concentration of mercury was found to be 195.0 ppb, assuming the concentration through 4 cm depth of bed sediment is uniform. In other words, the bed sediments contained 5.84 mg/m^2 of mercury in the study section. Hart (21) estimated that an amount of 31 kg of mercury was associated with the bed sediments which constitutes approximately 97% of the mercury distributed in the study section.

1.3 Study Objectives

This particular research project was primarily designed to investigate: (1) what types and fractions of bed sediments play important roles in mercury transport, and (2) how mercury is transported

due to bedload movement of sediments in a dynamic aquatic system using an experimental flume.

The project, which included a comprehensive programme of field surveys on the study section of the river, was divided into three separate sub-studies as follows:

1. Classification and spatial distribution of bed sediments in the 3-mile study section of the Ottawa River,

2. mercury sorption capacity and ion exchange capacity of various types and fractions of bed sediments; and

3. a study of the interaction between flowing water and bed sediments which included:

   a) Determination of the values of important flow parameters (velocity, boundary shear stress, etc.) at which incipient movement of sediment takes place.

   b) Transport of mercury associated with bed sediment.

The preliminary field surveys included collection of numerous samples of the bed sediments, at specific locations along the study section, using a "shipek" grab sampler attached to a raft.

In the laboratory representative samples, for each location, were analyzed for particle size distribution using the U.S. Standard Sieves (5). The mercury sorption and ion exchange capacities of the various fractions of bed sediments were determined using standard methods (to be described later). Prior to these analyses, samples were incubated, for approximately six months, with known concentrations

of mercury to reflect prototype conditions.

The third phase of the study initially included structural modifications to the 9.14 m experimental flume and, subsequent to this, a series of tests to check the hydraulic performance of same. The latter included calibration of the flow-metering device and preston tube (for measuring boundary shear stress), and several velocity distribution surveys, at the test section, in order to comment on the uniformity of the flow field there.

Finally, the interaction phenomena for mercury, with the solid and liquid phases, were observed using an "ORTEC" counter and a detector assembled above the test section.

CHAPTER 2

LITERATURE REVIEW

2.1 Mercury (Hg)

2.1.1 Sources of Mercury in the Environment

Mercury is probably the most widely distributed of the heavy metals existing in the environment. It is one of the most useful metals and it can also be one of the most toxic, depending on its form. The sources of mercury can be generally classified into two categories: (i) natural, and (ii) man-generated.

The amount of mercury present in the earth's crust is estimated to be approximately 0.08 ppm (56). A considerable amount of mercury in soils is present as elemental vapor, probably adsorbed on soil matter. Mercury ore is found in rocks of all classes, the common host rocks being limestone, calcareous shales, sandstone, serpentine chert, andesite basalt, and rhyolite. Mercury can be entirely recovered from sulfide ore (cinnabar, α-Hg's), which is 86.2 percent mercury.

In today's world, mercury is used in many forms and for many different purposes. As a result, in many instances, portions of mercury ultimately enter some phase of the environment, either accidentally or as part of an effluent from a manufacturing process. The mercury used in agriculture for seed treatment is intentionally added to the environment and may be one of the most hazardous sources.

Prior to the late 1960's, the pulp and paper industry utilized significant quantities of mercury compounds. The effluent from these industries resulted in an increase in the mercury level in the environment.

It can, therefore, be concluded that the sources of mercury to the environment are multifold both from natural and from man's activities.

2.1.2 Characteristics of Mercury

Mercury is present in nature, as in the laboratory, in three different oxidation states: the metallic state, the mercurous state and the mercuric state. Seven stable isotopes of mercury are known in nature with conventional abundance: ^{196}Hg (0.146%), ^{198}Hg (10.02%), ^{199}Hg (16.84%), ^{200}Hg (23.13%), ^{201}Hg (13.22%), ^{202}Hg (29.8%), ^{204}Hg (6.85%). Two radioisotopes of mercury have found use as tracers in environmental and biomedical studies. ^{197}Hg, half-life 65 hours, and ^{203}Hg, half-life 48 days, are both strong gamma emitters and are easily analyzed using scintillation counters.

Since mercury is present in various forms and in various types of strata, there will be release of the mercury through processes such as weathering, vaporization, dissolution and biological activities. Metallic mercury is relatively soluble under practically all Eh and pH values found in nature, while the ions have differing solubilities, depending upon the anionic species present and the Eh-pH regime. Canadian researchers observed that mercury in most sur-

facial waters can migrate as sulfate, nitrate, various chloride complexes, carbonate complexes, hydroxide complexes, ammonia complexes and other organometallic complexes resulting from the decay of plant and animal matter and the maturation of humus (27).

For more complete details about mercury, reference should be made to D'itri ed. (14), Krenkal et al (32) and Grdenic and Tunell (20).

2.1.3 Mercury in Bed Sediments

A significant amount of mercury, being absorbed by aquatic life, is contributed by bottom sediments of rivers and lakes. This is due to the fact that bed sediments of natural watercourses provide a large surface area for sorption and desorption of the contaminant across the sediment-water interface. This is also the case for the suspended sediments in rivers. It is therefore important to establish the back ground level of mercury and to locate those areas where mercury concentrations exceed this backgroud. It is also important to investigate the phenomena which control the transport and release of mercury from bed sediments.

Mercury pollution in the aquatic environment alarmed the public after hazardous mercury contamination was found in Japan, in Scandinavia, and in North America (14,39,45). A number of investigations of the concentration level of mercury in the various components of aquatic systems, and the transport mechanism of mercury among these components, was initiated. The factors governing the transport modes

of pollutants in stream systems are complex, however, the most important sink of pollutants is the sediment, qualitatively, and sometimes quantitatively (31, 32). This section discusses mercury contamination of bed sediments found in many parts of the world.

Matida and Kumada (40) found that the sediment of Minamata Bay contained up to 630 ± 10 ppm of mercury (dry weight) and the Agano River sediments up to 150 ppm, both in Japan. Axelsson and Hakanson (2) investigated Lake Ekoln sediments in Sweden, and found a minimum concentration of total mercury of 2.4 ppm at the mouth of the Fyris River.

Armstrong and Hamilton (1) commented that the "Wabigoon River-Clay Lake-English River-Winnipeg River" system in Western Ontario and Eastern Manitoba is one of the waterways in Canada most heavily contaminated with mercury. The source of this mercury is believed to be a chlorine-alkali plant at Dryden. They found that the total quantity of mercury in sediments in Clay Lake was somewhat more than 2,000 kg.

Thomas (65) investigated mercury concentration of bottom sediments in Lake Ontario and found an average concentration of 0.651 ppm for the entire lake. The highest mercury concentration was found to be 2.10 ppm.

A recent survey by the Tennessee Valley Authority (TVA) on Pickwick Lake, which was closed to fishing because of mercury contamination, indicated an average value of 5.3 ppm total mercury (on

dry weight basis), with a maximum value of 12 ppm and a minimum value of 1.2 ppm, all in the upper one inch (2.54 cm) of the sediment layer (31).

Zeller and Finger (75) investigated mercury concentrations in sediments in the vicinity of chlor-alkali plants in the southeastern United States and found a range from 0.04 ppm to 740 ppm total mercury on a wet-weight basis. Savannah River sediment showed a mercury concentration of 0.04 ppm above a chlor-alkali outfall and 1.2 ppm three-quarters of a mile below the outfall (wet weight basis). Brunswick Bay samples showed 0.57 ppm of mercury above a chlor-alkali outfall, 4.00 ppm at the outfall and 0.14 ppm below the outfall (wet weight basis). On the Mobile-Tombigbee River System, mercury concentration in the sediments above two chlor-alkali plants yielded values of 0.04 ppm (wet weight basis). 0.28 ppm was found several miles below one outfall and 0.3 ppm was detected 9 miles below the second outfall. However, later sampling after significant decrease in mercury discharged by the plants demonstrated generally reduced levels.

Turney (66) analyzed 24 sediment samples from the Michigan waters of the St. Clair and the mouth of the St. Clair River and found a mercury concentration of less than 0.5 ppm (dry weight basis). He investigated the sediment samples from the western shore of Lake Erie and found values less than 0.5 ppm and a variation of 1 to 2.1 ppm below the mouth of the Detroit River. Investigations in Washington State showed high concentration in the vicinity of mercury discharges (as high as 9348 ppm on a dry weight basis) to a low of 0.22 ppm (dry

weight basis), where no discharges occurred (38). California sediment investigations demonstrated values ranging from 0.04 ppm to 3.3 ppm on a dry weight basis (41).

Wood et al. (69), and Jensen and Jernelov (26) demonstrated that microorganisms living in the sediments can ingest the inorganic mercury and transform it into dimethyl or methylmercury. However, this transformation process is not well-understood, the rate constants are unknown and the various environmental factors involved need elucidation.

Cranston and Buckley (11) reported that the bottom sediments in the LaHave River (Nova Scotia, Canada)were affected by sedimentation of particulate matter containing high levels of mercury. They found the mercury concentration in the bottom sediments ranged from 0.09 to 1.07 ppm.

Oliver (51) reported heavy metal concentrations, including mercury, in the sediments of the Ottawa and Rideau Rivers near Ottawa, Canada. He found relatively low average values of 0.28 ppm and 0.20 ppm of mercury respectively (analyzing 48 and 68 samples collected from different locations along the Ottawa and Rideau Rivers, respectively). Relatively high mercury concentrations in sediments (1.99 ppm) were found in the vicinity downstream from effluents of paper mills on the Ottawa River. However, near the effluent of the sewage plant of Ottawa, mercury concentration was as high as 2.32 ppm.

As part of the "Ottawa River Project", Norstrom et al. (49) analyzed mercury concentration in 32 samples of the Ottawa River

sediment. They reported concentrations in these samples ranging from 0.025 ppm to 1.00 ppm. The value of 0.025 ppm of mercury is considered as a minimum background level for this region (27).

DeGroot (13) found mercury concentrations in the sediments of the Rhine River ranged from 4 to 14 ppm with an average of 8 ppm (not stated whether on a wet or dry weight basis). He placed emphasis on the importance of particle size and observed that the "heavy metals" concentration in the sediment fraction with particles less than 16 microns in diameter was important, inasmuch as some insight may be gained into mercury transport mechanisms by sediments.

2.1.4 Sorption and Desorption of Mercury by Bed Sediments

Sorption:

Sorption (uptake) may be described as the process of taking up and holding either by adsorption or absorption (57). In solutions, adsorption refers to the uptake and concentration of a solute at the surface of a sorbent, whereas absorption implies a generally uniform penetration of the solute into the sorbent. In the case of stream sediments, sorption phenomena generally belong in the adsorption category. However, in practice it is often impossible to separate the effects of adsorption from those of absorption. Consequently the more general term "sorption" will be used in the remainder of this section.

Sorption may occur wherever there is a surface or an interface. Sorption may occur at any surface; the most important and complex surfaces, however, are the interfaces between solutions and solids. The substances sorbed at an interface may be products of reaction or hydrolysis, unaltered molecules, or particular ions.

Sorption of solutes on the surface of sand and silt particles in streams is primarily physical, which is nonspecific in character and occurs on chemically inactive surfaces. Although physical sorption also occurs with colloidal clay particles, it is secondary to other types of sorption. Owing to the reversibility and rapid attainment of equilibrium which are typical of physical sorption, the concentration of solutes on the surface of sand and silt particles would tend to be quite sensitive to the concentration of solutes in the water. The sensitivity would be less when diffusion of the solute into the solid is a significant factor.

Sorption rate of pollutants by bed sediments can be expressed in two ways: (i) amounts of pollutants taken up per unit surface area of bed sediments (surface uptake rate), $\mu g/Cm^2$ per day, and (ii) amounts of pollutants taken per unit weight of bed sediments (mass uptake rate) $\mu g/g$ per day. The first expression is generally used since uptake by bed sediments is primarily a surface phenomenon. The latter is used mainly for suspended sediment uptake rate. Furthermore, the rate of transfer of mercury from solution to bed sediments is independent of the concentration of mercury in overlying water for a certain range provided it is expressed in correct units (36). Therefore, in this range the value derived from surface uptake rate divided by amount of mercury per unit volume of water (assuming density of water = 1.00), which is $\mu g/Cm^2$ per day $\div$ $\mu g/Cm^3$ = cm/day, has been found to be a useful parameter to express uptake rate by bed sediments.

Kudo and Hart (36) reported experimental results of mercury uptake rate by Ottawa River bed sediments in a laboratory model.

The uptake rates ranged from 1 cm/day to 10 cm/day depending on the environmental conditions. These values of mercury uptake rates were similar to those for various heavy metals such as Chromium (Cr), Cobalt (Co), Zinc (Zn), Strontium (Sr), and Cesium (Cs) taken up by Lake Austin sediments (74). Kudo and Hart also concluded that movements of water increased the uptake rates 70% to 100% compared with those in a stagnant system.

Desorption:

Any mercury accumulated in the sediments will be reintroduced into the suprajacent water column through the natural sediment-mercury-water equilibria (61). This process is referred to as desorption. Higher mercury-level sediments induce greater mercury contamination in the overlying waters.

Jensen and Jernelov (26) studied the desorption of methyl-mercury from sediments into water and found the desportion rates ranged from 0.0728 ng/cm^2 per day to 0.109 ng/cm^2 per day during a 1-week experiment.

Bongers and Khattak (4) investigated mercury desorption rates using fish. Tests indicated a desorption rate of mercury of 0.1 ng/cm^2 per day.

Kudo et al. (37) reported desorption rates (of total mercury) from the bed sediments of the Ottawa River. Their values ranged from 0.1 ng/cm^2 per day to 1.0 ng/cm^2 per day depending on the environmental conditions.

2.2 Sediment Transport

2.2.1 General

In a polluted river system, contaminants such as herbicides, pesticides, radioisotopes and mercury can attach to sediment particles and be transported with the suspended and bedloads. With regard to the latter mechanism, it may be possible to estimate the transport rate of such pollutants if the bed sediment transport rates are accurately known.

Many bedload equations, both theoretical and empirical, have appeared in the literature since the end of the last century (since Duboys, 1879) (19,46,53,71). The selection of one or more of these for use in a particular stream is a difficult task since the results of different formulas often differ drastically and it is not possible to determine positively which one gives the most realistic result. These bedload equations are based almost entirely on laboratory data. Since very little is known about how transport relations change, if at all, as the size of the stream changes, there is no basis for judging how well formulas based on data from small laboratory streams apply to large systems such as rivers. Further uncertainties are encountered because natural streams differ from laboratory flows in that their channels are irregular in cross section and alignment. The ideal method of evaluating formulas is to compare actually measured sediment discharges of a river with the values given by formulas.

There are two methods whereby the transport of sediment particles in a stream can be described (24). In one method observation

is made on a particular cross section of the channel and the concentration, discharge and characteristics of the sediment, as it passes the cross section, are described. This can be called an Eulerian description. In the other method attention is focused on a particular particle or group of particles, and the motion of the particles over a period of time is described. This is called a Lagrangian description. Although Eulerian experimental techniques provide a more direct method of determining quantities such as sediment discharge, Lagrangian techniques can yield information that is perhaps more instructive with regard to fundamental transport processes. For instance, Lagrangian experimental techniques permit direct evaluation of the rates of movement and dispersion of any type or combination of types of sediment particles.

Most of the theories and experimental techniques associated with current and past sediment transport research are based on the Eulerian system. However, investigations by Einstein (15), Crickmore and Lean (12), Hubbel and Sayre (24), Yang and Sayre (72), Shen and Cheong (59), are among the exceptions. The reason for not using the Lagrangian system more often is due largely to the experimental difficulties which have been associated with tracing the motion of a given particle or group of particles. With the recent development of radioactive (and other) tracer techniques, however, experimental techniques of a Lagrangian nature (i.e., groups of particles) have become feasiable for the study of sediment transport, both in natural streams and to a greatly increased extent in the laboratory.

Crickmore and Lean (12) attempted to develop a method of measuring the sand transport in streams by means of radioactive tracers. They conducted experiments in the laboratory using a 106.67 m long, 1.52 m wide flume under rippled bed conditions. They maintained a constant flow of 0.28 m^3/sec in the flume. The results of their experiments inferred that the transport rate can be deduced from the mass distribution of tracer particles initially laid to a depth sufficient to cover all levels of movement of the bed ripples, or by measuring the velocity of the centroid of the activity distribution together with an independent measurement of the ripple movements at a point.

Hubbell and Sayre (24) conducted one field experiment on the North Loup River in Nebraska and two subsequent laboratory experiments to study the transport and longitudinal dispersion of bed sediment materials using radioactive tracer techniques. They concluded that the discharge of bed material particles can be computed from the dispersion data collected by the radioactive tracer technique in conjunction with a continuity equation. The results of their experiments demonstrated the feasible application of Lagrangian experimental techniques to the observation of sediment transport processes both in the field and in the laboratory by using the radioactive tracer technique.

Yang and Sayre (72) extended a sediment transport study using the Lagrangian approach in a 18.29 m long laboratory flume. They performed a series of experiments with a range of sediment particle size

from fine to coarse sand using radioactive gold (^{198}Au) as tracers. They evaluated the velocities of bed sediments and found values ranged from 0.26 m/hr to 1.43 m/hr and the ratios of water and bed sediment velocity ranged from 1210:1 to 679:1 depending on the hydraulic conditions and type of sediment.

Shen and Cheong (59) investigated the downstream effects of an instantaneous injection of contaminated sediment particles at a given locality in a straight alluvial stream under steady uniform flow conditions. They concluded that with an instantaneous introduction of contaminants, the time-concentration distributions are highly skewed near the source and become progressively more symmetrical far downstream where they can be approximately represented by a Gaussian curve. They found that for a given degree of pollution, the critical duration increases downstream and the increase is in direct proportion to the square root of the distance from the source where the normality approximation is satisfactory.

The results of these and other similar investigations demonstrate the feasible application of radioactive tracer techniques to the observation of sediment transport processes, both in the field and in the laboratory. However, in all of these recent studies, no mass balance information of contaminants (radioactive tracers) was available and no indication of possible desorption of contaminants from the bed sediment to water above it during movement was given.

Kudo and Gloyna (34) introduced a radioactive cesium chloride solution (labelled with ^{137}Cs) in a 66 m-long model river

using Lake Austin sediments. They reported that, under normal operating conditions, approximately 45% of the contaminant was carried by the total sediment load compared to 31% by water. However, information relating to the transport capability of different fractions of sediments was not available.

The present study relates specifically to the transport of pollutants by the various sediment fractions, and in particular how the distribution of pollutant in the system may be predicted by appropriate laboratory studies.

2.2.2 Modes of Sediment Transportation

In this section the different ways, in which sediment is transported in dynamic aquatic systems such as rivers and streams, will be discussed.

Sediment particles in streams are transported mainly in two ways depending on the hydraulic conditions and the characteristics of the sediment: 1) The particles may be transported either by rolling or sliding with occasional bouncing along the bed (saltation). This kind of sediment transport is commonly referred to as the transport of the bedload or the contact load. The particle during its movement generally follows a sequence of alternating steps and rest periods of random length and duration. 2) In the turbulently moving water, sediments may also be transported in suspension. This is referred to as the suspended load. In addition, there will usually be a dissolved load, consisting of salts and other chemicals in solution; and a wash load, consisting of very fine particles carried along the channel with

no relation to the bed material. Although bedload and suspended load are usually considered separately, there is no sharp line of demarcation between them (46). Any given particle may be alternately carried in the bedload and in the suspended load. The bedload moves on or near the bed at the sediment water interface and the suspended load is carried in the fluid away from the bed and is supported by the surrounding fluid during its entire motion.

2.2.3 Definitions

Shen (58) defined the terms that are frequently used in sediment transport studies as follows:

Bedload: rate of particles moving near the bed in the bed layer.

Bed layer: a flow layer, 2 grains in diameter, immediately above the bed. The thickness of the bed layers varies with particle size.

Bed material: the sediment mixture which composes the moving bed.

Bed material load: the part of the sediment load which consists of the grain sizes represented in the bed and equals the sediment transport capability of the flow.

Bedload equation: the general relationship between bed load rate, flow condition, and composition of the bed material.

Suspended load: rate of particles moving outside the bed layer continuously supported by fluid.

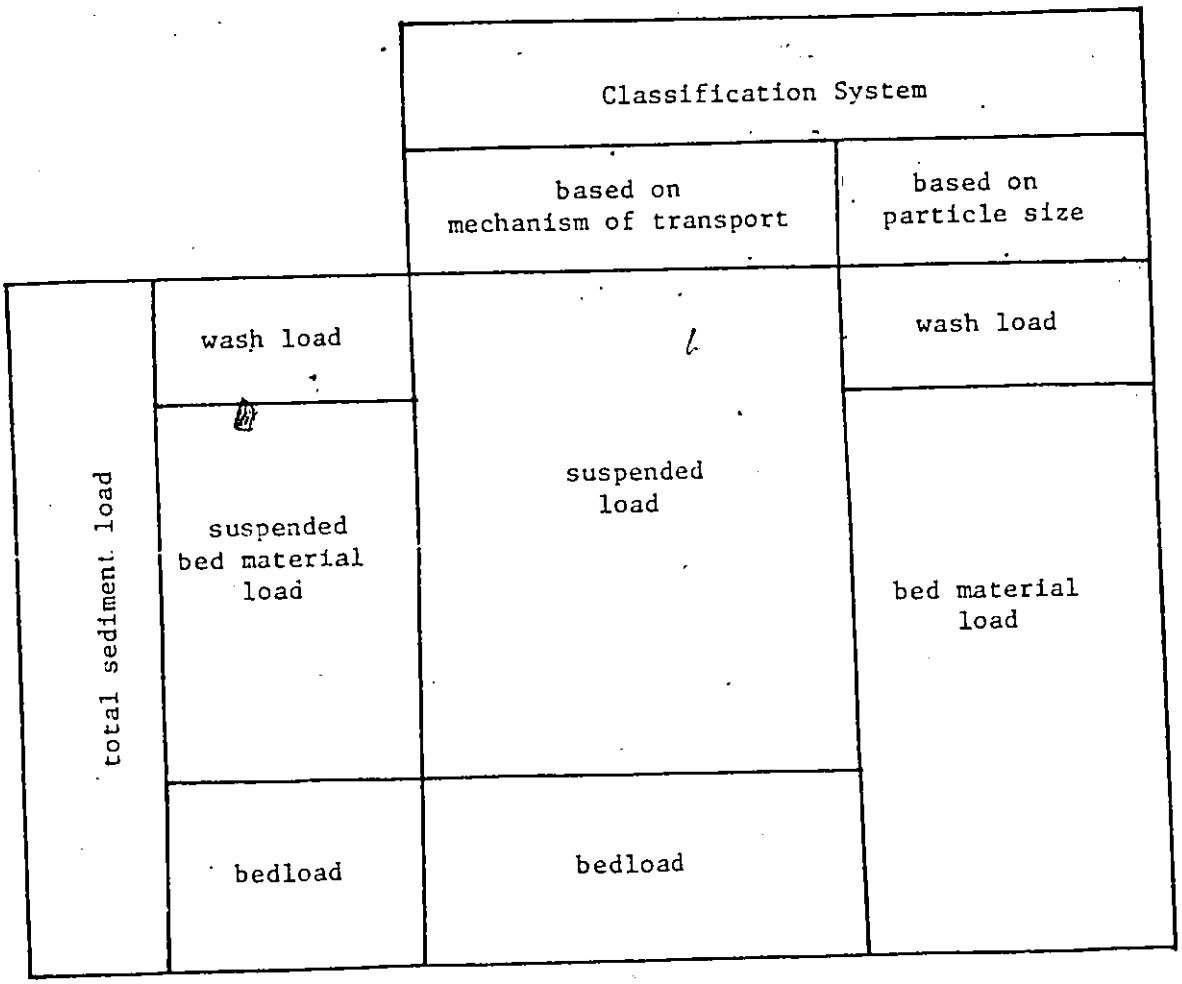

Fig. 2.5 Sediment Load Classification (from Cooper et al (10))

Wash load: that part of the sediment which consists of grain sizes finer than those of the bed and is determined by the available upslope supply rate.

Total sediment load: bedload plus suspended load or bed material load plus wash load. Cooper et al. (10) defined the total sediment load as consisting of wash load, suspended bed material load and bedload. Further, on the basis of mechanism of transport, total load consists of suspended bed material load and bedload, and on the basis of particle size, total load consists of wash load and bed material load. In the first case, suspended load = wash load + suspended bed material load, in the latter case, bed material load = suspended bed material load + bedload. This is consistent with the definition by Shen and is illustrated in Fig. 2.

2.2.4 Bedload Equations

The bedload equations which have been developed so far are so numerous that it is difficult to consider all of them here. However, some of the bedload equations (Duboys, 1879, Shields, 1936; Meyer Peter-Muller, 1948; Einstein, 1950; Colby, 1964) are presented in this section to illustrate the type of equations which have been developed by various researchers. These equations were developed for discharge of bed sediments under conditions of uniform steady flow. No detailed derivations have been attempted. For detailed derivations and for other formulas reference may be made to Raudkivi (53), Graf (19), Yalin (71), Task Committee (63,64) and Shen (58).

DuBoys Formula:

The classic analysis of bedload was first published by DuBoys in 1879. His model has influenced considerably many subsequent formulas. He proposed the idea of bed shear stress or tractive force and based his analysis on the assumption that the bed moves in a sort of laminar flow - each layer of thickness d (presumably the same magnitude as the particles or median diameter, d_{50} of particles for a mixture) sliding over the other, the velocity of the layers decreasing linearly with depth from maximum to zero.

Duboys equation is written as

$$q_s = C_s \tau_o [\tau_o - (\tau_o)_{cr}] \qquad 2.1$$

in which q_s = bed sediment discharge, in pounds per second per foot of width; $\tau_o = \gamma R_h S$, bed shear stress, in pounds per square foot; γ = specific weight of water in pounds per cubic foot; R_h = hydraulic radius in feet; S = slope of stream in feet per foot; $(\tau_o)_{cr}$ = critical bed shear stress at which sediment movement begins; $C_s = \frac{\upsilon_s d}{2(\tau_o)^2_{cr}}$ in fps (foot-pound-second) units, is a coefficient depending on sediment characteristics, υ_s = velocity of sediment layers, ft/sec.

Straub (22) found by examining the work of many investigators, that, for "grain-water" systems, C_s is equal to $0.173/d^{3/4}$. The behaviour of C_s has been verified only in the range of 1/8 mm < d < 4 mm. The values of the parameters of Eq. 2.1 can be determined either from Straub's table (19) or from graphs (19,63).

Shields' Formula:

Shields (60) applied successfully the modern concepts of fluid mechanics to the problem of critical shear stress. He developed his model for sediment transport based on the concept of an excess of shear stress (i.e. excess in relation to the critical value). His semi-empirical bedload equation is given as

$$q_s = 10 \frac{qS}{S_s} \frac{[\tau_o - (\tau_o)_{cr}]}{\gamma (S_s - 1) d} \qquad 2.2$$

where q = water discharge per unit width, S_s = specific gravity of sediment. Equation 2.2 is dimensionally homogeneous and thus can be used in any system of units. It fits fairly well to a wide variety of experimental data, the range of scatter is equivalent to a factor of 10 (19). Shields' equation is simply a form of Duboys' equation with a more specified C_s value.

Meyer-Peter and Muller Formula:

Meyer-Peter and Muller (43) developed a formula based on data from experiments in flumes ranging in width from 15 cm to 2 meters with slopes varying from 0.0004 to 0.02 and water depths ranging from 1 cm to 120 cm. The sediments used in the experiments ranged from coal with a low specific gravity, S_s = 1.25, to river sediments and barite, with a specific gravity more than 4. The sediments used were of mixed sizes as well as uniform sizes, consequently the results of their experiments cover a wide range of conditions, and the equation developed can be expressed mathematically as

$$q_s = 8\sqrt{\frac{g}{\gamma}\frac{\gamma_s}{\gamma_s-\gamma}}\,[\tau_o - (\tau_o)_{cr}]^{3/2} \qquad 2.3$$

in which 'g' is acceleration due to gravity and γ_s = unit weight of sediment. It is seen that this equation (Eq. 2.3) is basically of the same form as the DuBoys formula. Chien (58) has shown that the Meyer-Peter et al. equation can be modified as follows: $\phi = (\frac{4}{\psi} - 0.188)^{3/2}$, where ϕ and ψ (defined by Einstein) are discussed in the Einstein bedload function.

Einstein's Bedload Function:

The bedload equation developed by H.A. Einstein (15) proved to be the most popular among all the formulas proposed so far for the determination of sediment transport rate (71). Einstein departed from the tractive force concept and developed the first stochastic model to describe the motion of a sediment particle which moves along the bed in a series of alternating transport and rest periods. He assumed that 1) the velocity field is stationary in time and homogeneous in the lateral as well as in the longitudinal directions. 2) The transport periods of the sediment particles are insignificantly small as compared to the rest periods, and 3) the probability for a particle to be moved by flow is independent of its location. Einstein developed his bedload formula empirically in 1942 and then replaced it by an analytical function in 1950.

Einstein presented his first empirical bedload equation applicable for uniform sediment and mixtures acting like uniform

sediment in terms of ϕ and ψ given as follows:

$$p = A_*\phi = f(B_*\psi) \qquad 2.4$$

where, p = probability of erosion and depends on hydrodynamic lift and particle weight.

$$\phi = \frac{q_s}{\gamma_s} \sqrt{\left(\frac{\gamma}{\gamma_s - \gamma} \frac{1}{gd^3}\right)} \qquad 2.5$$

Einstein called this dimensionless number (ϕ) the "intensity of bedload transport".

$$\psi = \frac{\gamma_s - \gamma}{\gamma} \frac{d}{SR_h'} \qquad 2.6$$

He called this term the "flow intensity".

R_h' is the hydraulic radius attributed to the sediment grain.

The two constants A_* and B_* and function 'f' are determined empirically by using the data of Gilbert (18) and of Meyer-Peter et al. (42); the range of the data is indicated in Fig. 3 where values of ψ are plotted against values (on logarthmic scale) of ϕ.. From Fig. 3 it appears that all data with ϕ less than 0.4 can be represented with a single curve (curve 1), the equation of which is

$$0.465\phi = e^{-0.391\psi} \qquad 2.7$$

The curve given by Eq. 2.7 deviates from the data for large values of ϕ, i.e., when ϕ is greater than 0.4. This is due to strong bed-load movement. Equations 2.4 and 2.7 were developed for weak sediment

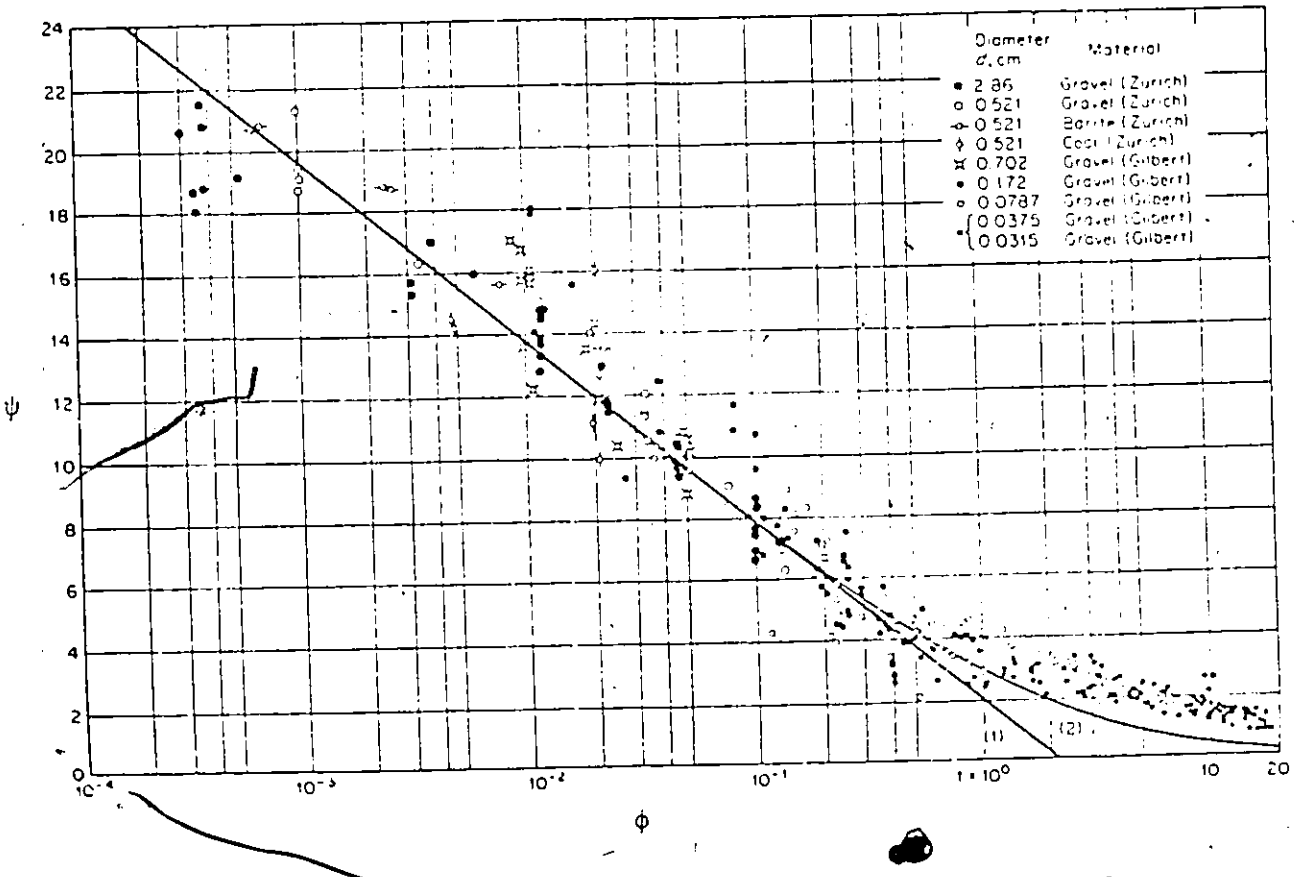

Fig. 3. - Einstein's Bedload Equations [after Einstein (1942)]

transport, i.e., $\phi < 0.4$. However, the basic equation, which is in the general form (19), was found to predict a curve such as curve 2 in Fig. 3 and explains the data better. Nevertheless, the scatter still existed which may be attributed to the fact that the experimental data included suspended load material.

As mentioned earlier, Einstein replaced his empirical relation (presented in 1942) by an analytical one in 1950. The latter is probably the most generally applicable, but also the more complex bedload equation. The final, or second, bedload equation suggested by Einstein is given as:

$$p = 1 - \frac{1}{\sqrt{\pi}} \int_{-B_*\psi_*-1/\eta_o}^{+B_*\psi_*-1/\eta_o} e^{-t^2}\, dt = \frac{A_*\phi_*}{1+A_*\phi_*} \qquad 2.8$$

where A_*, B_* and η_o are universal constants determined experimentally to be 43.5, 0.143 and 0.5 and t is the time (the only variable of integration). Einstein introduced two correction factors in his analytical derivation for sediment of mixed sizes. He observed that small particles seemed to lodge between larger ones or remain in the laminar sublayer, such that their lift must be corrected. This correction factor he termed the "hiding factor" and is denoted by ξ. The other correction factor, termed the "pressure correction", denoted by γ, describes the change of the lift coefficient in mixtures with various roughnesses. Both these factors have been determined experimentally by Einstein (19).

A second plot of the "ϕ_* versus ψ_*" relationship is shown in Fig. 4.

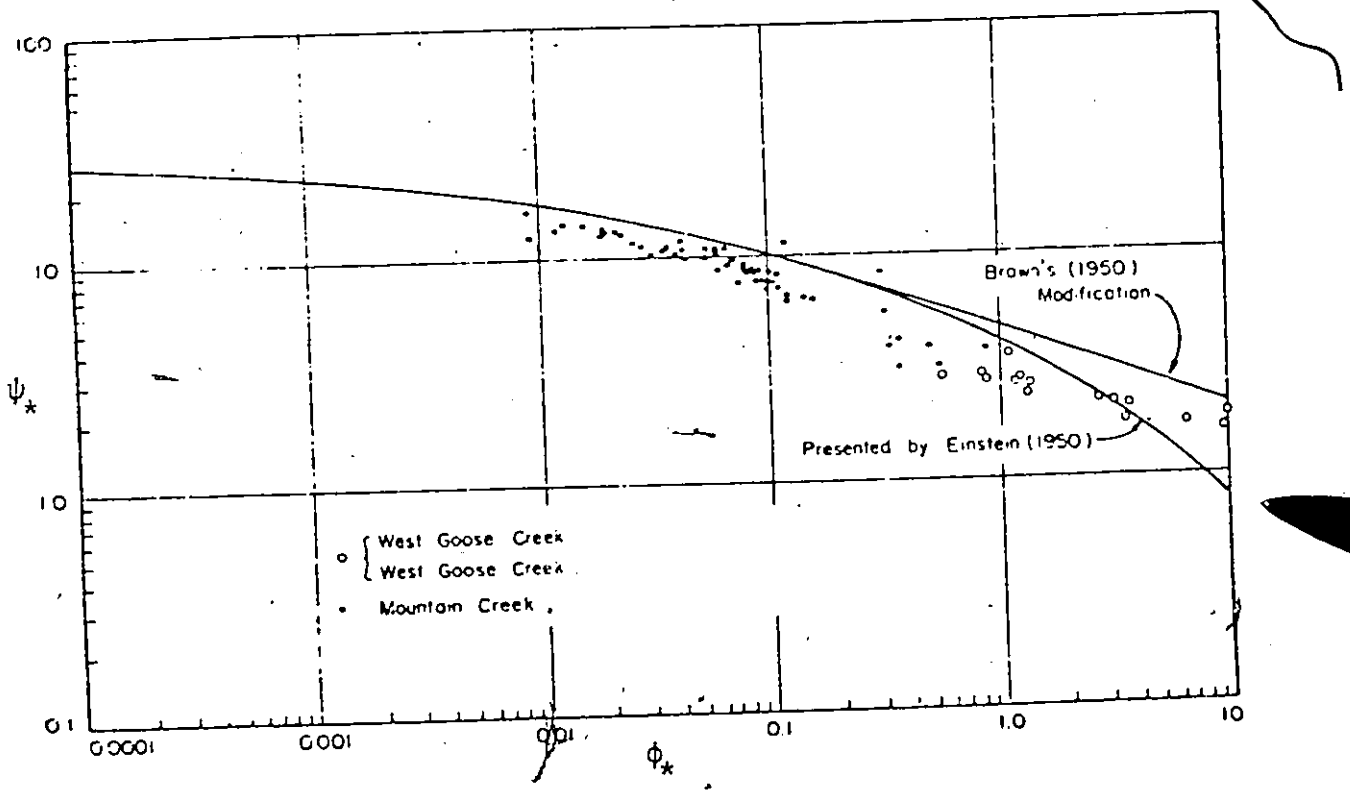

Fig. 4. - Plot of Einstein's functions, ϕ_* versus ψ_* [after Einstein (1950)]

Einstein's bedload equation appears to be rather complicated to apply, but, in fact this is not so. An ASCE Task Committee (63) has presented a table, which shows the necessary steps required in the calculation of sediment discharge using Einstein's bedload function.

Colby's Sediment Discharge Relations:

Colby (8) investigated the effects of mean velocity, shear, shear velocity, stream power of flow, flow depth, viscosity, water temperature, sediment size, and concentration of fine sediment on the discharge of sand bed sediment per foot of channel width. He presented four graphs, Fig. 5, where the sediment discharge as a function of mean velocity of water, water depths and the median size of the sand particles (d_{50}), are shown. These four sets of curves were obtained for water depths of 0.1 ft, 1 ft, 10 ft and 100 ft respectively. Each curve in each set was developed for a water temperature of 60°F, and a given d_{50}. Curves are presented for d_{50}'s of 0.1 mm, 0.2 mm, 0.3 mm, 0.4, 0.6 mm and 0.80 mm.

Colby (9) also developed curves for observed bed sediment discharge (per foot of width) versus mean velocity at average temperatures of about 60°F for five rivers, Fig. 6. He recommended that Fig. 6 can be used to calculate sediment discharge whenever the characteristics of the stream (such as bed sediment size, mean velocity of water, temperature) being studied are even approximately the same as those of the streams quoted in the figure (Fig. 6) or it can be used to check roughly all calculations.

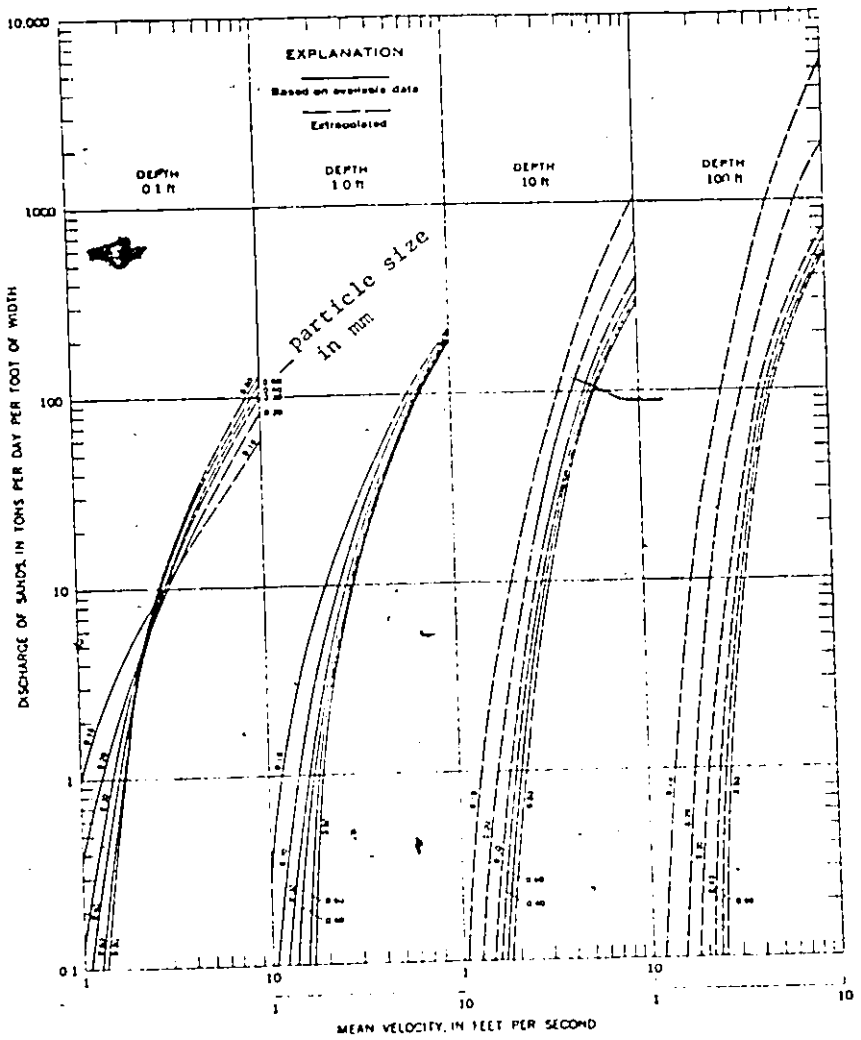

Fig. 5. – Relationship of discharge of sands to mean velocity for six median sizes of bed sands, four depths of flow, and a water temperature of 60°F, after Colby (8)

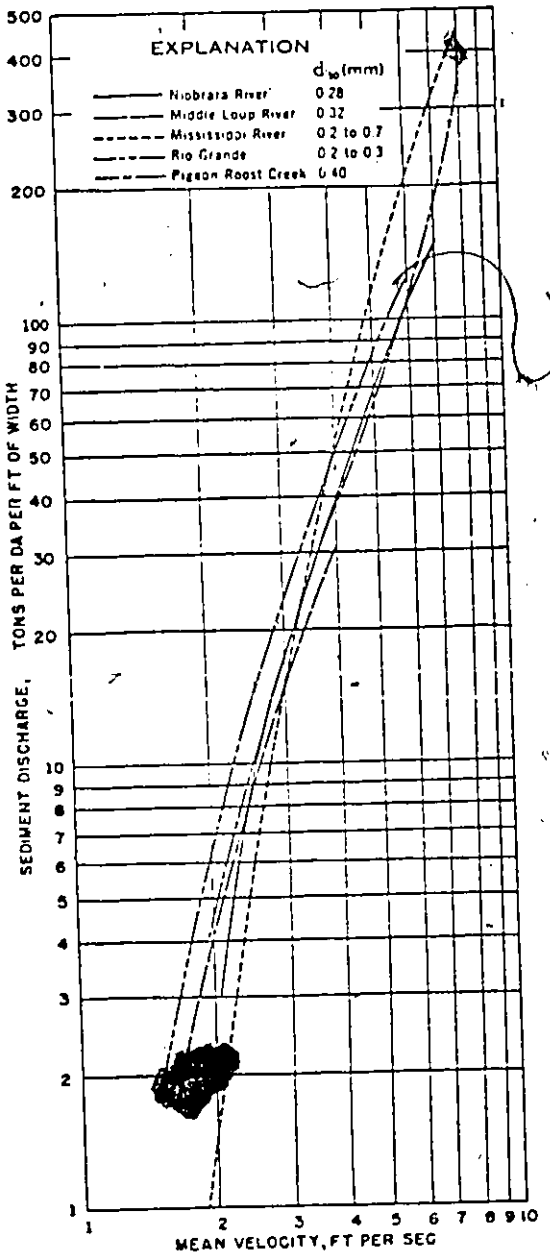

Fig. 6. – Relationship between observed discharge of sands and mean velocity for 5 sand-bed streams at average temperatures of about 60°F, after Colby (9)

2.2.5 Field Measurements and the Bedload Formulas

As stated earlier, the best way to evaluate a formula is to compare the results of calculations using it with bed sediment discharge rates actually measured in natural streams. The comparison of calculated and observed sediment discharge can be done in two ways: 1) both the observed and calculated sediment discharges are plotted against water discharge to obtain a sediment transport curve for the stream. By this method, calculated values, using several formulas, can be displayed and compared directly with each other and with the observed sediment discharge, 2) comparison is done by plotting the observed values against the calculated ones. In this method, results from only one formula can be shown in any one graph but the observed results can be obtained from any number of streams including laboratory flumes.

One of the major problems in developing and evaluating formulas is that very few direct measurements of the rates of sediment transport of rivers have been made due to practical difficulties. However, direct measurement of sediment transport rates were made on the Colorado River (at Taylor's ferry) and the Niobrara River (near Colby, Nebraska). Vanoni, Brooks and Kennedy (67) compared those field data with the results calculated using many of the established formulas (63). The results are shown in Figs. 7 and 8. These are modifications of curves presented by Vanoni et al. It appears from these figures (Figs. 7 and 8) that sediment discharges, given by the DuBoys, Shields, and Einstein-Brown formulas, tend to be high and

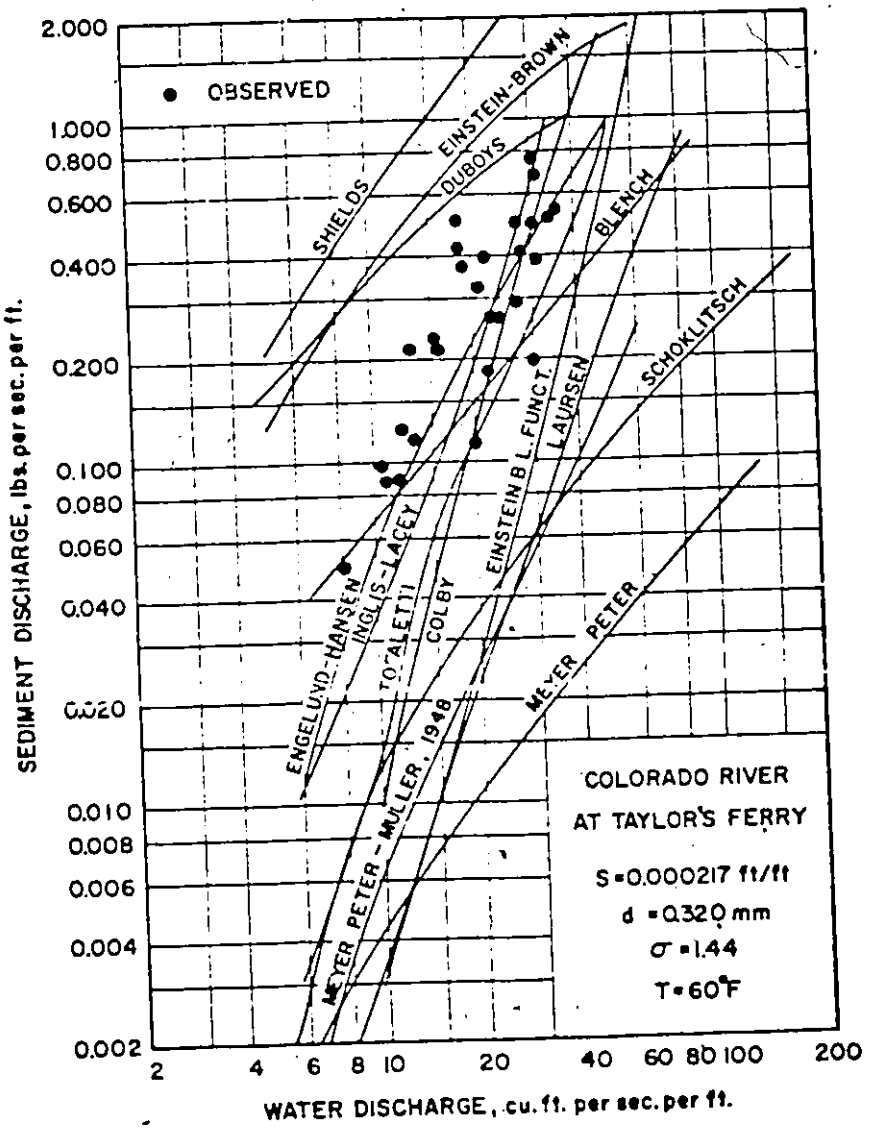

Fig. 7. – Sediment discharge as function of water discharge for Colorado River at Taylor's Ferry obtained from observations and calculations by several formulas (63)

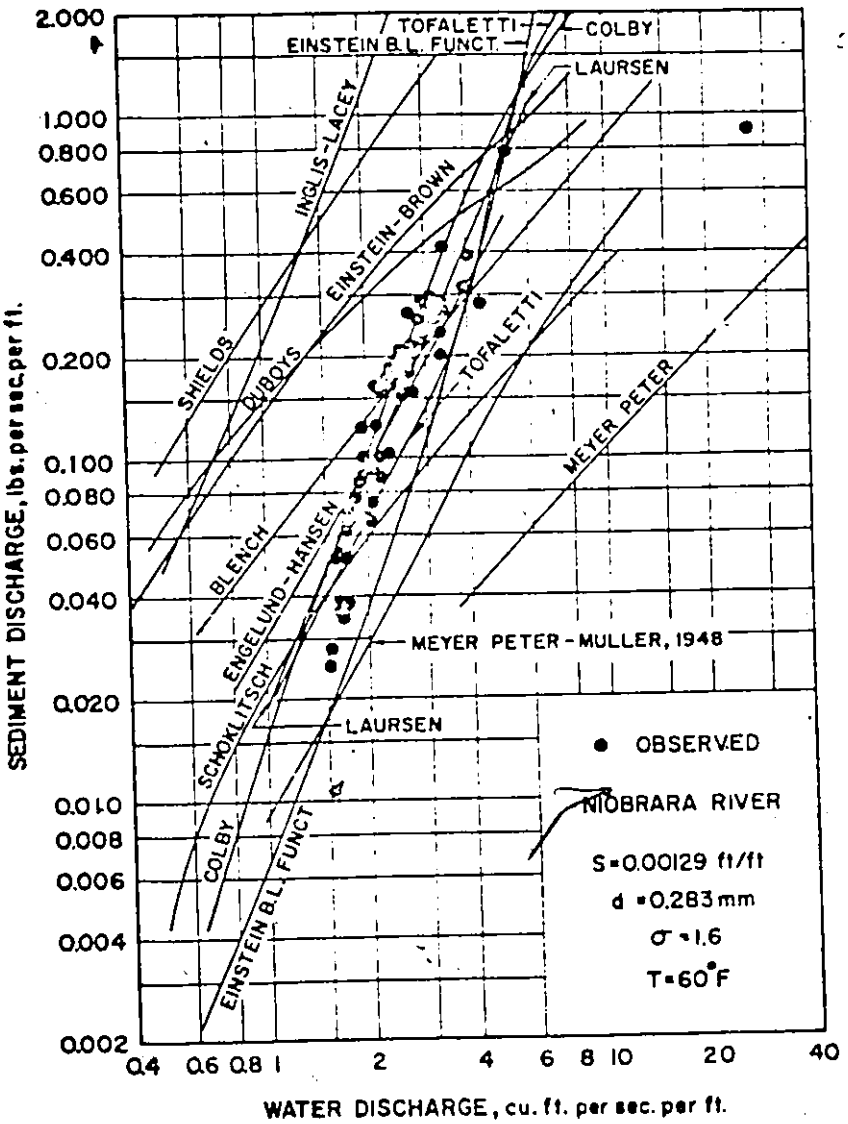

Fig. 8. - Sediment discharge as function of water discharge for Niobrara River near Cody, Nebraska obtained from observations and calculations by several formulas (63)

those by the Meyer-Peter formula tend to be low. These formulas and the Schokiitch (63) formula give curves with considerably less slope than straight lines fitted to the data in Figs. 7 and 8. The formulas which give best agreement with the observed sediment discharges are those of Colby, Tofaletti, and Engelund-Hansen (63). The curves for these formulas have slopes that are close to those of lines fitted to the field data. The slopes of the curves for the Einstein bedload function and the Laursen (63) and Inglis-Lacey (63) formulas are also close to those of a mean line for the data but the curves do not fit the data as well as several others. The curve for the Blench (63) formula intersects the data but it has too small a slope.

It is observed from the figures (Figs. 7 and 8) that the amount of scatter in the field measurements is quite formidable, and that the differences between the various formulas and the field measurements are equally great. In view of these scatters, it is clear that the formulas are still far from being able to make accurate predictions of the rate of sediment transport in rivers and streams. Since Colby, Tofaletti and Engelund-Hansen relations have been found to agree reasonably well with a large body of data from streams and flumes, there is a tendency to rely more on them than on others. All formulas mentioned so far were developed to calculate the transport rates of cohesionless sand-type sediments. No formula has yet been developed to compute the movement rate of bed sediments which are primarily composed of organic materials or which are cohesive in nature. This is a major problem faced in the Ottawa River Project.

2.2.6 Incipient Motion of Sediment Particles

Determination of incipient motion of sediment particles in rivers and streams is important not only to the study of sediment transport mechanisms but also to the study of pollutant transport associated with sediment movements (17,19,48,52,62,71,73). Incipient movement of the bed sediment, (frequently called the critical condition or initial scour), can be explained in two ways.

1) With critical velocity equations; considering the effect of the overlying liquid on the particles;

2) With critical shear stress equations; considering the frictional drag of the flow on the particles.

The above approaches might appear to be different but they are not entirely different from each other.

Critical Velocity Equation

Theoretical Development (Yang's approach (73)) -

The forces acting on a sediment particle (assumed to be spherical) at the bottom of an open channel are shown in Fig. 9. For most natural streams, the channel slopes are small enough so that the component of gravitational force in the direction of flow can be neglected as compared with other forces acting on a spherical sediment particle.

The drag force F_D can be expressed as:

$$F_D = C_D \frac{\pi d^2}{4} \frac{\rho}{2} U_d^2 \qquad 2.9$$

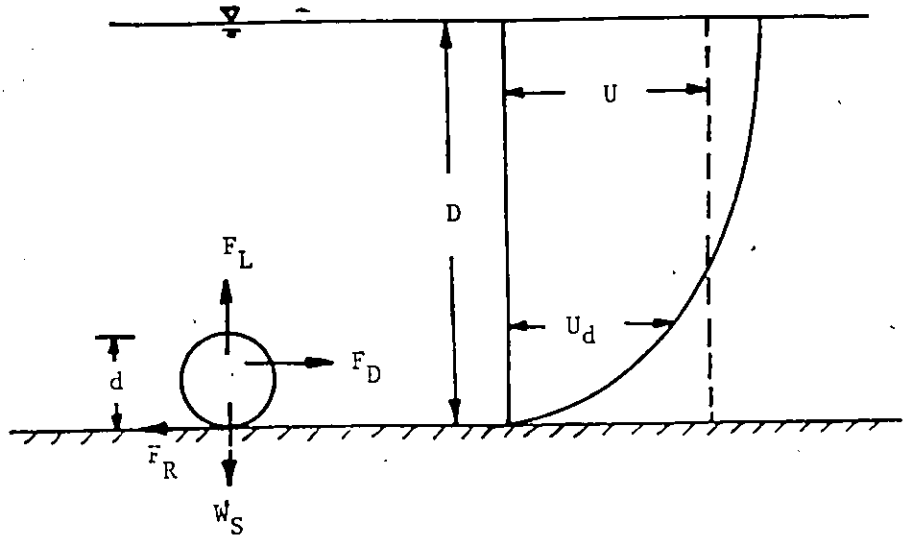

Fig. 9. - Diagram of forces acting on sediment particle

in which C_D = drag coefficient at velocity U_d; d = particle diameter; ρ = density of water; U_d = local velocity at a distance, d, above the the bed.

The terminal fall velocity of a spherical particle is reached when there is a balance between drag force and submerged weight of the particle, i.e., when,

$$C_D' \frac{\pi d^2}{4} \frac{\rho}{2} \omega^2 = \frac{\pi d^3}{6} (\rho_s - \rho) g \qquad 2.10$$

in which C_D' = drag coefficient at ω; ω = terminal fall velocity; and ρ_s = density of sediment particles.

By substituting C_D' with $k_1 C_D$ and eliminating C_D from Eqs. 2.9 and 2.10, the drag force becomes,

$$F_D = \frac{\pi d^3}{6 k_1 \omega^2} (\rho_s - \rho) g \, U_d^2 \qquad 2.11$$

If we assume that the logarithmic law for velocity distribution can be applied in this case, then

$$\frac{U_Y}{U_*} = 5.75 \log \frac{Y}{d} + B \qquad 2.12$$

in which U_Y = local velocity at distance Y above the bed, B = roughness function, U_* = shear velocity.

Then the local velocity at Y = d becomes

$$U_d = B\, U_* \tag{2.13}$$

The average velocity can be obtained by integrating Eq. 2.12 from $Y = \varepsilon$ to $Y = D$ with $\varepsilon \to 0$, that is:

$$U = U_* \left[5.75 \left(\log \frac{D}{d} - 1\right) + B\right] \tag{2.14}$$

from Eqs. 2.11, 2.13 and 2.14

$$F_D = \frac{\pi d^3}{6k_1} (\rho_s - \rho) g \left(\frac{U}{\omega}\right)^2 \left[\frac{B}{5.75 \left(\log \frac{D}{d} - 1\right) + B}\right]^2 \tag{2.15}$$

The lift force F_L acting on the particle can be expressed by

$$F_L = C_L \frac{\pi}{4} d^2 \frac{\rho}{2} U_d^2 \tag{2.16}$$

The relationship between lift coefficient C_L and drag coefficient C_D can be determined experimentally. Assuming $k_2 C_L = C_D$, and following the same procedure as in obtaining Eq. 2.15, we have

$$F_L = \frac{\pi d^3}{6k_1 k_2} (\rho_s - \rho) g \left(\frac{U}{\omega}\right)^2 \left[\frac{B}{5.75 \left(\log \frac{D}{d} - 1\right) + B}\right]^2 \tag{2.17}$$

The submerged weight of the particle is

$$W_s = \frac{\pi d^3}{6} (\rho_s - \rho) g \tag{2.18}$$

Then the resistance force F_R becomes

$$F_R = k_3 (W_s - F_L) \tag{2.19}$$

or

$$F_R = \frac{k_3 \pi d^3}{6} (\rho_s - \rho) g \left[1 - \frac{1}{k_1 k_2} \left(\frac{U}{\omega}\right)^2 \left(\frac{B}{5.75 \left(\log \frac{D}{d} - 1\right) + B}\right)^2\right] \qquad 2.20$$

In which k_3 = friction coefficient.

Assuming that the incipient motion occurs when $F_D = F_R$, then from Eqs. 2.15 and 2.20

$$\frac{U_{cr}}{\omega} = \left[\frac{5.75 \left(\log \frac{D}{d} - 1\right)}{B} + 1\right] \sqrt{\frac{k_1 k_2 k_3}{k_2 + k_3}} \qquad 2.21$$

where U_{cr} = the average critical velocity at incipient motion and $\frac{U_{cr}}{\omega}$ = the dimensionless critical velocity.

Equation 2.21 is the basic equation which specifies the flow condition when a sediment particle is about to move on the bottom of an open channel. The terminal fall velocity, ω, of a spherical grain, can be computed from the following equation

$$\omega = \upsilon_s - \upsilon = \frac{2}{9} \left(\frac{d}{2}\right)^2 g \frac{\rho_s - \rho}{\mu} \qquad 2.22$$

The values of the coefficients k_1, k_2 and k_3 have to be determined experimentally.

The roughness function B, depends on whether the boundary is in a "hydraulically smooth", "transitional" or "completely rough" regime.

In the hydraulically smooth regime, B is a function of only the shear velocity Reynolds number $\frac{U_* d}{\nu}$ shown in Fig. 10 and obtained by Nikuradse.

$$B = 5.5 + 5.75 \log \frac{U_* d}{\nu} \quad , \qquad 0 < \frac{U_* d}{\nu} < 5 \qquad 2.23$$

Then Eq. 2.21 becomes

$$\frac{U_{cr}}{\omega} = \left[\frac{\log \frac{D}{d} - 1}{\log \frac{U_* d}{\nu} + 0.956} + .1\right] \sqrt{\frac{k_1 k_2 k_3}{k_2 + k_3}} \qquad 2.24$$

which is a hyperbola on a semilog plot between $\frac{U_{cr}}{\omega}$ and $\frac{U_* d}{\nu}$.

In the completely rough regime, the laminar friction contribution can be neglected as the protrusions reach outside the laminar sublayer and B is constant, and is a function of only the relative roughness d/D.

$$B = 8.5 , \quad \frac{U_* d}{\nu} > 70 \qquad 2.25$$

then Eq. 2.21 becomes

$$\frac{U_{cr}}{\omega} = \left[\frac{\log \frac{D}{d} - 1}{1.48} + 1\right] \sqrt{\frac{k_1 k_2 k_3}{k_2 + k_3}} \qquad 2.26$$

Equation 2.26 shows that in the completely rough regime, the plot of $\frac{U_{cr}}{\omega}$ against $\frac{U_* d}{\nu}$ is a straight horizontal line. The position of this horizontal line depends on the value of relative roughness $\frac{d}{D}$, and the coefficients k_1, k_2 and k_3.

In the transitional regime given by the condition $5 < \frac{U_* d}{\nu} < 70$ the value of B cannot be obtained analytically. Depending on the given value of the Reynolds number $\frac{U_* d}{\nu}$, the value of B can be estimated from the graph in Fig. 10.

The flow condition, corresponding to incipient motion, depends more or less on the investigators definition of incipient

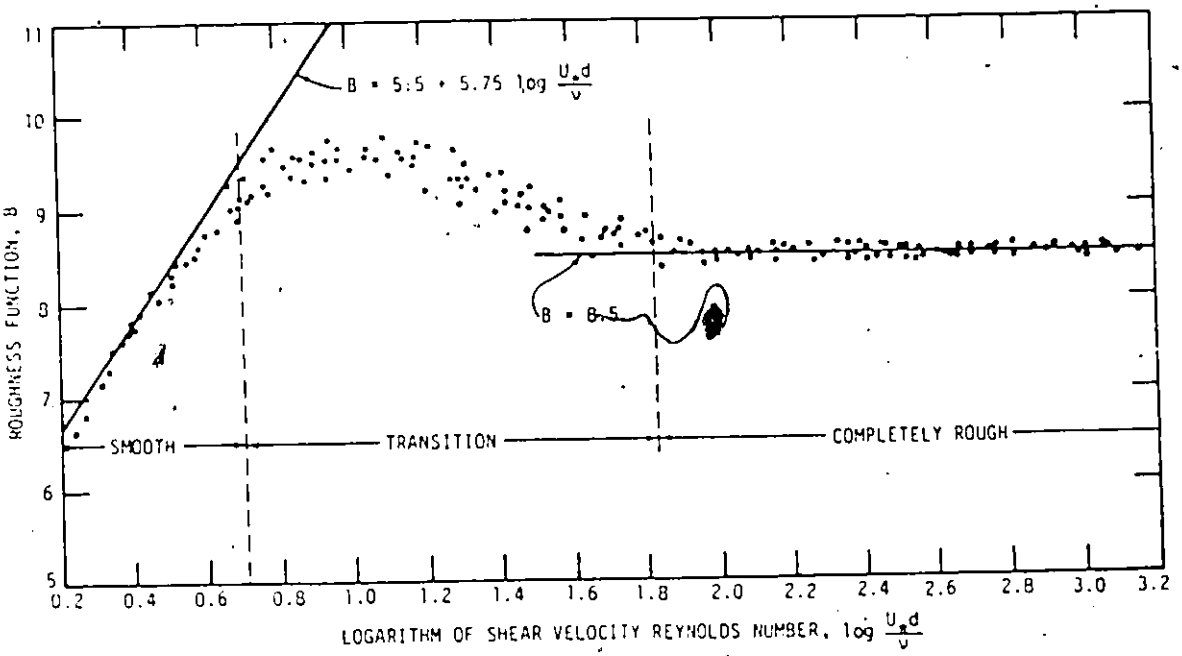

Fig. 10.- Relationship between roughness function and shear velocity Reynolds number (73).

motion (62). Yang (73) developed a curve for the relationship between dimensionless critical velocity $\frac{U_{cr}}{\omega}$ and shear velocity Reynolds number $\frac{U_* d}{\nu}$ at incipient motion, using the data of several investigators, see Fig. 11.

As shown in the figure (Fig. 11) when the shear velocity Reynolds number is smaller than 70, the data follows the hyperbola

$$\frac{U_{cr}}{\omega} = \frac{2.5}{\log\left(\frac{U_* d}{\nu}\right) - 0.06} + 0.66, \qquad 0 < \frac{U_* d}{\nu} < 70 \qquad 2.27$$

fairly well in accordance with Eq. 2.24. Yang determined the coefficients in Eq. 2.27 by trial and error to minimize the deviation between the observed and predicted values. When the shear velocity Reynolds number is greater than 70, $\frac{U_{cr}}{\omega}$ is no longer a function of $\frac{U_* d}{\nu}$ according to Eq. 2.26. Yang represented the data in this case by

$$\frac{U_{cr}}{\omega} = 2.05, \qquad 70 < \frac{U_* d}{\nu} \qquad 2.28$$

Yang concluded that Eqs. 2.27 and 2.28 would provide a useful criterion for incipient motion. His approach to the problem of incipient motion was well received by other investigators (7,33).

Critical Shear Stress Equation

Shields (60) described the problem of initiation of motion in terms of the following functional relationship,

$$\frac{(\tau_o)_{cr}}{(\rho_s - \rho) g d} = f\left[\frac{(U_*)_{cr} d}{\nu}\right] \qquad 2.29$$

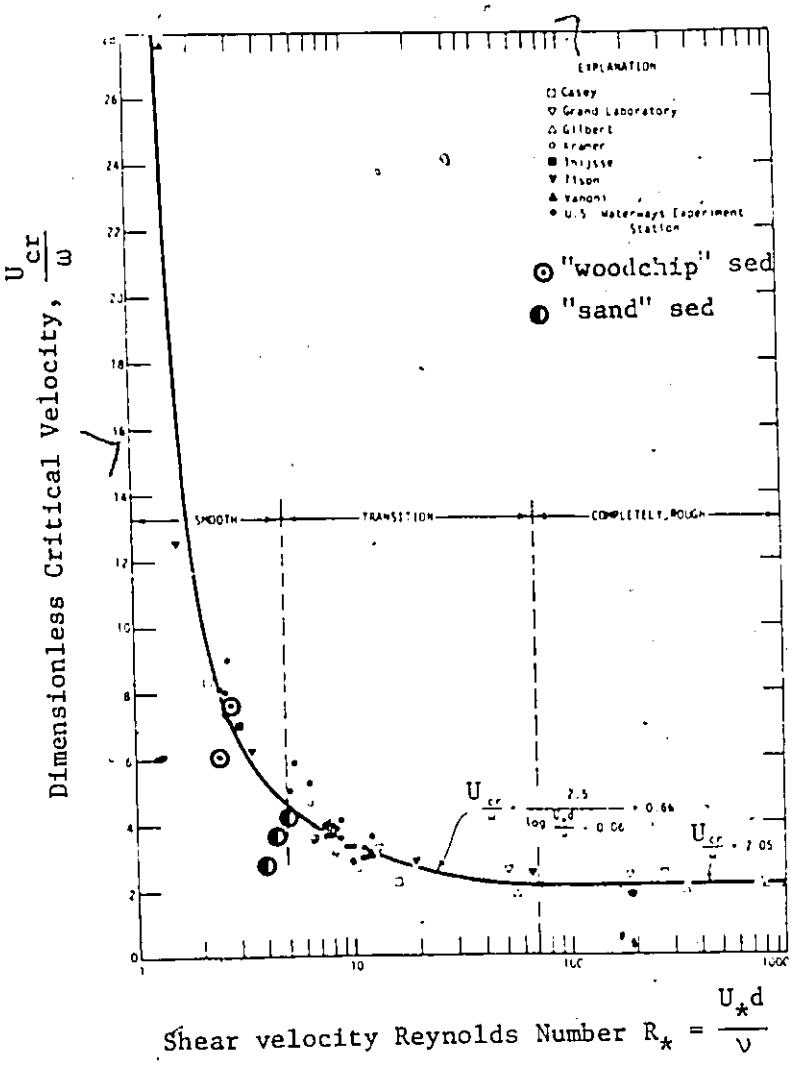

Fig. 11.-Relationship between Dimensionless and shear velocity Reynolds Number at Incipient Motion (73)

in which $(\tau_o)_{cr}$ = critical average shear stress when bed particles begin to move; ρ_s = sediment density; ρ = the fluid density; ν = kinematic viscosity; d = bed sediment diameter; $(U_*)_{cr} = \sqrt{\frac{(\tau_o)_{cr}}{\rho}}$ = critical bed shear velocity; and f denotes "a function of". The left hand side of Eq. 2.29 is called the dimensionless critical shear stress, (usually denoted by $(\tau_*)_{cr}$), and the variable on the right is called the boundary critical Reynolds number, (denoted by $(R_*)_{cr}$). When values of bed stress τ_o other than $(\tau_o)_{cr}$ are used in the two quantities they are termed dimensionless shear stress and boundary Reynolds number and are denoted by τ_* and R_*, respectively (62). Figure 12 is a graph of the data used by Shields to determine the function of Eq. 2.29. The data delineating the curve were obtained by Shields and several other workers from experiments in flumes with fully developed turbulent flows and artificially flattened beds of non-cohesive sediments (19,62). Shields' results, shown in Fig. 12, have been widely accepted although some workers have reported somewhat different values for the parameters (19).

To facilitate the calculation of $(\tau_o)_{cr}$ when the sediment and fluid properties are known an auxiliary scale, having lines with positive slopes of 2.0, is included in the figure (Fig. 12). To find $(\tau_o)_{cr}$ the value of $d/\nu \sqrt{0.1 (\frac{\gamma_s}{\gamma} - 1)gd}$ is calculated using a consistent set of units such as feet, pounds and seconds, and this value is located on the auxiliary scale. A line is then drawn through this point parallel to the inclined lines and the values of $(\tau_*)_{cr}$ is read at the intersection with the Shields curve from which $(\tau_o)_{cr}$ can be calculated (62).

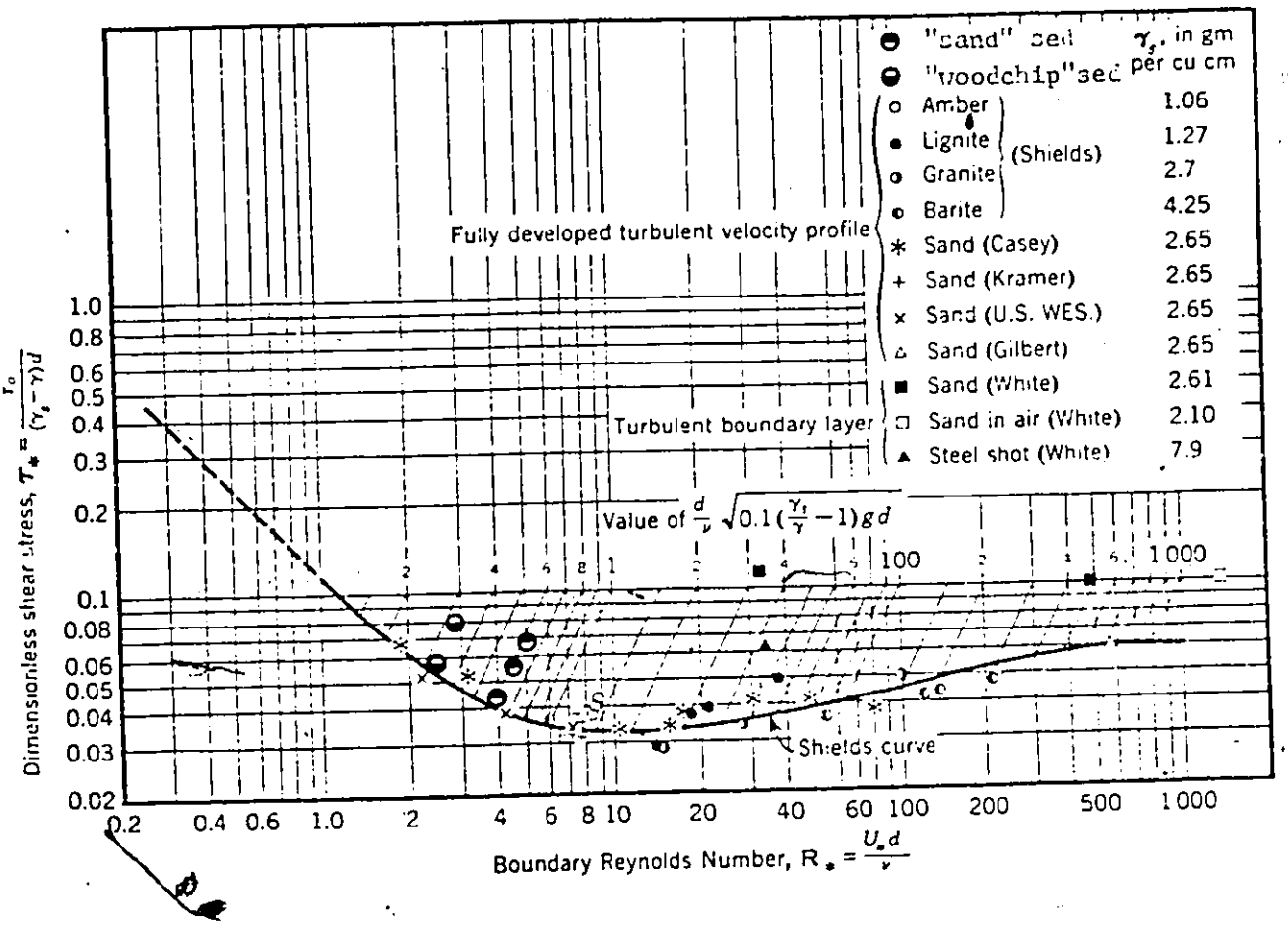

Fig. 12 - Shields Diagram (62)

White (68) concluded that true critical shear stress required to move a particular grain has a fixed value. His equation for $(\tau_o)_{cr}$ for sediment in a horizontal bed is given as

$$(\tau_o)_{cr} = 0.18\ (\gamma_s - \gamma)\ d \tan \theta \qquad 2.30$$

where θ = the angle of repose of the submerged sediment.

The constant in Eq. 2.30 is obtained from experiments with laminar flows.

The fact that the definition of critical conditions for incipient movement of sediments is rather indefinite, as a consequence the variation in the results of different workers can be expected. Despite this fact however there seems to be reasonable agreement among a considerable number of published results from several sources.

CHAPTER 3

EQUIPMENT AND PROCEDURES

In this Chapter, the equipment used and procedures adopted to carry out the studies will be presented.

3.1 Classification and Spatial Distribution of Bed Sediments in the 4.88 km (3-mile) Study Section of the Ottawa River

3.1.1 Equipment

The following equipment was used in this study:

1) Shipek grab sampler
2) 12 ft x 20 ft (3.66 m x 6.1 m) raft
3) U.S. Standard sieves (Nos. 20, 30, 40, 60, 80, 100, 140, 200, 270, 400, pan)
4) Mechanical shaker
5) Balance

3.1.2 Procedure

Field Program - In the summer months of 1973, a large number of samples of bed sediments were collected from 35 locations of the study section using the Shipek grab sampler and the raft of the Department of Geology, University of Ottawa. Figure 13a shows the Shipek sampler and Fig. 13b shows the sampler mounted on the raft. From each sampling location 35 to 40 lbs of bed sediments were collected in plastic bags and brought back to the laboratory for detailed analysis and for future use in the flume studies.

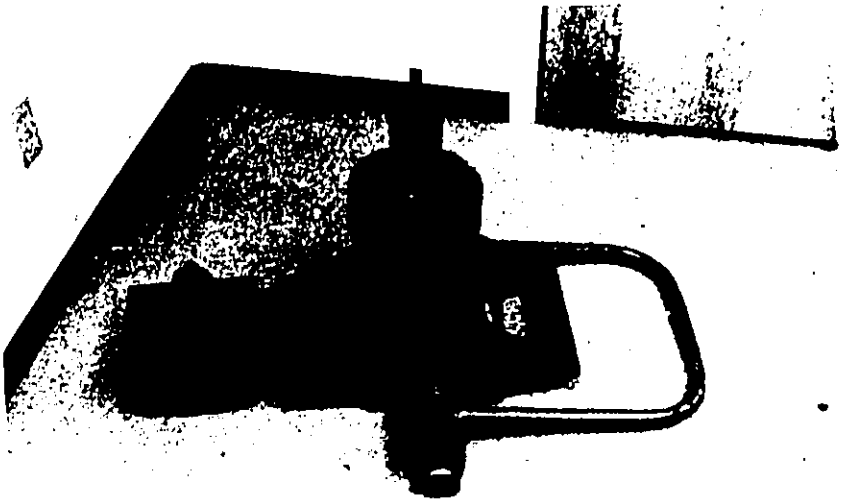

(a)

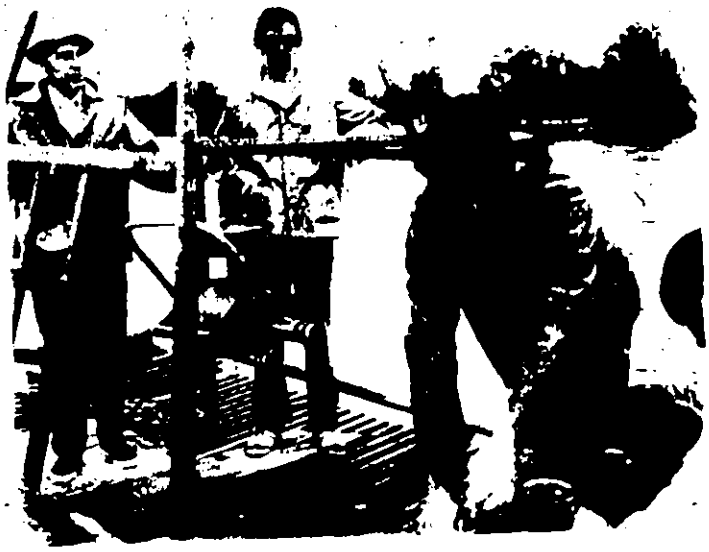

(b)

Fig. 13. - (a) Shipek grab sampler, (b) Sampler mounted on the raft

Laboratory Study - Grain size distribution analyses of the bed sediments were performed using the U.S. standard sieves. In each test 500 grams of sample was sieved very carefully for 15 minutes using the mechanical shaker and the weight of each fraction measured very accurately. The necessary computations associated with the grain size distribution analysis are presented in Appendix A.

3.2 Cation Exchange Capacity and Mercury Sorption Capacity of Various Types and Fractions of Bed Sediments

3.2.1 Equipment

The equipment used in this study are listed below:

1) "Nuclear Chicago" deep well gamma counter, (Fig.14)
2) Variable speed shaker
3) Centrifuge
4) Vials, pippettes
5) Millipore filter apparatus

3.2.2 Procedure

Cation Exchange Capacity - The ion exchange capacities of different fractions of main channel and C.I.P. channel bed sediments, (obtained from the sieve analysis), were determined using both the radioactive cesium and mercury methods (3). The procedure for determining the ion exchange capacities of the sediment fractions by both the methods are similar. In both methods duplicate samples (200 mg) from each size fraction were placed in the vials to which was added 5 ml of 0.25 N solution (mercuric chloride labelled with ^{203}Hg/cesium

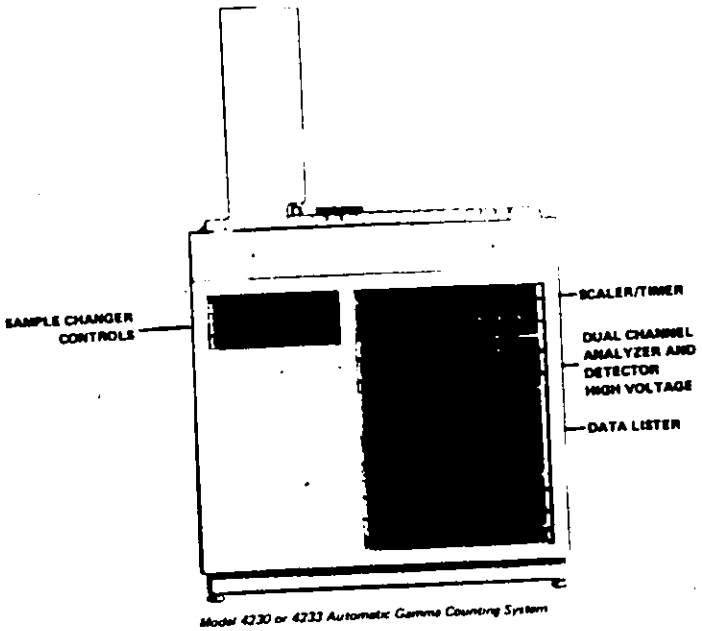

Fig. 14. - "Nuclear Chicago" Deepwell Gamma Counter

chloride labelled with ^{137}Cs). The vials were then placed in the shaker and shaken for four hours. This treatment saturated the cation exchange sites with mercury/cesium. The solid and liquid phases were then separated by centrifuging and the supernatant liquid was decanted. This procedure was repeated once more. The excess solution from the sample was then removed by repeated washing (at least three times) with approximately 15 ml portions of 95 percent ethyl alcohol, agitating thoroughly (15 minutes), centrifuging completely, and decanting the supernatant liquid after each additional centrifugation until the decanted alcohol was free of chloride.

After the washing was completed the vials were thoroughly cleaned (on the outside) with tap water; dried and placed in a well-type automatic gamma scintillation counter (Nuclear Chicago Corporation model). Counting rates of the adsorbed cesium-137/mercury-203 were determined. An aliquot (4 ml) of the solution used to saturate the samples with cesium/mercury was counted using the same gamma counter. Exchange capacities of the samples were then calculated by comparing the counting rate of the sample with that of the equilibrating solution using the following equation:

$$\text{Exchange Capacity} = \frac{\text{sample counts per minute}}{\text{counts per minute/milliequivalent of cesium/mercury}} \times \frac{100}{\text{sample wt. expressed in grams}}$$

or

$$\frac{\text{sample cpm}}{\text{cpm/milliequivalent}} \times \frac{100}{\text{sample wt. in grams}} = \text{milliequivalent per 100 grams}$$

Sorption Capacity - The mercury sorption capacity of the three major fractions; fines (consisting of clay, silt and wood fibres); sands; and wood chips of the "CIP" channel bed sediment was determined using radioactive mercuric chloride solution labelled with ^{203}Hg. Four sediment samples were treated with four different concentrations (0.1 ppm, 10 ppm, 100 ppm, and 1000 ppm) of mercuric chloride solution.

The samples were then incubated for 6 months to simulate field conditions. Fine fractions from each of the samples were [redacted]ted by agitating with distilled water and then the distilled water (together with fines in suspension) was decanted and filtered on a 0.45μ filter paper using the millipore filter apparatus. Wood chips fraction from the samples could be separated very easily with the help of forceps. The three fractions from each sample were placed in separate vials, weighed, and their counting rates were determined by the "Nuclear Chicago" counter.

3.3 Study of the Interaction between Flowing Water and Bed Sediments

In this section the laboratory model, instrumentation of the model, procedure for mercury transport study and determination of the values of important flow parameters at incipient motion of sediment particles are discussed.

3.3.1 Laboratory Model

Figure 15a is a schematic diagram of the laboratory model (flume). The elements of the model consist of a 9.14 m long (30.48 cm x 5.08 cm) rectangular conduit with a 121.9 cm long test section, an

inlet head tank, a supply tank, a sediment catcher, an outlet gate, an outlet tank, a 30 gpm constant speed pump, a supply valve, a flow rate control valve, supply pipes, and an overflow return pipe.

The flume walls are made of 1.27 cm thick plexiglass. Section A-A (Fig. 15b) shows a cross section of the conduit. The bottom and sides of the test section (working section) are made of brass and the top is made of plexiglass. A plexiglass side window is located on one side of the test section to enable one to observe sediment movement and a slot is provided on the top to accommodate measuring instruments. Section B-B (Fig. 15c) shows a cross sectional view of the test section and Fig. 15d shows part of the test section.

The 5.08 cm diameter supply pipe leading from the pump branches into two pipes (each 5.08 cm diameter) at the control valve in order to ensure balanced flow into the head tank. The piping for the overflow return from the head tank to the supply tank consists of a single 7.62 cm diameter pipe. All the pipes used are polyvinyl-chloride (PVC) pipes. The flow regulation in the system can be expressed as

$$Q_s = Q_f + Q_o$$

where Q_s is the total water supply in the head tank, Q_o is the excess water flowing through overflow return pipe (for the purpose of maintaining a constant supply pressure in the head tank). Q_f is the flow through the working section.

The selection of a pressurized rectangular conduit system for this study, rather than a free surface flume, was made in order

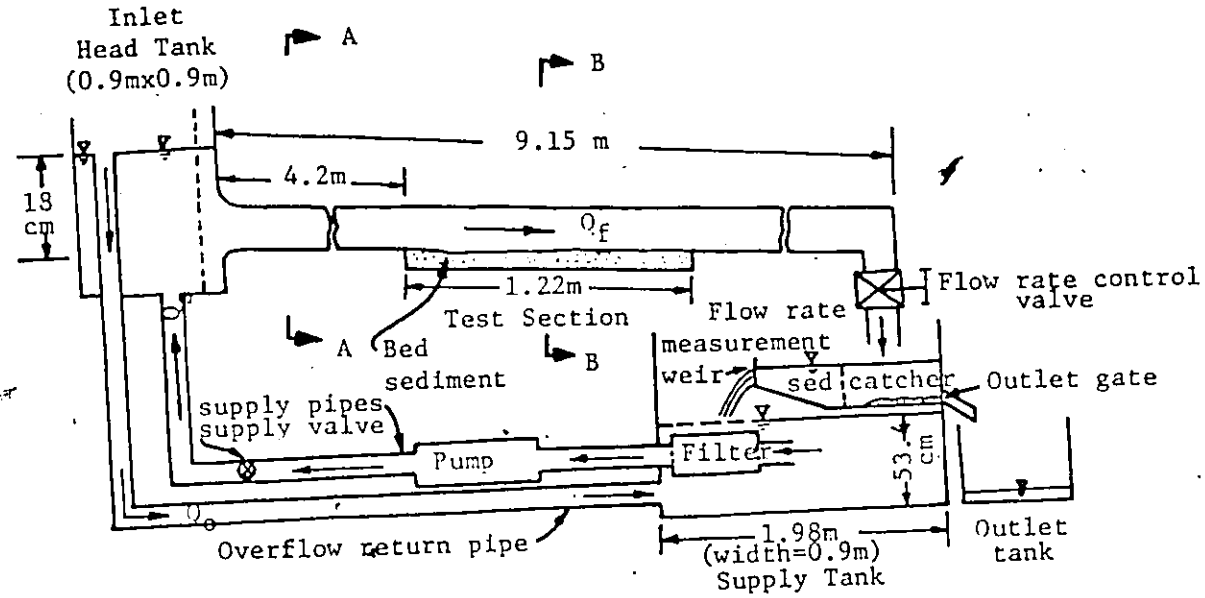

(a) Schematic diagram of the laboratory model

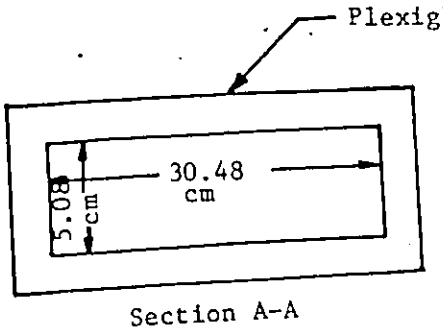

(b) Cross sectional view of the conduit

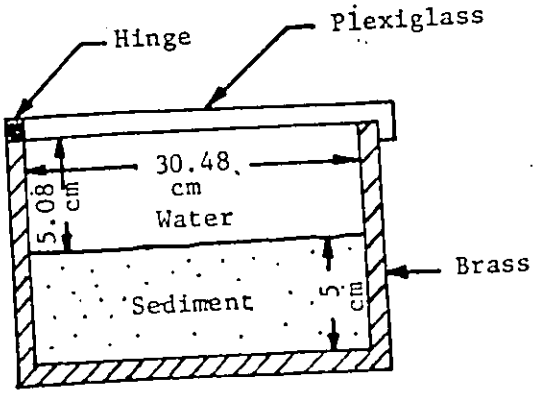

(c) Cross sectional view of the 1.22 m test section

Fig. 15. - (continued)

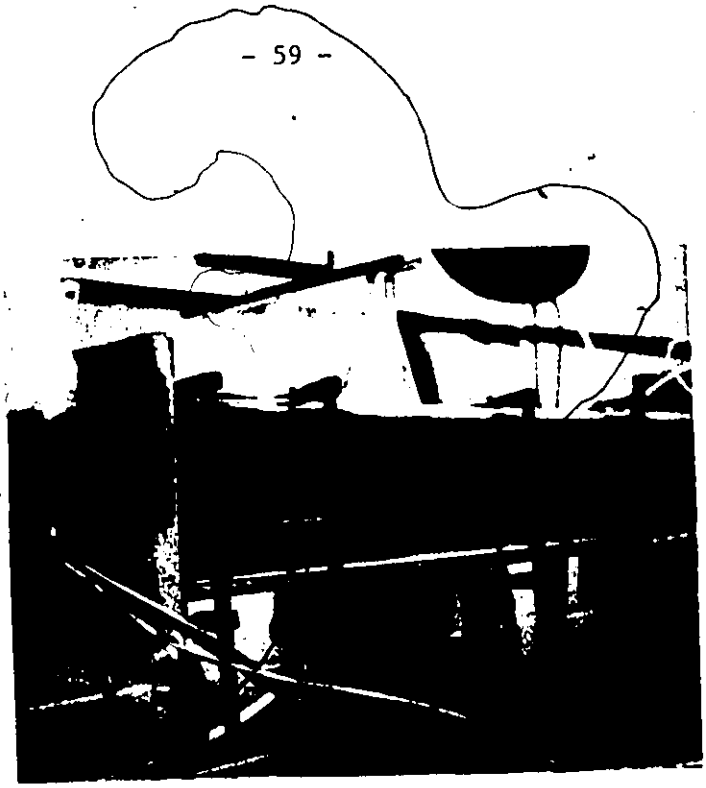

(d) part of the test section

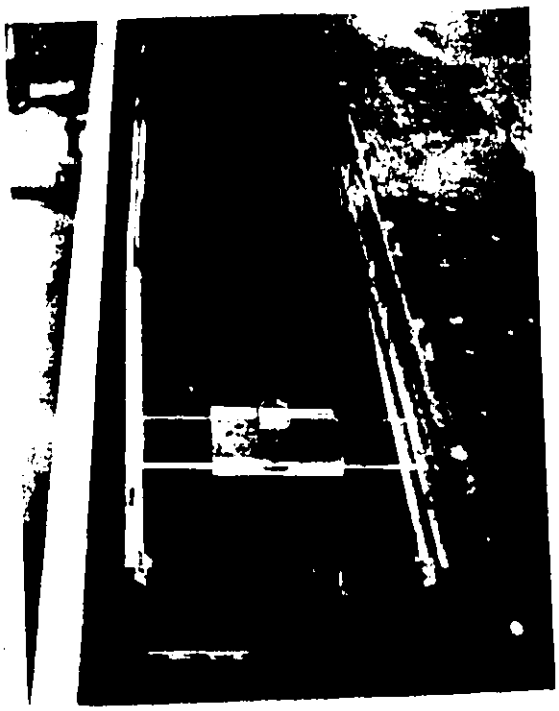

(e) sediment catcher with v-notch
and point gauge

Fig. 15. - (a) Schematic diagram of the laboratory model, (b) sectional view of the conduit, (c) sectional view of the test section, (d) part of the test section, (e) sediment catcher with v-notch and point gauge

to measure and reproduce flow conditions with a high degree of confidence. Control of the geometry also insured reproducible conditions at the desired points in the test section. Free surface flows simulated in a flume are complicated by the depth of flow, surface wave interaction at high Froude numbers, and the physical length and size. The advantages of using the closed conduit system compared to a comparable free surface system are as follows:

1) The flow parameters can be measured with more simplicity and accuracy

2) The physical size is reduced

3) The geometry is controlled.

3.3.2 Instrumentation

The flow through the flume was measured by a 90° v-notch installed downstream from a sediment catcher (Fig. 15e). Baffles were placed in the catcher to suppress turbulence and the discharge heads at the weir were measured by a point gage. The weir was calibrated for different flow conditions. Figure 30 in Appendix C shows the calibration curve for the weir.

Point velocities across the flow field were measured using a pitot tube (outside diameter 4 mm) and a piezometer unit attached to the flume. Boundary shear stress measurements were supplied using the preston tube technique. The preston tube was calibrated and the calibration procedure is presented in Appendix C.

The temperature of the water was measured by a thermometer.

The data acquisition system used in the experiments was equipped to monitor radioactivity movement. The system consisted of a detector (positioned at different locations on the test section with proper shielding with lead brick) connected with "ORTEC" Gamma Counter, Fig. 16. The radioactivity in the water samples (collected in vials during tests), in the sediment in the test section after the tests and in the transported sediment collected in vials was determined by the "Nuclear Chicago" counter.

Before proceeding with the various experiments, the flume was tested for a range of operating flow conditions to ensure that the velocity field was symmetrical about the centreline of the test section. The results of these preliminary tests are presented in Appendix C. They confirm that the profiles are normal and free of any significant distortion in the 1.22 m long working section. Subsequent to these tests the following studies were performed.

3.3.3 Mercury Transport Study Associated with Bed Sediments

A sample of the bed sediment was placed in the test section. The flume was then filled very slowly with water by gradually opening the supply valve while keeping flow rate control valve closed. When the flume was completely filled with water it was kept in that state for some time until the sediment in the test section became totally saturated. Water was then drained out of the flume by opening the flow rate control valve. Sediment mixed with radioactive mercury

Fig. 16. - "ORTEC" counter

(labelled with ^{203}Hg) was then placed in the test section in a 5 cm strip across the full width of the sample up to a depth of 1 cm (Fig. 17). The flume was then refilled with water as before. When the flume was completely full the desired flow was produced by adjusting the supply valve and the flow rate control valve and measuring the desired flow rate with the aid of the v-notch. The radioactivity movement was recorded (at 1/2 hour intervals) by placing the detector along the test section (Figs. 18a, b, and c). At each interval water samples were collected in vials (10 ml) and in jars. At the end of each experiment the supply valve was closed, water was drained out of the system and sediment samples were collected in vials from the test section at the locations as shown in Fig. 17. Samples were also collected from the sediment mass transported downstream from the working section. The water samples collected in jars were filtered on 0.45μ filter paper using millipore filter apparatus to obtain suspended sediment. The activity of these samples were determined by the "Nuclear Chicago" counter apparatus. The total amount of sediment transported was determined by adding the amounts obtained in the sediment catcher and on the floor of the flume downstream from the test section after each experiment.

3.3.4 Determination of the Flow Parameters (Velocity Boundary Shear Stress) Corresponding to Incipient Motion of the Particles

The test section was filled with sediment, levelled, and

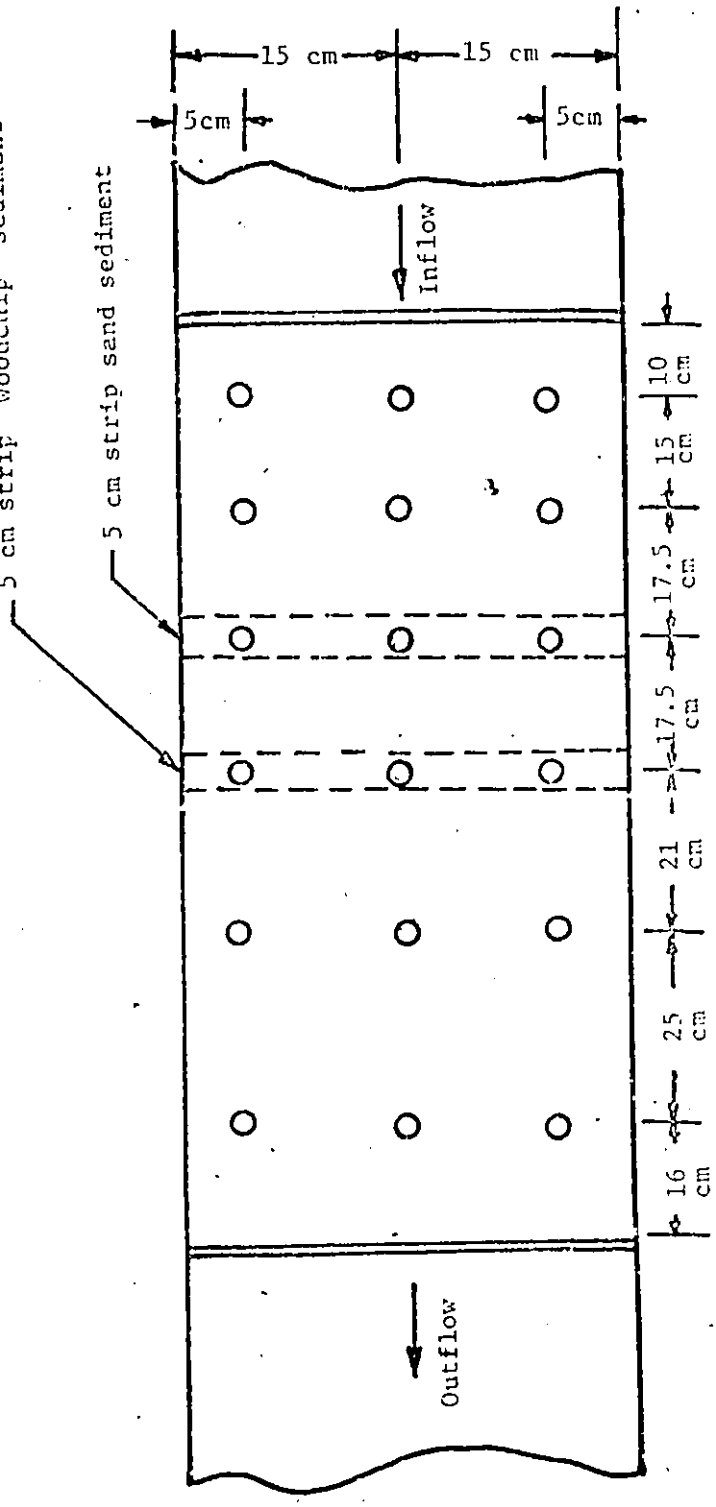

Plan of Test Section

Fig. 17. - Location of the sources for sand bed sediment and "woodchip" bed sediment. The circles show the sampling locations at the end of each run.

(a) Detector placed over the test section

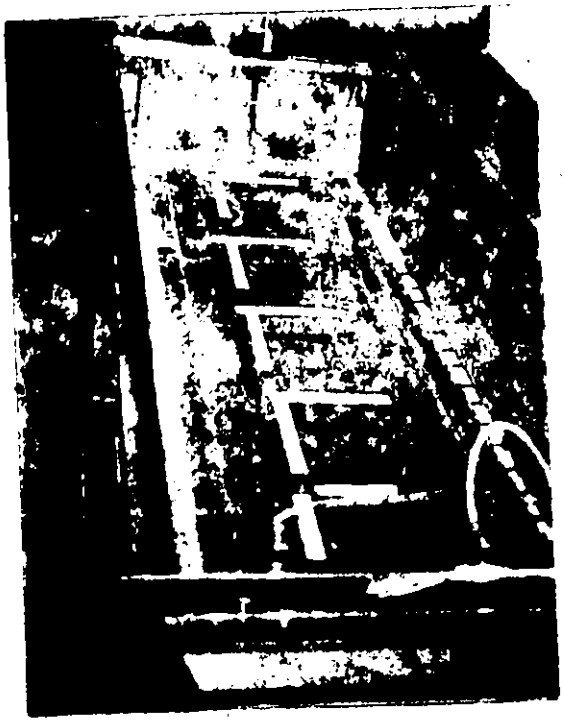

(b) Detector positions on the test section

Fig. 18. - (continued)

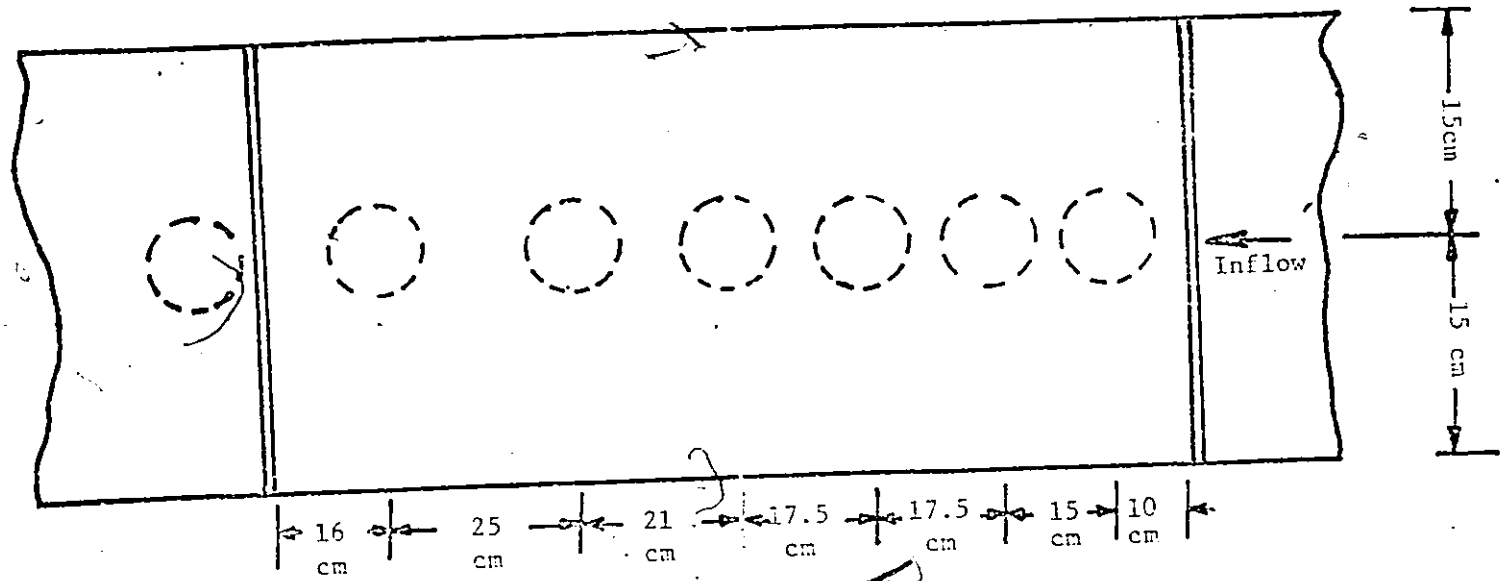

(c) Locations of the detector positions on the test section

Fig. 18. - (a) Detector placed over the test section

(b) Detector positions on the test section

(c) Locations of the detector positions on the test section

saturated with water in the same way as described in the preceding section. When the bed sediment was saturated completely, water was allowed to flow over the sediment by slowly opening the flow rate control valve and adjusting the supply valve. Simultaneously careful observation was made on the test section to determine the beginning of movement of the bed sediment particles.

Because of the totally random nature of the movement process, there is no truly critical condition corresponding to the initiation of particle motion. In fact Kramer (62) defined the following three "intensities" of sediment motion near the critical condition:

"1. Weak movement indicates that a few or several of the smallest particles are in motion in isolated spots in small enough quantities so that those moving on one square centimeter of the bed can be counted.

2. Medium movement indicates the condition in which grains of mean diameter are in motion in numbers too large to be countable. Such movement is no longer local in character. It is not yet strong enough to affect bed configuration and does not result in appreciable sediment discharge.

3. General movement indicates the condition in which sand grains up to and including the largest are in motion and movement is occurring in all parts of the bed at all times."

Velocity gradients near the bed, across the width of the test section, were measured by placing a pitot tube near the sediment/

water interface. The limiting distance was 2 mm from the bed to the centre of the tube. Flow rate was deduced from the calibration curve of the 90° triangular notched weir (Fig. 50) by measuring the head upstream from same and the mean velocity (U_{cr}) through the flume for these critical conditions was calculated from the flow rate. Boundary shear stresses for these conditions were measured using the Preston tube technique described in Appendix C.

CHAPTER 4

PRESENTATION AND DISCUSSION OF RESULTS

4.1 Bed Sediments of the 4.88 km (3 mile) Study Section of the Ottawa River

4.1.1 Classification and Spatial Distribution of Bed Sediments

Due to the presence of the Kettle Island and Upper and Lower Duck Islands, the study section of the Ottawa River is divided into a main channel and two small subsidiary channels. The main channel is located south of Kettle Island, in between Kettle Island and Upper Duck Island and passes north of the Upper and Lower Duck Islands as shown in Fig. 1. One of the subsidiary channels is located to the north of Kettle Island along the Quebec shore and is referred to as the "CIP" (Canadian International Paper Company) channel. The other subsidiary channel flows to the south of Upper and Lower Duck Islands. These two subsidiary channels eventually merge with the main channel.

The bed sediment in the main channel is mainly medium sand (d_{50} = 280 μm) except near the southern bank (Ontario province), where a strip consisting of mixture of silt and clay is present. In the CIP channel, the bed sediment consists of a complex mixture of fine sand (d_{50} = 180 μm), wood fibres, wood chips and bark. These organic contents vary from 1 percent to nearly 100 percent depending on the location and time of year. Because of the presence of wood

chips in high proportion, the bed sediment of the CIP channel will hereafter be referred to as "woodchip" sediment. This channel is the most heavily polluted zone in the study section due to the presence of the CIP mill on the north shore. The bed sediment in the other subsidiary channel is coarse sand mixed with gravel. The results of the studies presented in this chapter are confined to the "sand" sediment of the main channel and "woodchip" sediment of the CIP channel, since, when taken together, these two sediment types constitute the major portion of "mobile" bed sediments.

Figure 19 shows the transects A-A, B-B, C-C, D-D, E-E, and F-F along which the bed sediment samples were collected. The points along the transects indicate the locations where samplings were done. Figure 20 shows pictures of a typical sand sediment from the main channel and a "woodchip" sediment from the CIP channel. The clay sediment obtained near the Ontario bank is also shown in the same figure, (in crushed form), for the purpose of grain size comparison, but it actually occurs in the river bed in a very stiff consolidated state. This type of clay sediment is called "Leda clay" geologically and is a marine clay of the Champlain Sea (6).

The sand sediment of the main channel also contains some wood chips as shown in Fig. 20. The presence of organic fractions in this and other parts of the river bed is a unique characteristic of the Ottawa River system.

Figure 21 shows the lateral variation of median sizes of bed sediments along the transects A-A, B-B and C-C of the main channel

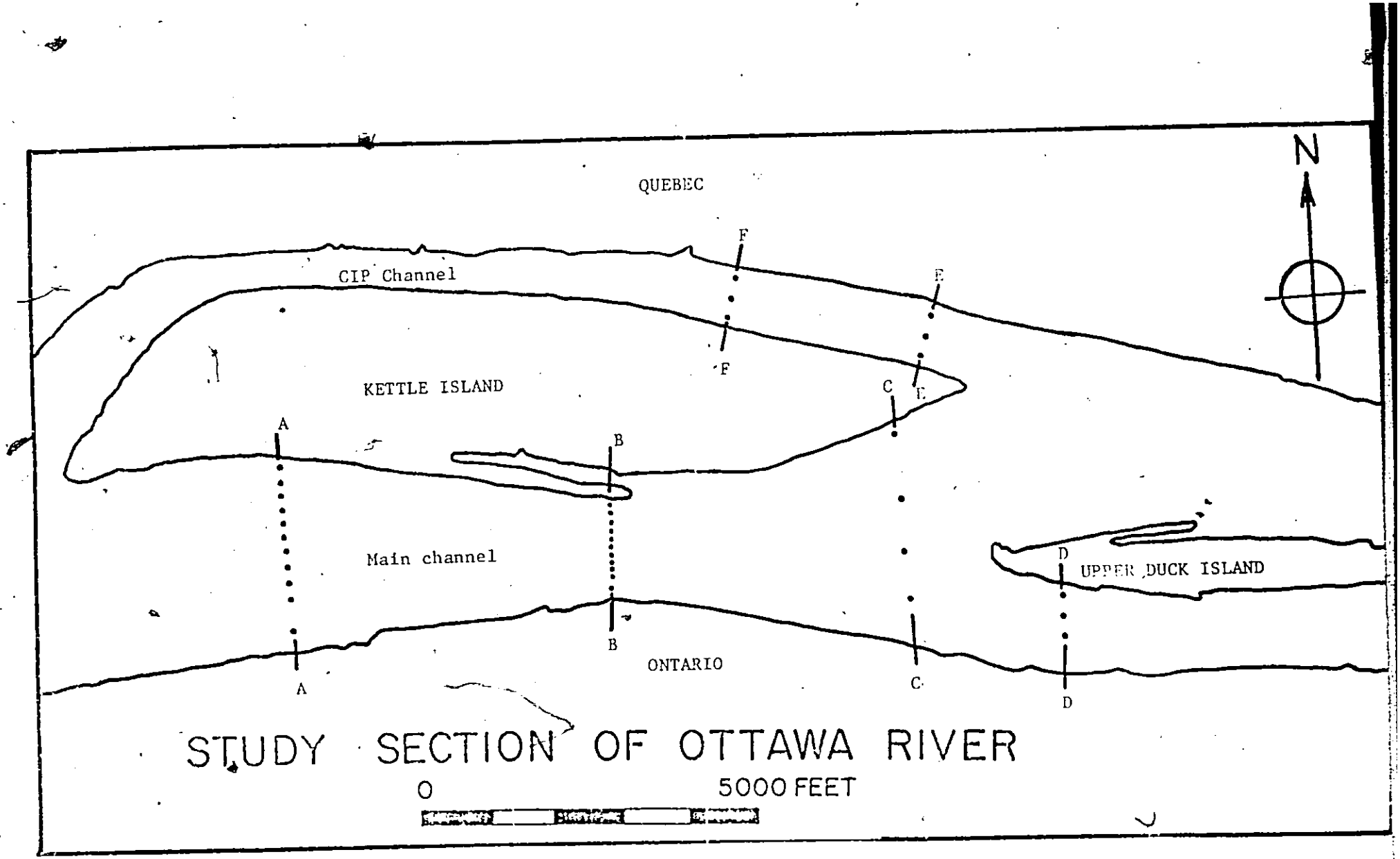

Fig. 19. - Transects showing sampling locations in the study section of the Ottawa River

Fig. 20.-OTTAWA RIVER BED SEDIMENTS

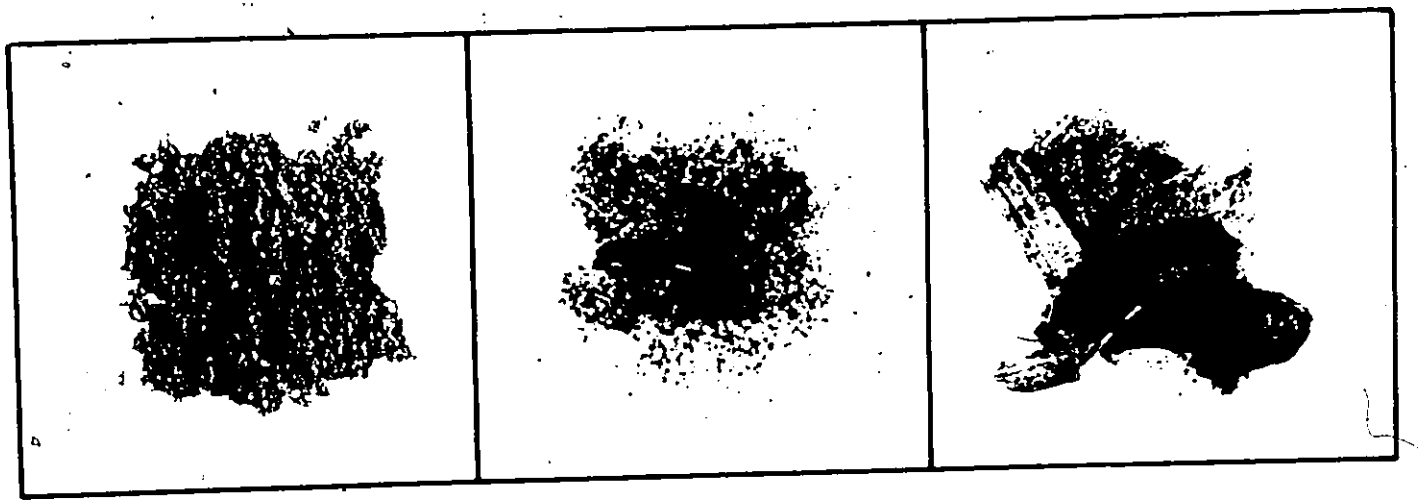

CLAY SAND WOOD CHIP

0 1 2 3 4 5

SCALE: CM

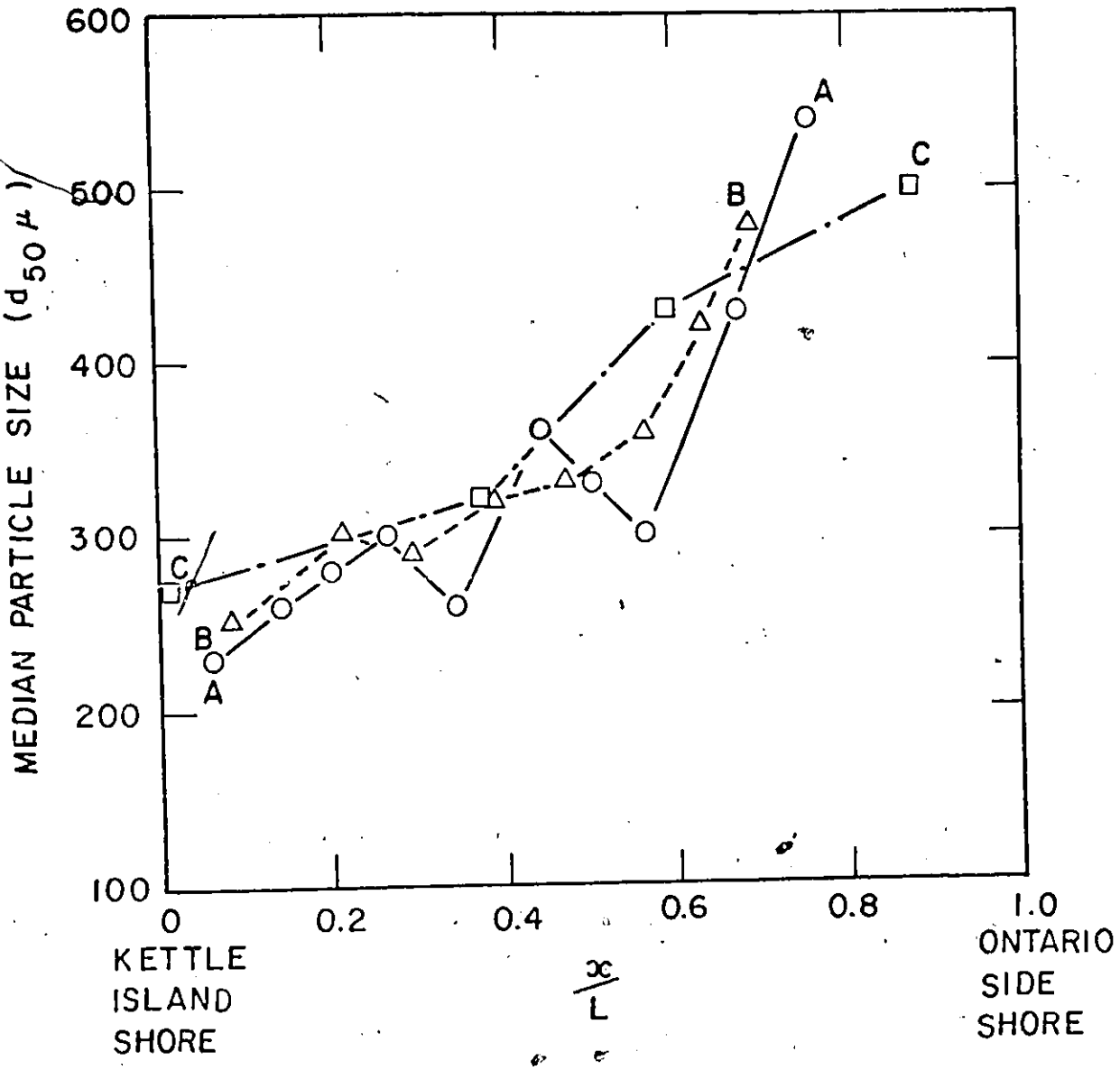

Fig. 21 - Lateral variation of the median sizes (d_{50}) of bed sediment particles along the transects A-A, B-B, C-C of the main channel

From these curves, it is clear that the coarsest sediment in the study reach is confined to the main channel, where the water depth is greatest. Median grain size gradually decreases as the Kettle Island shore is approached. Figure 22 shows detailed distributions of the different types of bed sediments found in the various zones along the study section. Some of the information for preparing this figure (Fig. 22) were obtained from Dr. B. Rust of Geology Department, University of Ottawa.

4.1.2 Particle Size Distribution Analysis

Particle size distribution appears to be the single most important factor for bed sediment transport, as well as for pollutant transport associated with bed sediment movements (34). A detailed particle size distribution analysis was performed for both types of sediments, i.e., sand sediment from the main channel and "woodchip" sediment from the CIP channel. Particular attention was given to analyzing the "fines" components (less than 100 μm) since, as will be shown later, these fractions play an important role in the sorption (uptake) and subsequent transport of mercury in dynamic aquatic systems.

Particle size distribution curves, plotted on probability graph paper for sand sediments and "woodchip" sediments, are shown in Fig. 23. The median diameter for the sand and "woodchip" sediments are 280 and 180 μm, respectively. The distribution of both sediments are not log-normal, as might be expected for stream bed sediments (23).

In the case of "woodchip" sediments, particles with diameters less than 100 μm represented 1.97% of the total weight, whereas particles, less than 50 μm in diameter, represented only 0.26% total

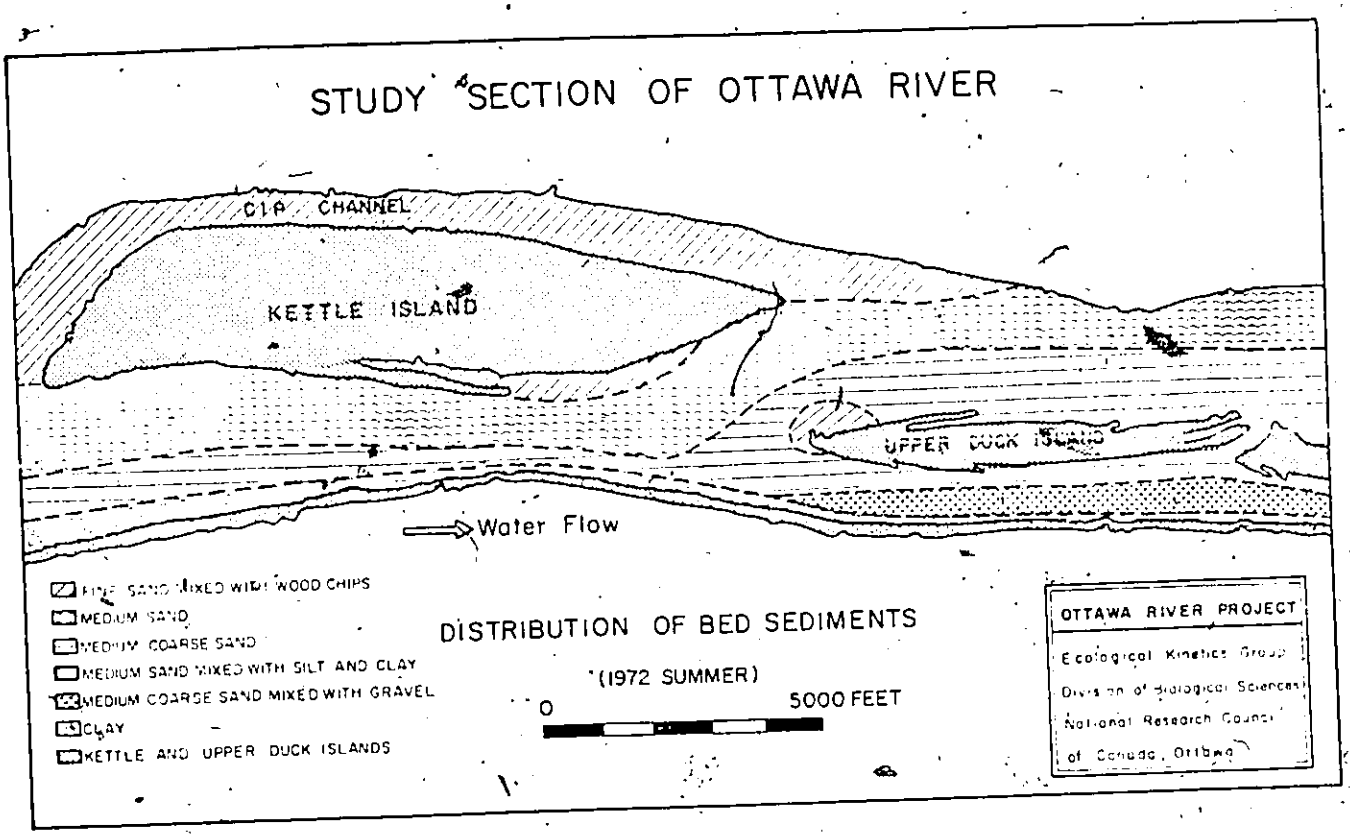

Fig. 22. - Distribution of bed sediments in the study section of the Ottawa River

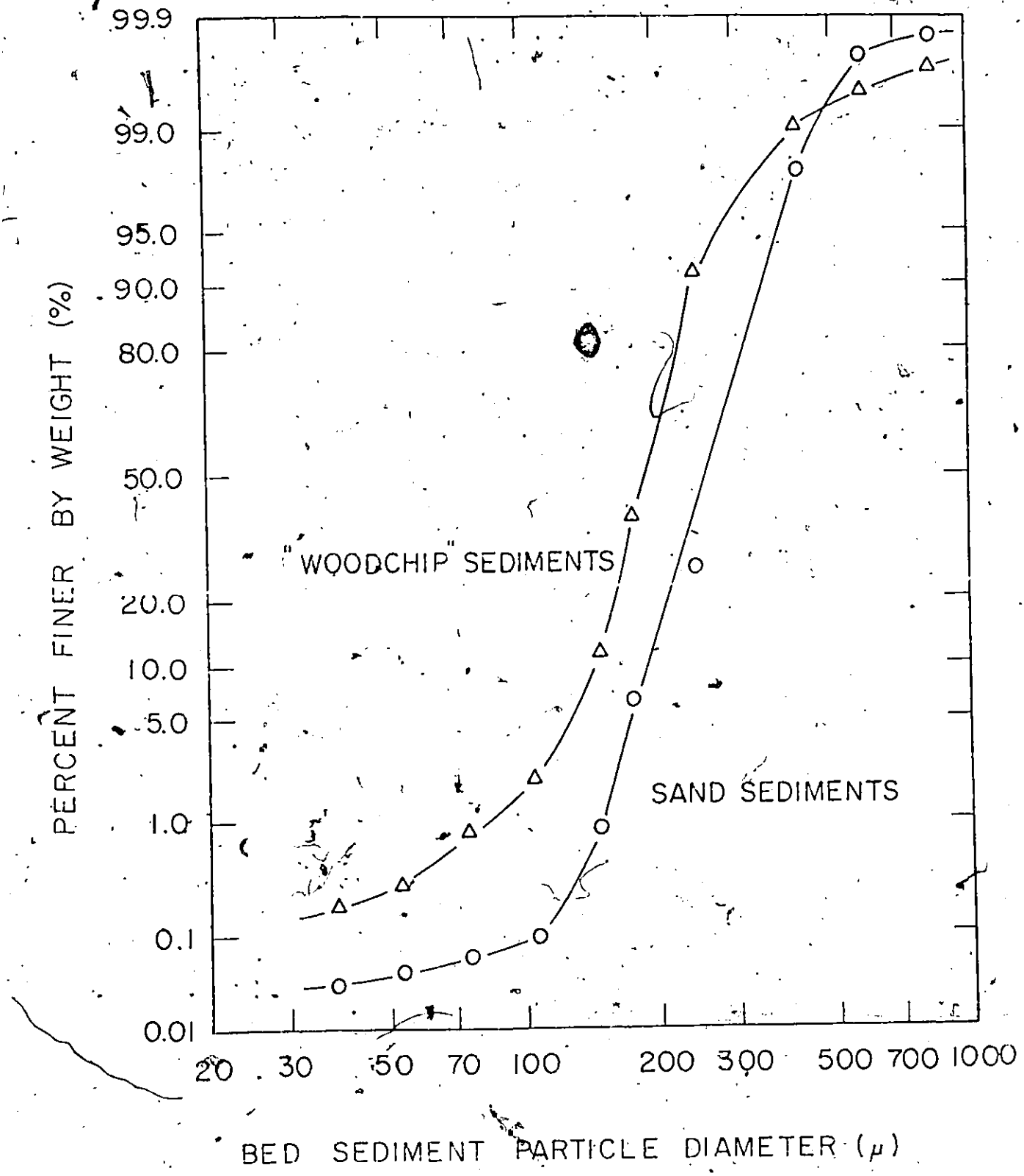

Fig. 23. - Grain size distribution curve

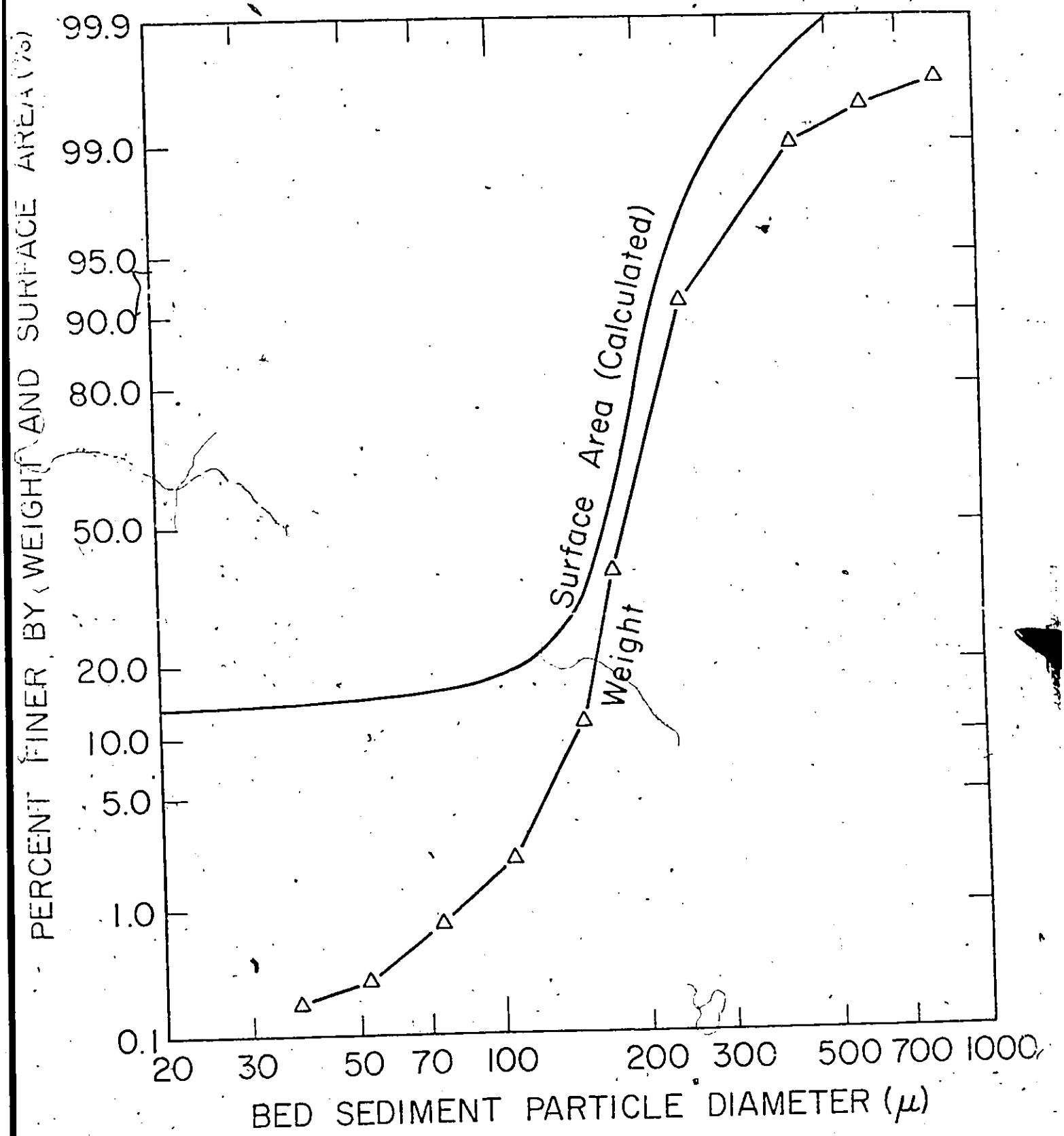

Fig. 24. - Accumulative surface area and weight curves of "woodchip" sediments

weight. It could be assumed, however, that the cumulative surface area of the "fines" particles would represent a greater proportion of the total surface area - since this component contains more grains (by unit weight) Fig. 24. This is to be expected regardless of exact shape of the particles involved.

4.2 Mercury Sorption Capacity and Cation Exchange Capacity of the Different Fractions of Bed Sediment

4.2.1 Sorption Capacity

Table 1 shows the concentrations of mercury in each sediment fraction, in water and in "woodchip" sediments as a whole (values shown are for total mercury; chemical form was ignored). Also shown are the concentrations per unit mass of the component fractions. In the case of the "0.1 ppm" mercury concentration experiment, fractions of wood chips and fines contained 1.12 ppm and 2.58 ppm of mercury respectively, whereas the sand fraction contained only 0.026 ppm. Since similar results (i.e., significantly higher mercury concentrations in fines and wood chips) were observed for all mercury concentrations considered, it is clear that mercury distribution, within bed sediment fractions, is certainly not uniform. Therefore, great care must be taken to retain the total volume initially extracted when collecting representative bed sediment samples from rivers for the purpose of studying pollutant concentrations in same.

The final values in Table 1 are distribution coefficients for mercury between water and the three sediment fractions for the

Table 1. - Distribution of Mercury in "Woodchip" Bed Sediments and Water

Mercury Concentrations (ppm)				
Whole sediments	0.1	10	100	1,000
Sands	0.026	1.79	52.1	896
Wood Chips	1.12	126	724	1,730
Fines	2.58	203	3,040	28,100
Water (ppb)	0.043	1.03	69.5	550
Fractional Amounts				
Sands (93.5%*)	24.3%	16.7%	48.6%	83.7%
Wood Chips (6.3%*)	70.8%	79.4%	45.5%	10.9%
Fines (0.19%*)	4.9%	3.9%	5.9%	5.4%
Distribution Coefficients (K**)				
Sands	610	1,740	750	1,630
Wood Chips	26,200	123,000	10,400	3,130
Fines	60,400	198,000	43,600	51,100

*By dry weight

**$K_{sand} = \frac{[Hg]_{sand}}{[Hg]_{water}}$ = 610, 1740, 750, 1630 = 1200 average

$K_{fine} = \frac{[Hg]_{fine}}{[Hg]_{water}}$ = 90,000 average

different concentrations considered. Although there is a noticeable variation, (at least an order of magnitude), numerical averages can be suggested for sands and fines respectively, i.e., $K_{sand} = 1.2 \times 10^3$ and $K_{fines} = 90 \times 10^3$. These values would, naturally, vary widely in different environments, however they appear to be quite consistent with field data obtained from the Ottawa River.

For wood chips, it seems clear that the K-value shifts in favour of the water component for high mercury concentrations. This result suggests possible saturation of binding sites. For low concentrations, however, a distribution coefficient of the order of $K_{wood\ chip} = 50 \times 10^3$ seems indicated.

Comparison of these laboratory results with field data is reasonably satisfactory. In the study section, total mercury concentration in water was found to be 0.038 ppb during the 1972 summer (21), and 0.018 ppb during the 1973 summer (44). The aforementioned "laboratory" distribution coefficients would suggest values of mercury concentration in sediments (1972) ranging from about 0.05 ppm for pure sand to about 2.0 ppm for pure wood chips. Actual field values averaged 0.08 ppm in the sandy main channel and 0.27 ppm in the north (CIP) channel, where high organic content is common (55); the heterogeneous character of the field samples would naturally suggest values in between the predicted extremes.

For 1973, the comparison is equally reasonable. Consideration of the concentration of mercury in the water column leads to predictions of 0.012 ppm for pure sand and 0.5 ppm for pure wood chips, field values for main channel samples averaged 0.023 ppm and, for CIP channel samples, the average was 0.17 ppm (50).

Table 1 also lists fractional amounts of mercury within the bed sediment components. For example, the wood chips fraction contained 70.8% of the mercury in the "0.1 ppm" bed sediment, though it was only 6.3% of the total sediment (dry weight). Again, 79.4% of the mercury was associated with the wood chips fraction of the "10 ppm" sample.

The relative amounts of mercury in the different sediment components (relative to sand) were also calculated and are shown in Fig. 25. This presumably means that fines and wood chip fractions have higher sorption capacities than sands for all mercury concentrations. For the 0.1 ppm mercury concentration, sorption capacities of fines and wood chips were 99 and 43 times higher, respectively, than that for sands.

4.2.2 Cation Exchange Capacity

Sediment is known to affect the chemical composition of stream waters in various ways. Some minerals will dissolve, some may cause precipitation of certain dissolved ions, and others, because of their exchange capacity, may help stabilize the composition of stream water (29). The study presented in this particular section was carried out to obtain information about variation of exchange capacity with size and type of sediment particles.

The cation exchange capacities of different fraction sizes in the bed sediments are presented in Tables 2 and 3. Capacity was determined using both cesium (monovalent ions) and mercury (divalent

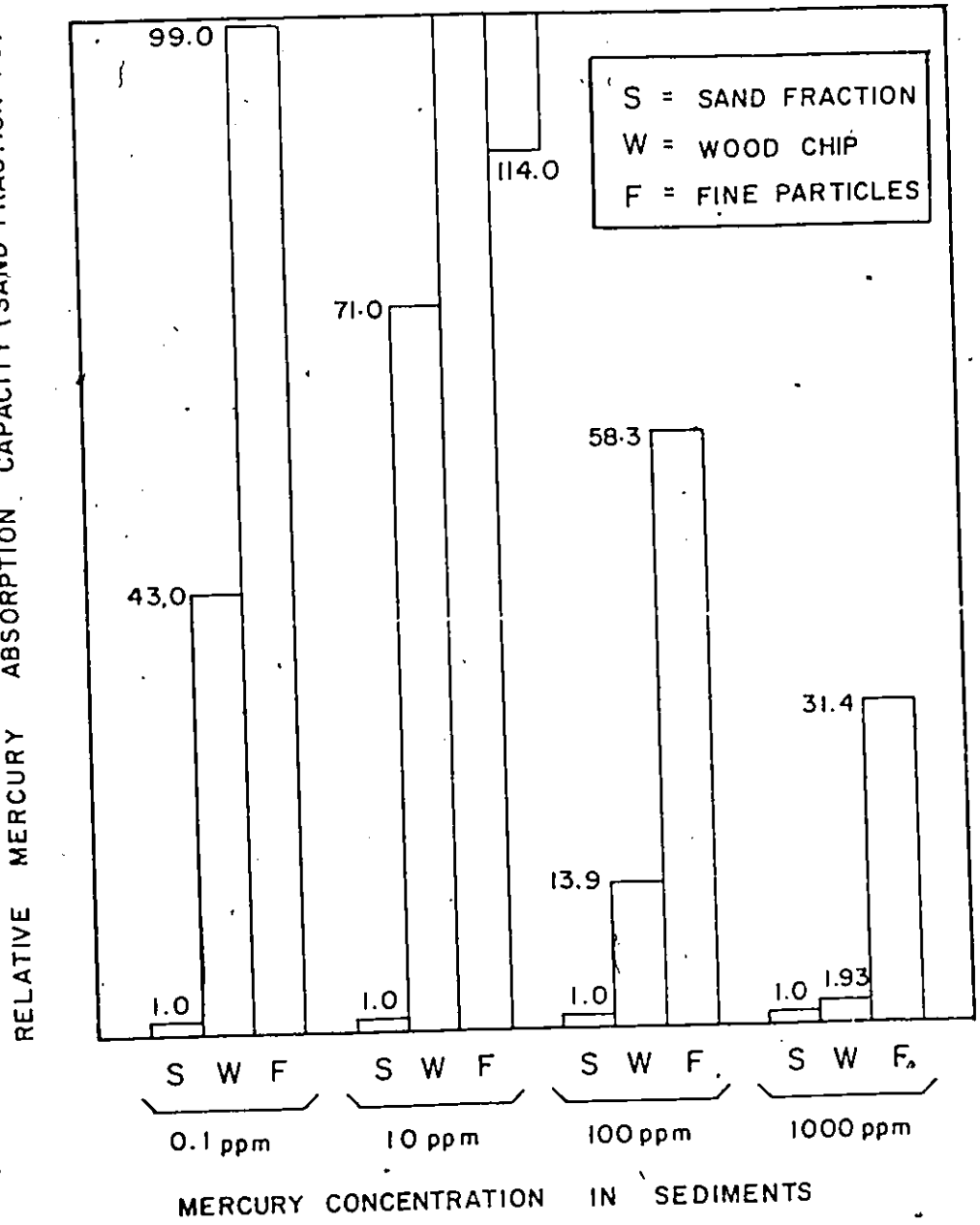

Fig. 25. - Relative mercury sorption capacity of different fractions of "woodchip" sediment

Table 2. - Cation Exchange Capacity (sand sediment)

Particle Diameter μm	Ion Exchange Capacity meq/100 gm	
	Cesium Method	Mercury Method
840	0.54	0.39
590	0.64	0.75
420	1.92	1.76
246	0.51	0.43
177	0.42	0.29
149	0.45	0.61
106	0.56	0.42
75	2.61	2.98
53	6.04	14.85
38	9.05	22.00
<38	13.91	43.00

Table 3. - Cation Exchange Capacity ("Woodchip" sediment)

Particle Diameter μm	Ion Exchange Capacity meq/100 gm Cesium Method	Mercury Method	Remarks
840	24.70	57.0	Wood chips, bark
590	14.75	32.15	wood chips
420	12.20	22.60	fine wood chips
246	13.30	9.74	very fine wood chips
177	0.92	1.44	fine sand
149	0.63	0.96	fine sand
106	0.73	0.96	very fine sand
75	1.27	1.57	very fine sand
53	2.70	3.38	coarse silt
38	5.20	8.88	coarse silt mud
<38	12.20	26.45	very fine fraction (clay,silt,etc.)

ions). Figures 26 and 27 show the variation of ion exchange capacity with particle size. It was found that the exchange capacity increases as the grain size decreases. The higher exchange capacities are characteristic of samples containing high proportions of montmorillonite and/or vermiculite (29). The ion exchange capacities of both sand sediment and "woodchip" sediment were somewhat higher for mercury than with cesium as can be seen from the tables.

For the sand sediment, the ion exchange capacities of the sand particle fraction ranged from 0.54 to 2.61 meq per 100 grams (cesium) and 0.39 to 4.98 meq per 100 gram (mercury). For the silt fraction (less than 75 μm), the values ranged from 6.09 to 9.05 meq per 100 grams (cesium) and 19.85 to 22.00 meq per 100 grams (mercury). For the fine fraction (less than 38 μm), the exchange capacity was found to be much higher. The values obtained were 13.91 meq per 100 grams (cesium) and 43.00 meq per 100 grams (mercury).

In the case of the "woodchip" sediment, the ion exchange capacity of the sand particle fraction ranged from 0.92 to 1.27 meq per 100 grams (cesium) and 0.96 to 1.57 meq per 100 grams (mercury). For the silt type fraction the values ranged from 2.70 to 5.20 meq per 100 grams (cesium) and 3.38 to 8.88 meq per 100 grams (mercury); and for the fine fraction (less than 38 μm), the values obtained were 12.20 meq per 100 grams (cesium) and 26.45 per 100 grams (mercury). The exchange capacities of the wood chip fraction in the "woodchip" sediment were also determined. The values ranged from 13.30 to 24.70 meq per 100 grams (cesium) and 9.74 to 57.0 meq per 100 grams (mercury). The higher values are characteristic for the organic materials. All the weights mentioned above are dry weights.

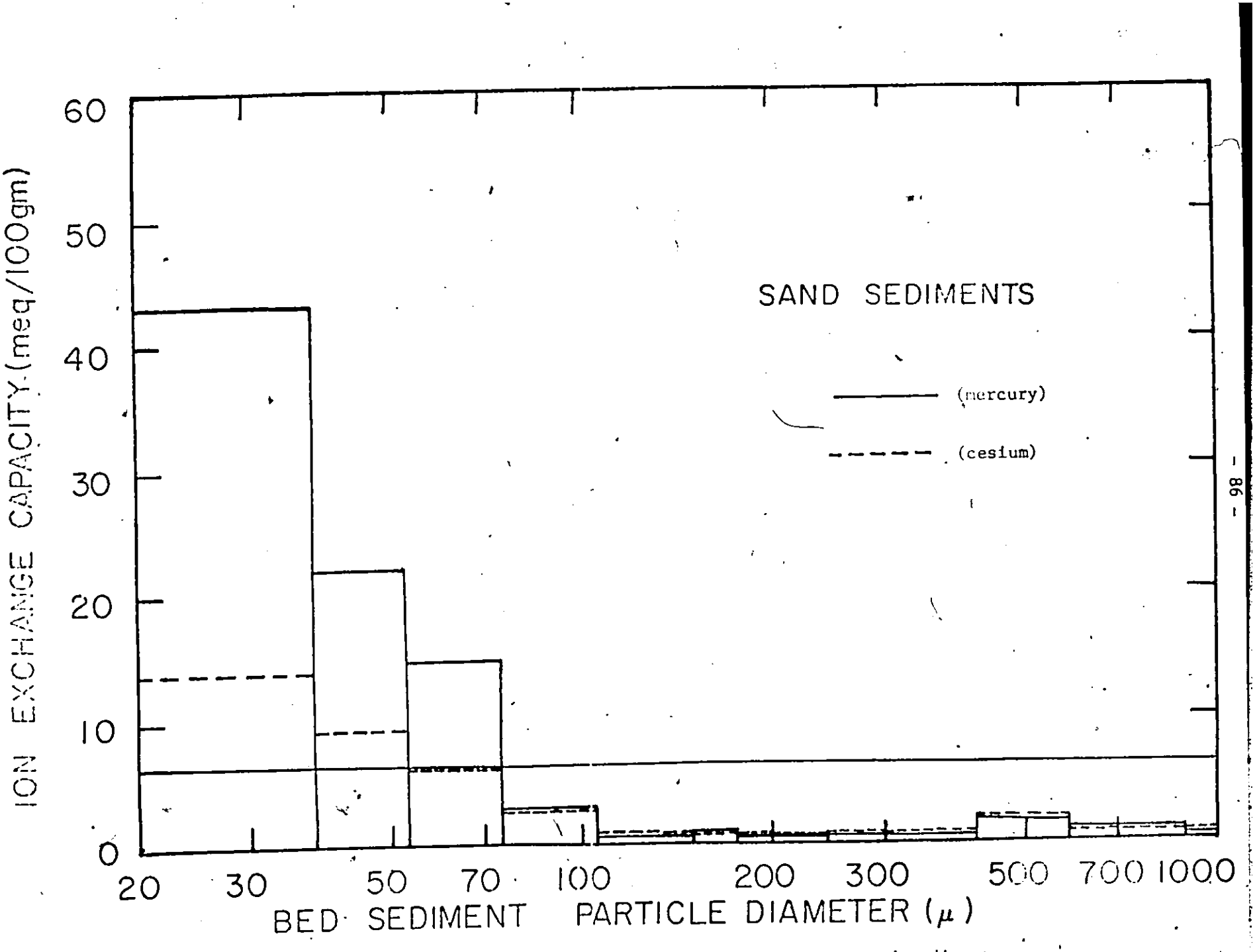

Fig. 26. - Cation exchange capacities of different fractions of sand sediments

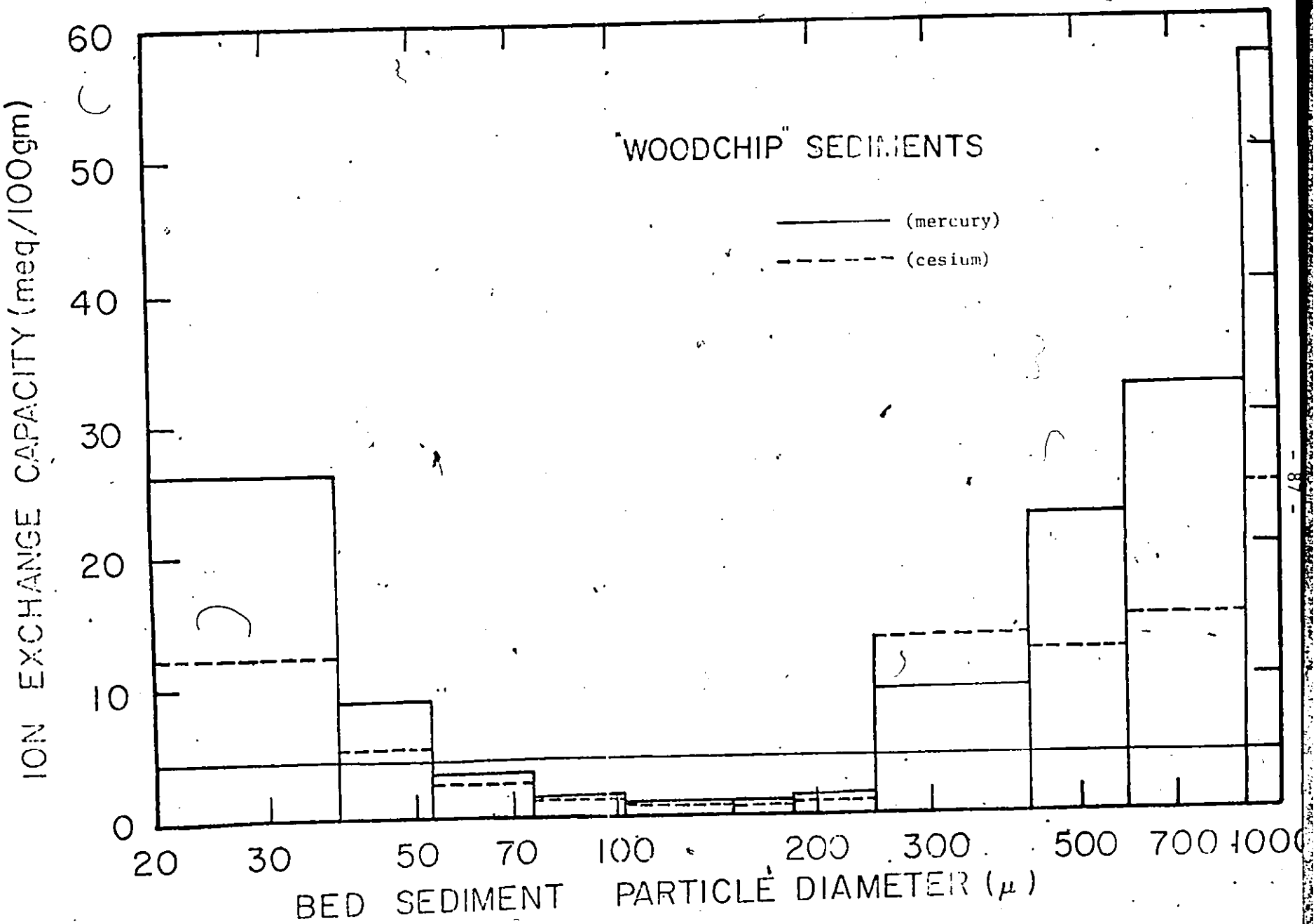

Fig. 27. - Cation exchange capacities of different fractions of "[illegible]" sediments

This information concerning the range of exchange capacities for different sizes and types of sedimentary material is useful in estimating the uptake (sorption) by sediments of ions dissolved in stream water. For example, stream sediments having a high exchange capacity can generally be expected to remove more ions than those having a low exchange capacity. Another use for information on exchange capacity is in estimating the proportion of industrial waste which may be carried adsorbed on the sediment fractions, (as compared to the proportion remaining in solution).

4.3 Study of the Interaction between Flowing Water and Bed Sediments using a Laboratory Model

In this section, the results of the following two studies are presented.

1) Transport of mercury associated with bed sediments during bedload movement, and

2) Flow parameters (velocity, boundary shear stress) at incipient motion of bed sediment particles.

4.3.1 Transport of Mercury Associated with Bed Sediments during Bedload Movement

Two types of bed sediments, "sand" sediment (d_{50} = 280 μm) from the main channel and "woodchip" sediment (d_{50} = 180 μm) from the CIP channel, were used in this study. Each sediment sample was subjected to two different hydraulic conditions: (1) mean velocity = 20 cm/sec, corresponding to an average flow rate = 3.2 ℓ/sec;

(2) mean velocity = 30 cm/sec, corresponding to an average flow rate = 4.7 ℓ/sec.

The samples were placed in the 1.22 m test section of the experimental flume and a "source" volume (5 cm long x 30 cm wide x 1 cm deep) was contaminated with mercuric chloride labelled with ^{203}Hg to produce a total mercury concentration of 1.00 ppm. The contaminated volume was incubated at 21°C for one month to simulate "field" conditions before being placed in the test section sample. Table 4 shows the specific activity of mercury in the contaminated sediments used in each of the experiments.

The counts indicated in Table 4 made it possible to detect the transport of mercury within an acceptable accuracy range from outside the flume (i.e., without causing disturbance to the water and bed sediment movements).

Figures 28 and 29 show the mercury levels (in percent) associated with bed sediments at the contaminated location (source) in the test section at different times for different flow conditions. Table 5 shows the amount of mercury (in percent relative to the original amount) which remained at the source location just before the end of each run.

The results in Table 5 indicate that the transportability of "woodchip" sediment (and the contaminants bound to this material) is much higher than the sand sediment for the same flow conditions.

Figures 30, 31, 32 and 33 show the relative mercury concentration in the bed at various locations downstream from the source for each test run. These figures indicate the movement of mercury

Table 4. - Specific Activity of Mercury (Labelled with Hg-203) in the Contaminated Sediments at the Source

Run No	Flow Condition (velocity cm/sec)	Specific Activity		Type of Sediment
		* Ncpm per gram	** Øcpm per 150 cm^2	
1	20	25,738	71,366	sand
2	30	128,666	258,763	sand
3	20	103,915	211,432	"woodchip"
4	30	103,915	211,432	"woodchip"

*Ncpm = Nuclear counter per minute

**Øcpm = Ortec count per minute

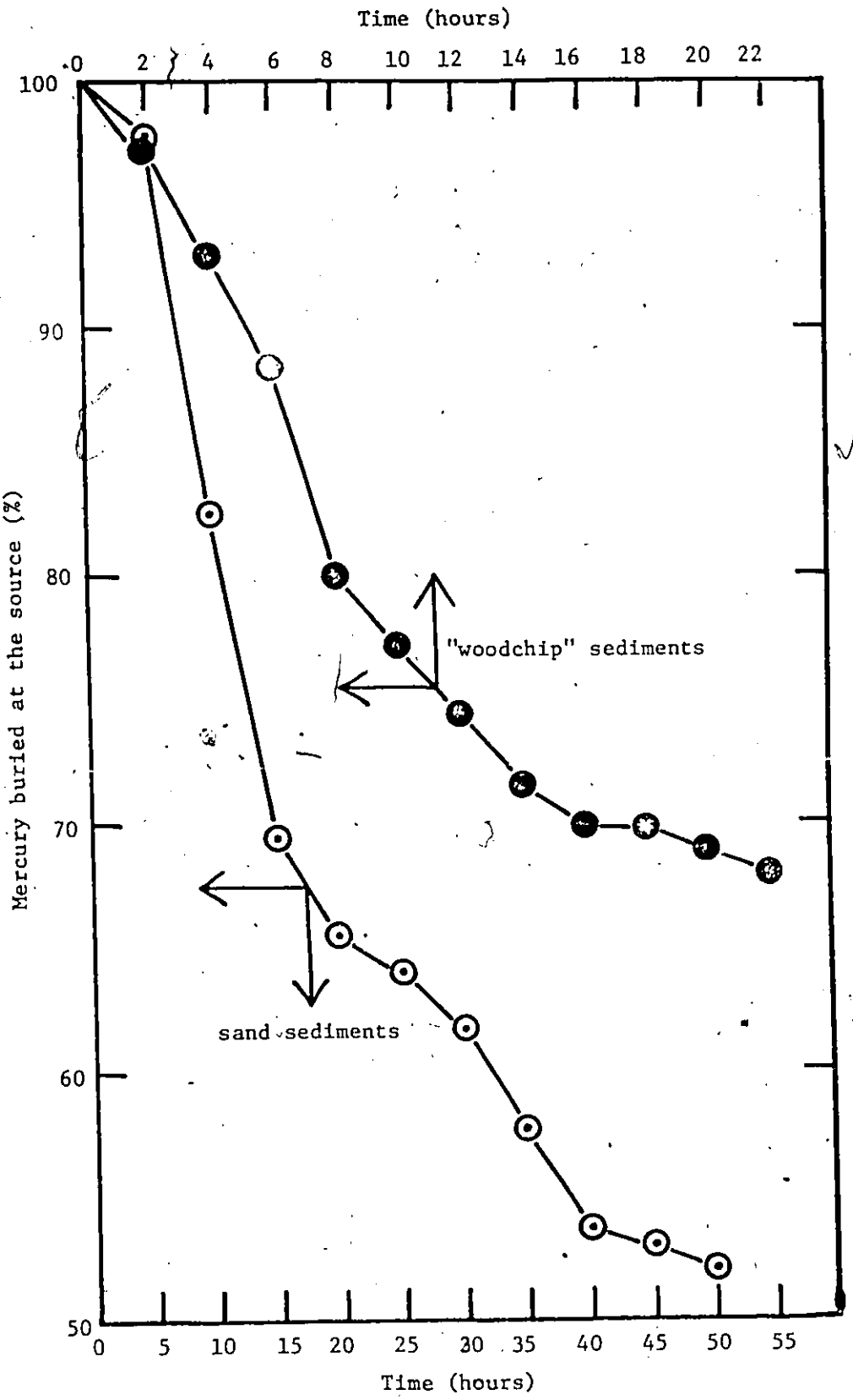

Fig. 28. - Amounts of mercury remaining at original location (source). Runs 1 and 3

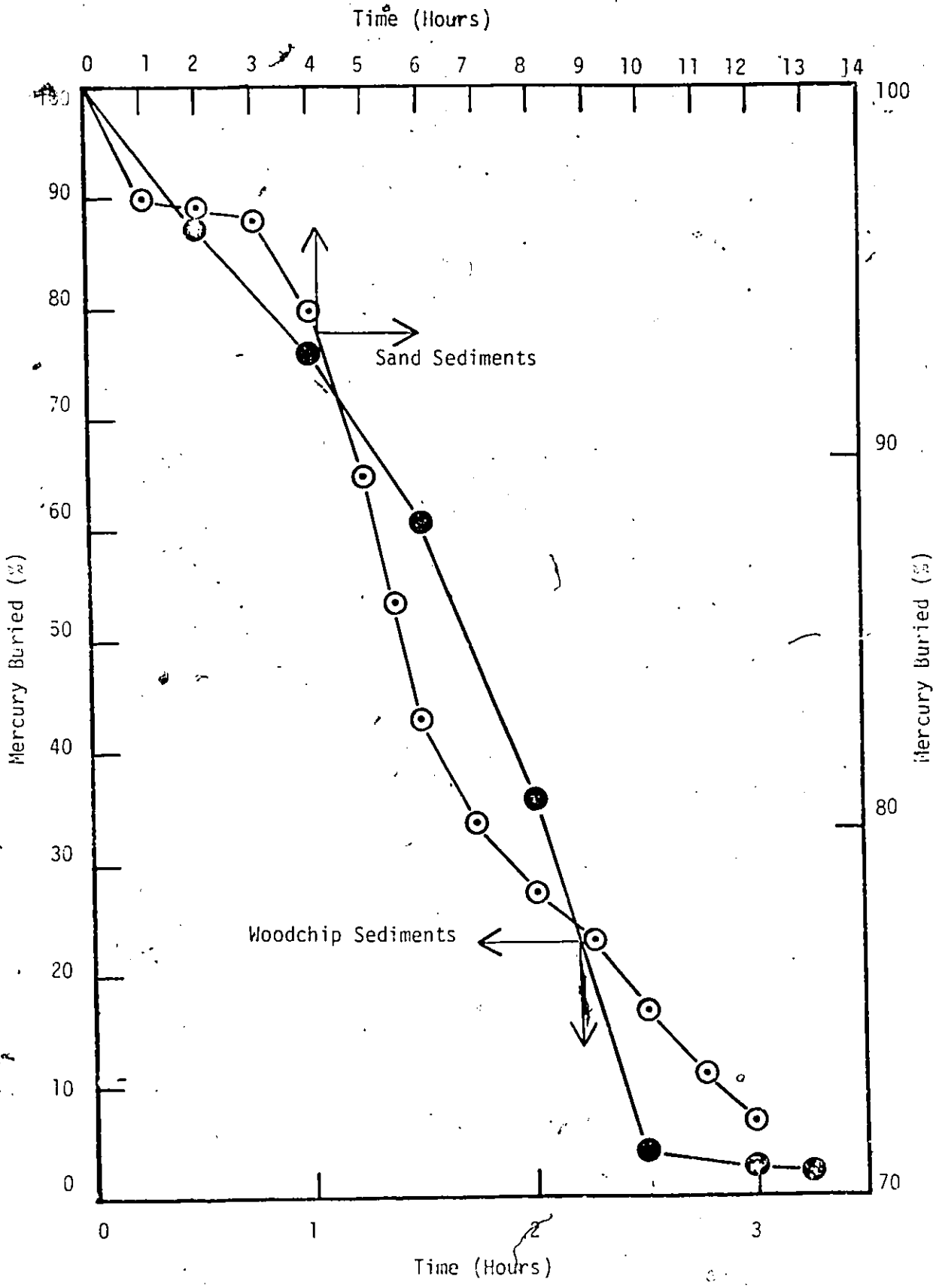

Fig. 29. Amounts of Mercury Remaining at Original Location (source) (Runs 2 and 4)

Table 5. - Mercury Level (in percent) at the Source just Before the End of Each Run

Run No	Time of Run hrs	Mercury Level at the Source (in percent)	Rate of Sediment Transport (kg/hr)
1	50	51.9	0.117
2	12	71.36	0.923
3	22	67.9	0.971
4	3-1/2	2	2

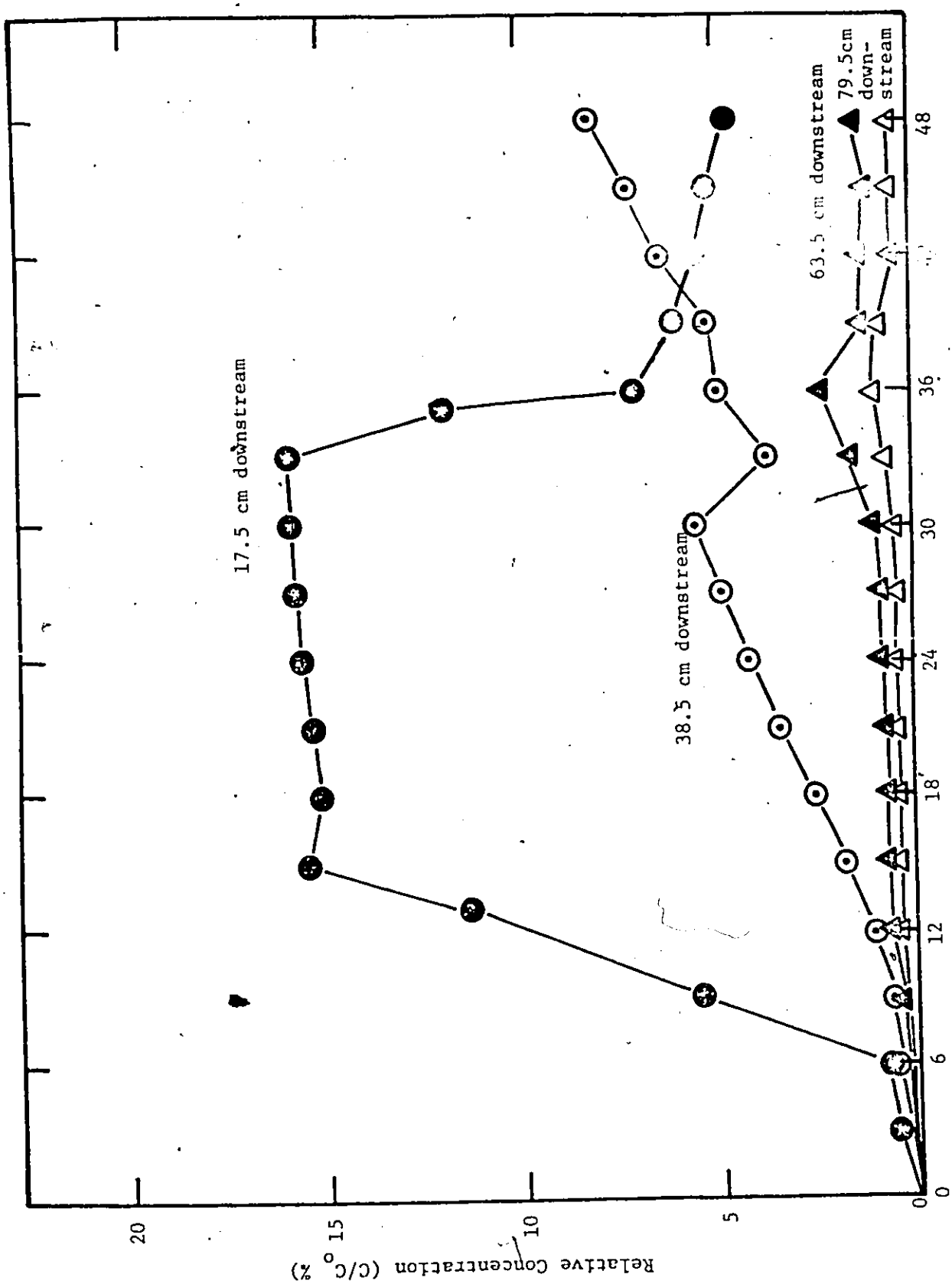

Fig. 30. - Mercury concentrations in bed sediments at various locations downstream from source (Run 1)

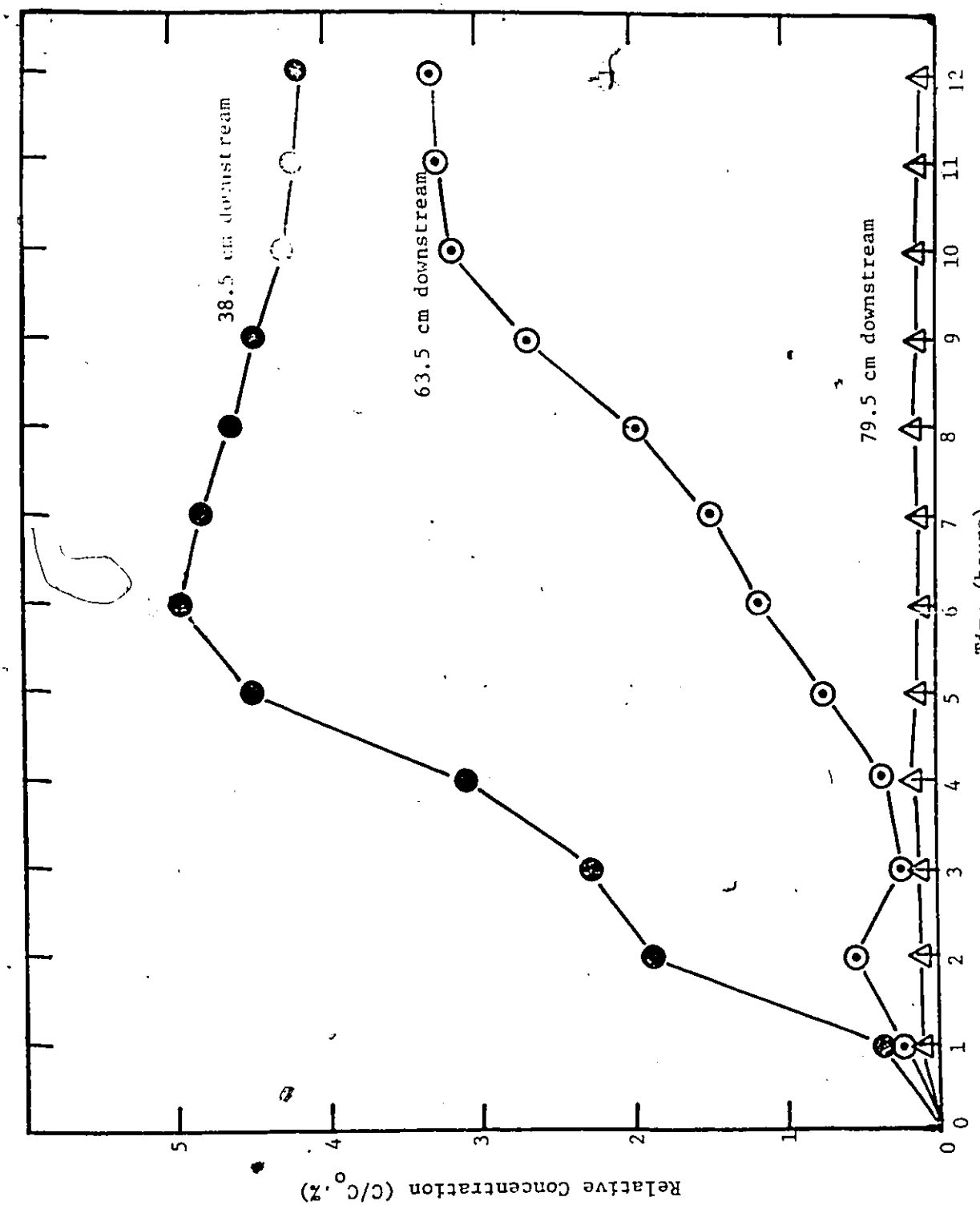

Fig. 31. - Mercury concentrations in bed sediments at various locations downstream from source (Run 2)

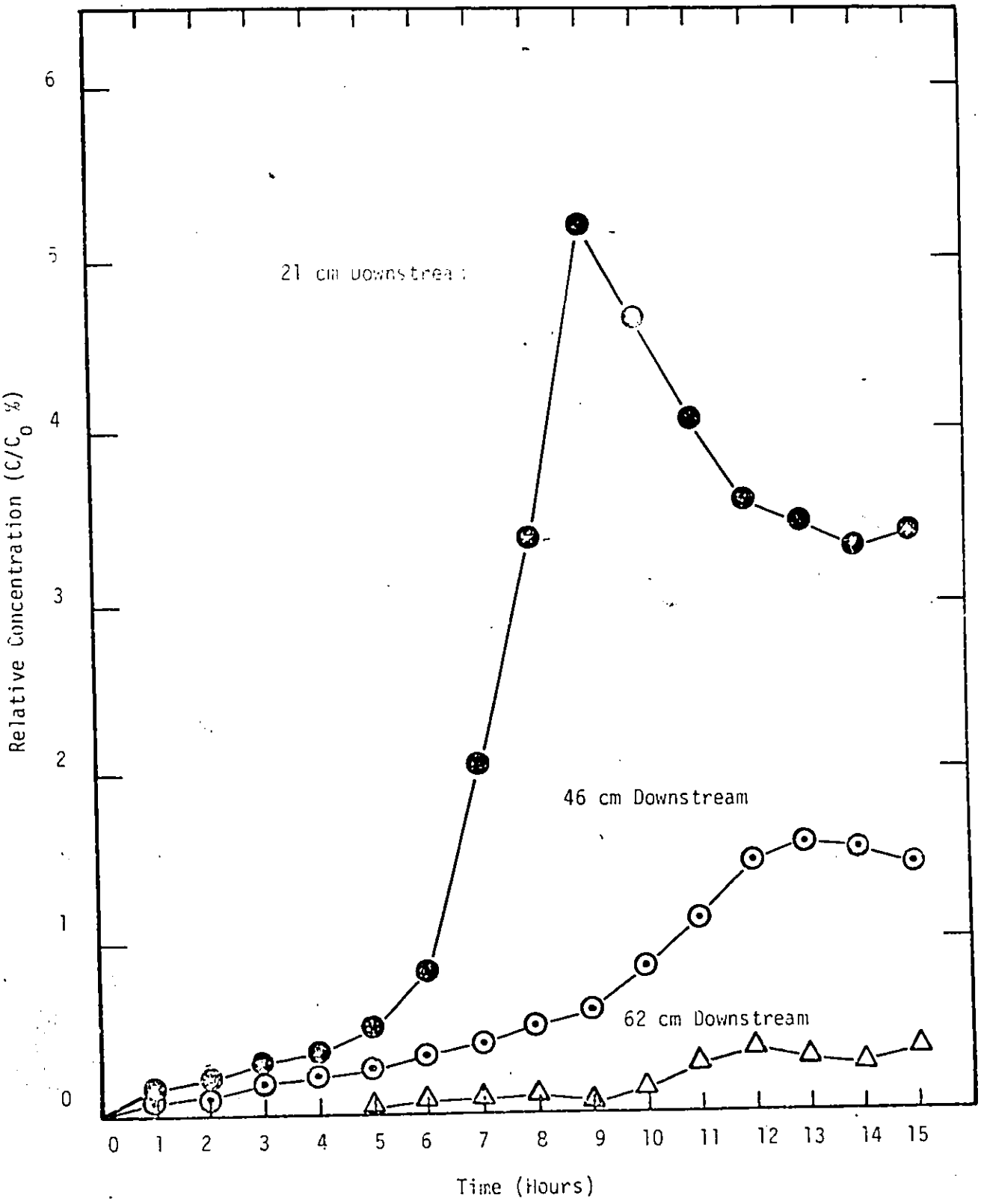

Fig. 32. Mercury Concentrations in Bed Sediments at Various Locations (Run 3)

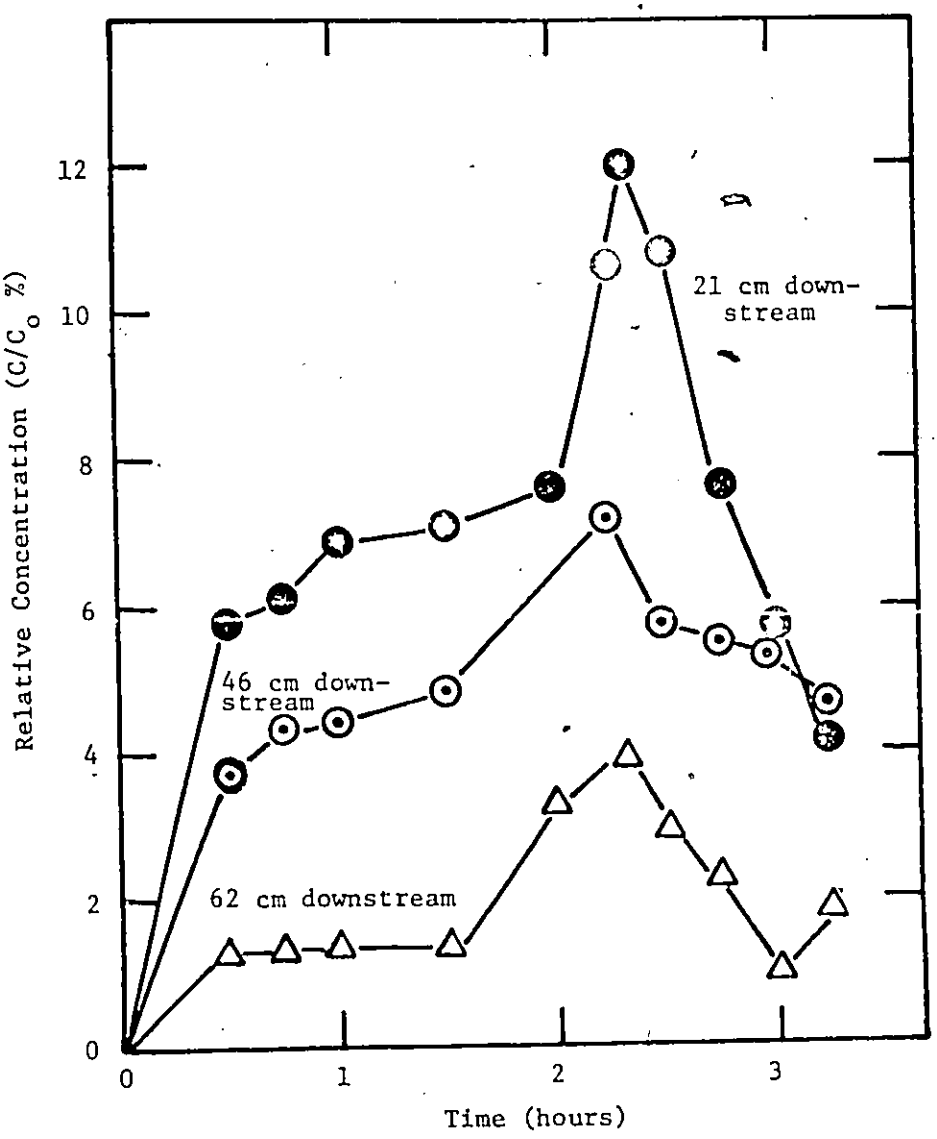

Fig. 33. - Mercury concentration in bed sediments at various locations downstream from source (Run 4)

downstream from the source with time due to bedload movement. The average velocity of mercury transport associated with bed sediment movements was evaluated for each run. A relationship between mean water velocity and mercury velocity is shown in Fig. 34. A significant difference in velocity of mercury transport associated with bed sediments was obtained between the "woodchip" and sand sediments. For a mean water velocity of 30 cm/sec, mercury attached to "woodchip" sediments moved downstream at a velocity of 36 cm/hr compared to 2.5 cm/hr for sand sediments. In other words, mercury associated with "woodchip" sediment was transported 14 times faster than that with sand sediment, (for a mean water velocity of 30 cm/sec). The difference in velocity of mercury transport between the two sediments decreased with a decrease of mean water velocity. At a water velocity of 20 cm/sec, the speed of mercury transport became 1.7 cm/hr for "woodchip" sediment and 0.68 cm/hr for sand sediment.

With a decrease of mean water velocity a considerable decrease in velocity of total mercury transport was also observed. For the sand sediment, only 0.4% of mercury was moved downstream during a 2-hour experiment (at a water velocity of 10 cm/sec). Most of the movement was considered to be due to the initial disturbance of the sediment. In other words, at this velocity no mercury transport was noticed.

A comparison of the data reported by Hubbel and Sayre (24), for the North Loup River study in Nebraska, was made. They placed 18.1 kg of tracer particles labelled with 40 millicuries of Iridium-192 on the bed sediment (median diameter 290 μm). For an average water discharge of 7.36 m^3/sec mean depth 0.76 m and bed slope 0.00083, they measured the velocity of the iridium-traced sediment as 91 cm/hr at a

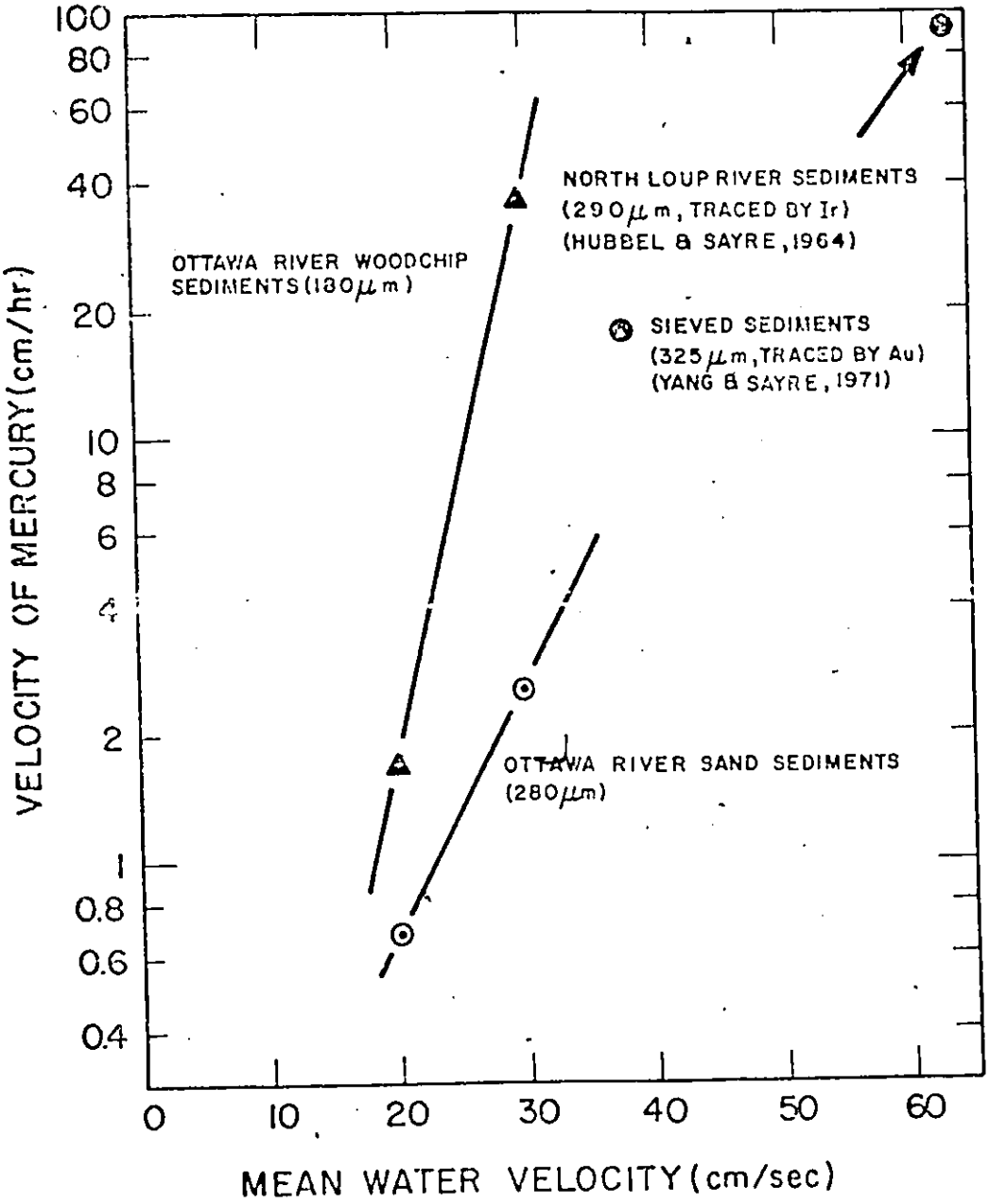

Fig. 34. - Velocity of mercury associated with bed sediments

mean water velocity of 63.5 cm/sec. Another comparison was made with the experimental data presented by Yang and Sayre (72). They used a recirculating flume 18.28 m long, 0.61 m wide and 0.76 m deep. The size and amount of tracers used were 325 μm (labelled with gold-198), and 1600 grams respectively. The activity of the tracers were 260 micro-curies. They found that for a water surface slope of 0.088×10^{2}, water discharge of 32 ℓ/sec, normal depth of 15.8 cm, and velocity of water, 38 cm/sec, the velocity of tracer sediment was 17.8 cm/hr. These results, plotted on the same figure (Fig. 34) agree reasonably well with the data obtained in this laboratory study.

Figure 35 shows the typical movement of "woodchip" bed sediment downstream from the test section during Run 4. Figures 36 and 37 show the bed formation and sampling locations in the test section after Runs 2 and 4. Figures 38 and 39 show the distribution of mercury in the test section downstream from the "source" after Runs 2 and 4.

Mass balance of mercury, for "woodchip" and sand sediments, was obtained during Runs 2 and 4. The results are presented in Tables 6 and 7. These results are also plotted in Figures 40 and 41. In both experiments no rapid desorption of mercury from bed sediments into flowing water was observed during the initial period of interaction between uncontaminated flowing water and contaminated bed sediments. However, suspended load contained a significant portion of mercury when bed sediment transport was vigorous as observed in Run 4. After 3.5 hours (Run 4) for "woodchip" bed sediments, the bedload and suspended load carried 35.9% and 20.3% of total mercury introduced, respectively, 15.7% was transported by water itself, which recycled the flume 61 times in the same time period. At

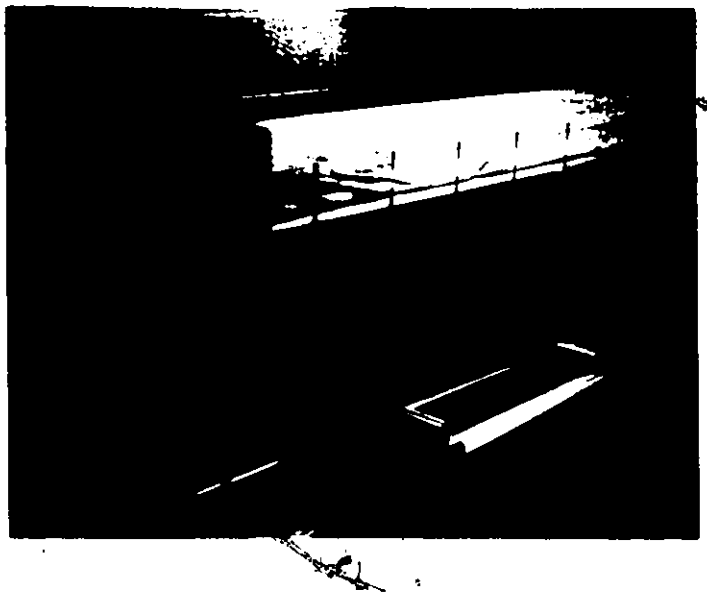

Fig. 35. - Typical bed sediment movement (Run 4)

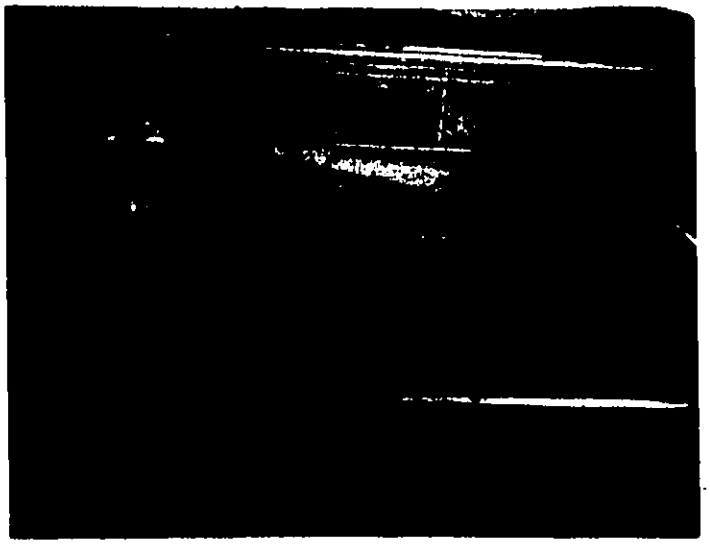

Fig. 36. - Typical bed formation after the Run (Run 2)

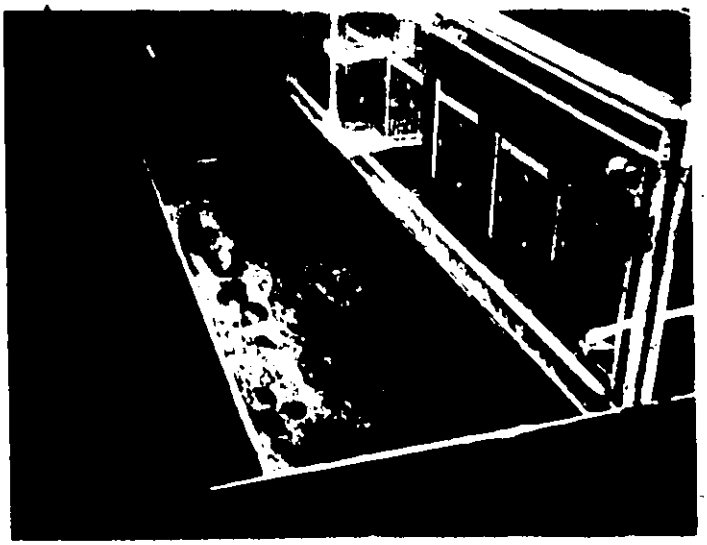

Fig. 37. - Typical bed formation after the Run (Run 4)
Also showing the sampling done after the run

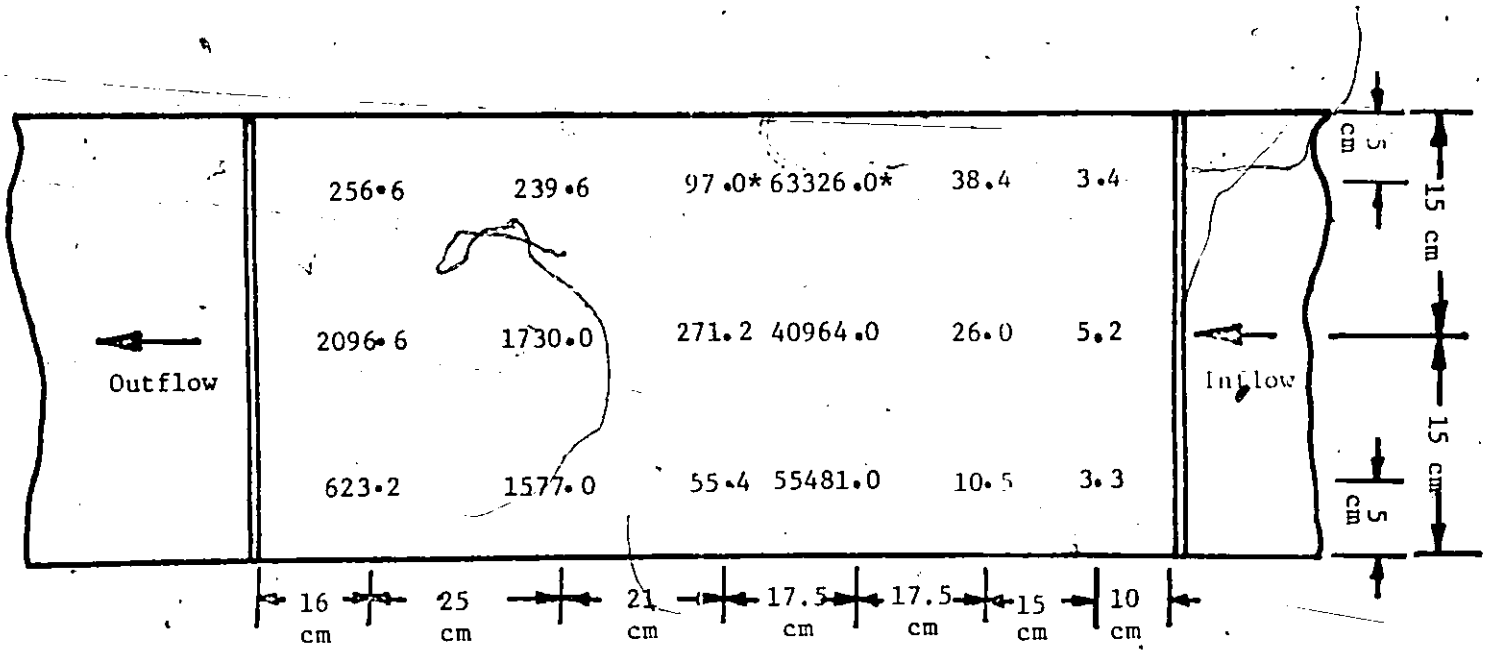

*NCPm/g = Nuclear count per minute per gram

Fig. 38. - Mercury distribution in bed sediments (NCPm/g) after Run 2

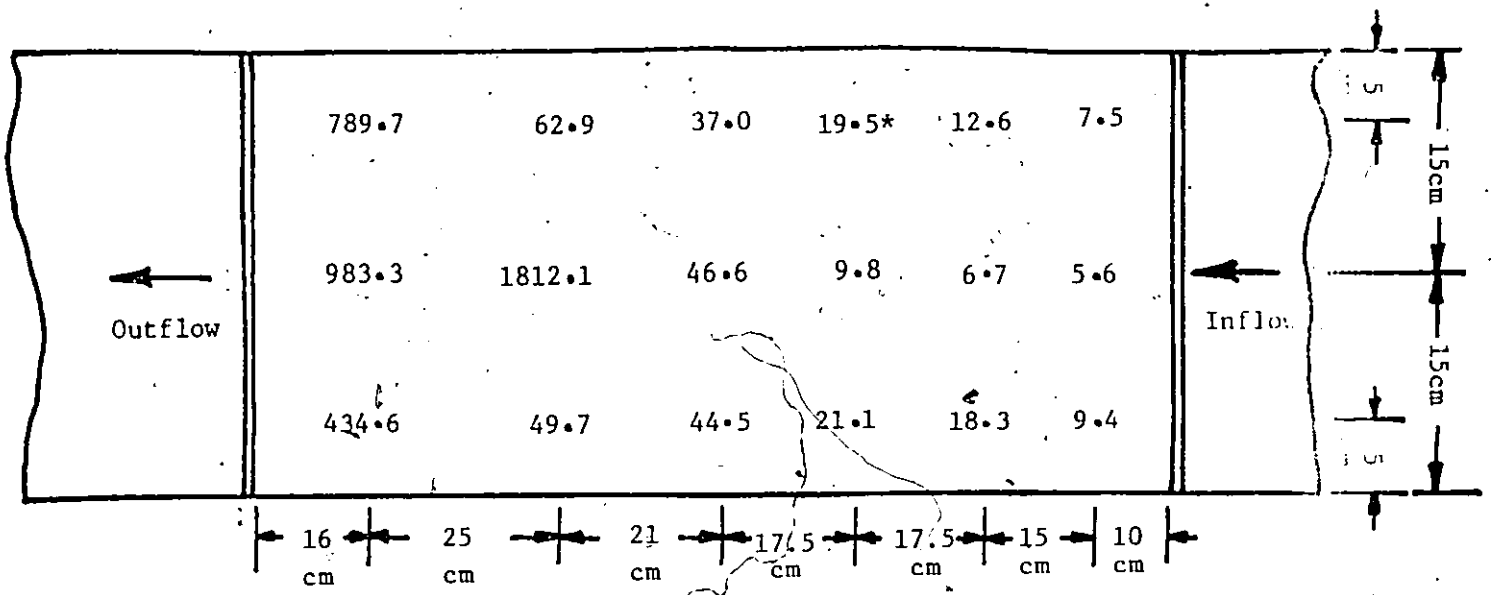

*NCPm/g = Nuclear count per minute per gram

Fig. 39. - Mercury distribution in bed sediments (NCPm/g) after Run 4

Table 6. - Mass Balance of Mercury (Run 2)

Time hrs	2	3	4	5	6	7	8	9	10	11	12
Water and suspended load %	1.33	2.49	2.97	3.31	3.64	3.90	4.15	4.21	4.24	4.29	4.31
Bedload %	0.57	0.86	1.14	1.43	1.71	2.00	2.28	2.57	2.86	3.14	3.43
In the bed sediment downstream from source %	2.09	3.24	2.54	4.58	7.60	8.53	8.61	8.35	10.19	10.94	11.36
In the source %	96.57	96.43	94.0	89.57	82.90	80.11	78.25	77.01	75.10	73.38	72.18
Attached with walls and unknown %	-0.56	-3.02	-0.65	1.11	4.15	5.46	6.71	7.86	7.61	8.25	8.72
Total %	100	100	100	100	100	100	100	100	100	100	100

Table 7. - Mass Balance of Mercury (Run 4)

Time hrs	1	2	3	3-1/2
Water %	7	8	13	15.7
Suspended load %	8	23	23	20.3
Bedload %	2.58	11.72	32.14	35.9
In the bed sediment downstream from "source" %	5.16	13.08	14.50	11.20
In the "source" %	76.2	35.4	2.46	2
Attached to walls and unknown %	1.06	8.8	14.9	14.9
Total %	100	100	100	100

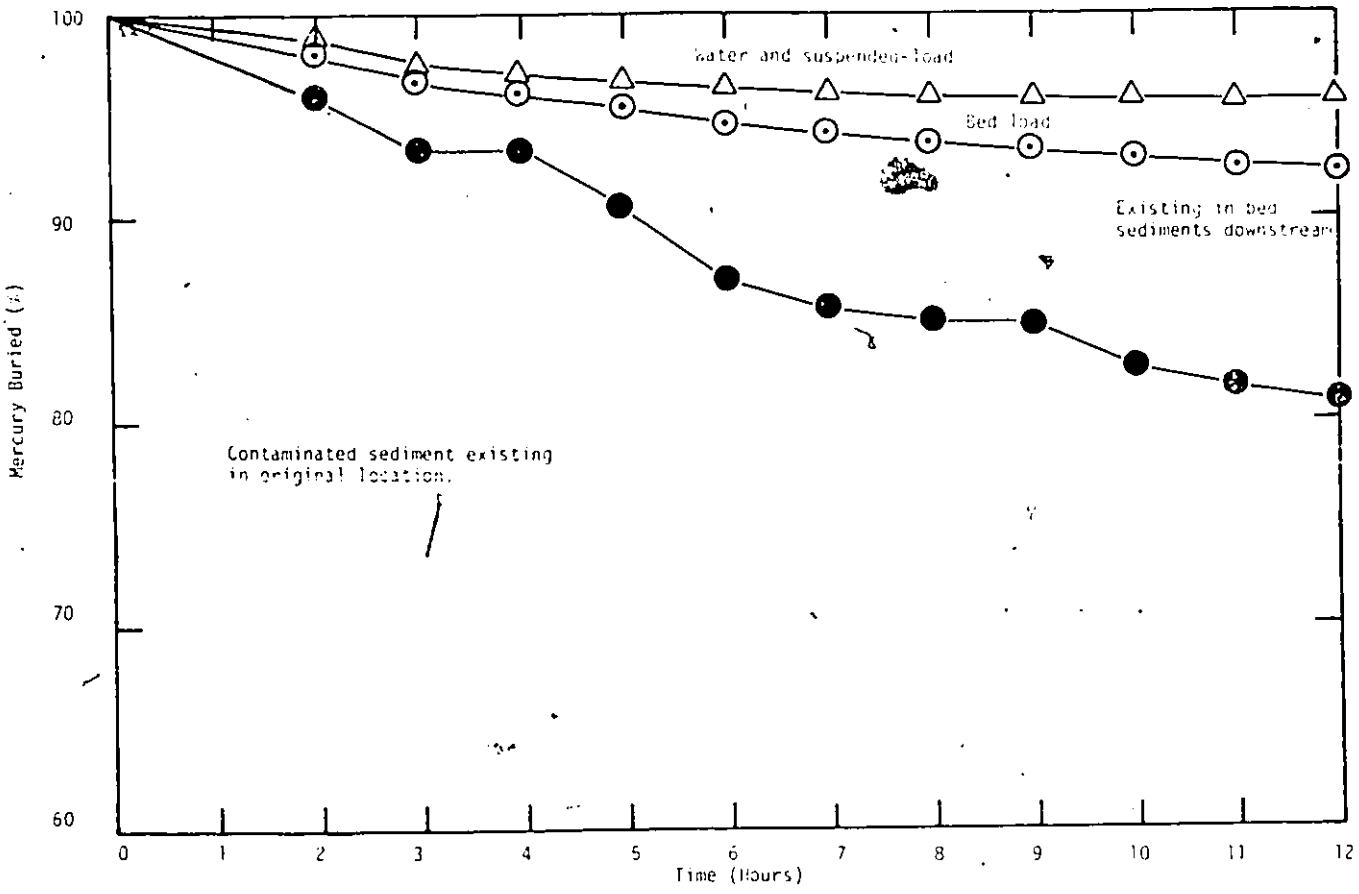

Fig. 40. - Mass balance of mercury associated with sand sediments (Run 2)

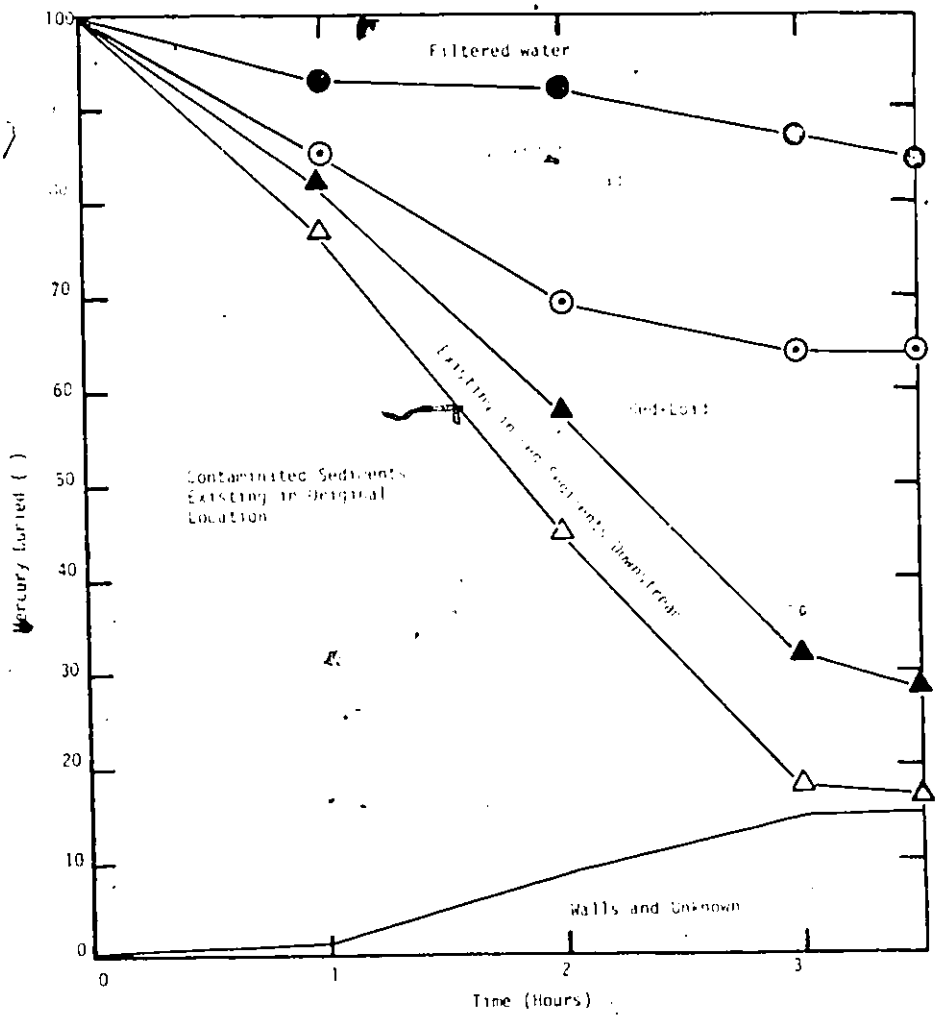

Fig. 41. - Mass balance of mercury associated with "woodchip" sediments (Run 4).

this point in time only 2.0% of mercury remained at the source. Also, 11.2% of mercury introduced into the system was in the bed sediments up to 62 cm downstream from the source. The amount of mercury attached to the walls (and unknown) was estimated to be 14.9%. This value can be considered reasonable on the basis of previous work (47).

These results indicated that 84.3% of mercury was still associated with the solid phase after 3.5 hours of interaction with flowing water and most of the mercury was transported downstream attached to sediment particles being moved. The average sediment transport rate for this Run (Run 4) was 2 kg/hr per 30.48 cm (per ft) width of the flume with a water flow rate of 4.7 ℓ/sec through the flume.

In the case of sand sediment (Run 2) most of the mercury remained in the source volume because of the sand's lower transportability compared to woodchip sediment. After 12 hours, mercury in suspension was 4.31%, in the bed sediment downstream from the source the percentage was 11.36%, in the bed load it was calculated as 3.43%, whereas 72.18% of mercury remained at the source. The average bed sediment transport rate for this Run (Run 2) was 0.923 kg/hr per 30.48 cm width of the flume with a mean water flow rate of 4.7 ℓ/sec.

4.3.2 Flow Parameters (velocities, boundary shear stresses) at Incipient Motion of Bed Sediment Particles

Critical values of velocities and boundary shear stresses, for both "woodchip" sediment and sand sediments, were determined for the conditions of weak and general movements of the sediment particles. It was observed that the transport characteristics of wood chip particles were entirely different from those of sand particles. The wood chip particles, once lifted by water from the bed, travelled downstream a few cm above the bed sediment surface in suspension. This unique movement of wood chip particles can be explained by their low specific gravity compared to that of sand particles. In this study the critical values of velocities and boundary shear stresses were determined for the medium sand sediment (d_{50} = 280 μm) of the main channel and fine sand sediment fraction of the "woodchip" sediment (d_{50} = 180 μm) from the CIP channel.

Figures 42 and 43 show the dimensionless velocity distribution near the bed at which two types of movements (weak and general) occurred in the case of "woodchip" sediments. Weak and general movements of the sediment particles were observed for mean water velocities of 18 cm/sec and 23.33 cm/sec, respectively. The corresponding average flow rates were 2.9 ℓ/sec and 3.6 ℓ/sec. The average critical velocities near the bed for these conditions were 12.71 cm/sec and 17.6 cm/sec respectively.

The average critical boundary shear stresses computed for the above two flow conditions (presented in Tables 8 and 9 in

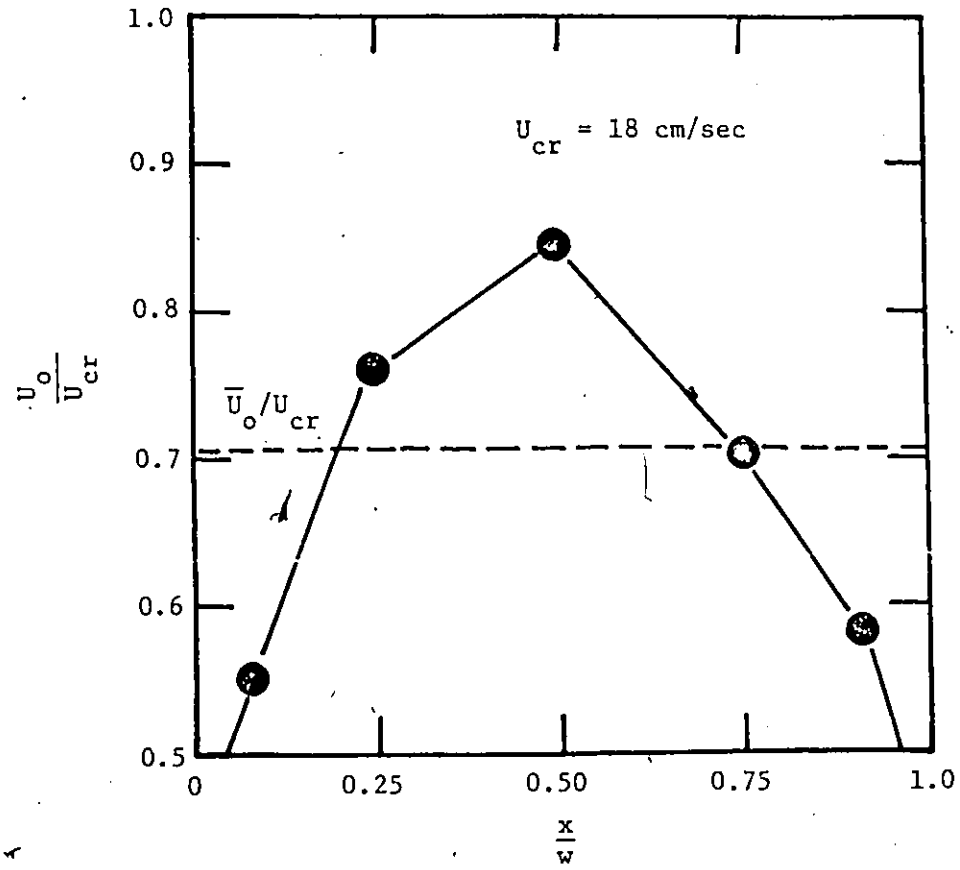

Fig. 42. - Dimensionless velocity distribution near the bed (weak movement) in the case of "woodchip" bed sediment.

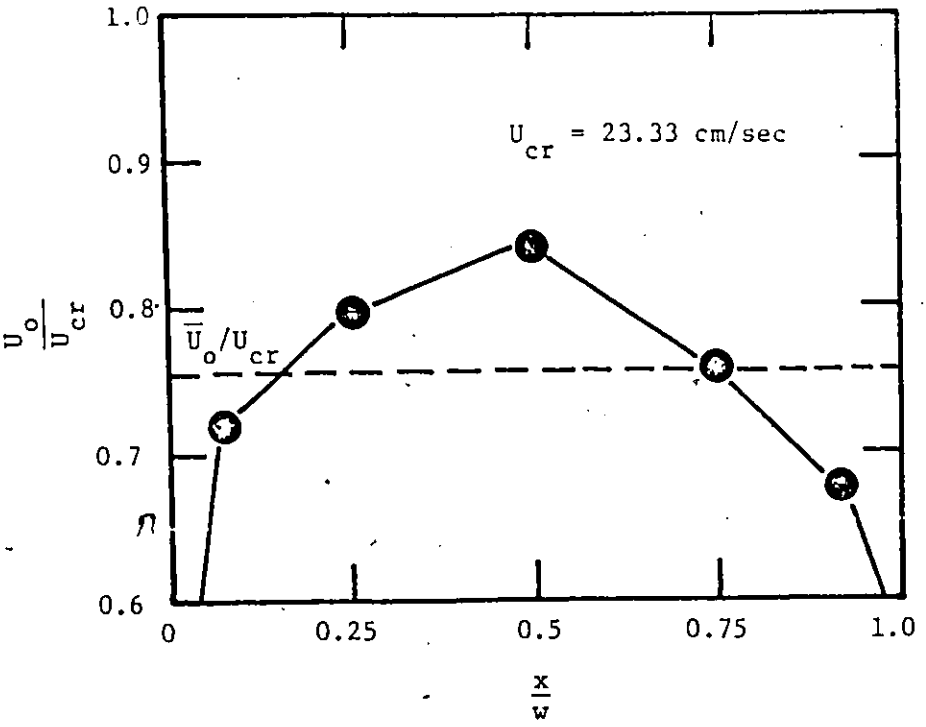

Fig. 43. - Dimensionless velocity distribution near the bed (general movement) in the case of "woodchip" bed sediment

Appendix B) were 1.59×10^{-5} N/cm^2 and 2.32×10^{-5} N/cm^2 respectively. Figures 44 and 45 show the dimensionless critical boundary shear stress distributions near the bed for the above flow conditions.

In the case of sand sediment, weak movement of sediment particles occurred at a mean water velocity of 20 cm/sec (mean flow rate = 3.2 ℓ/sec). The average velocity near the bed was 14.91 cm/sec. However, general movement of the sediment particles was observed for mean water velocity of 25 cm/sec and corresponding mean flow rate of 3.8 ℓ/sec). The average velocity near the bed for the later condition was 18.78 cm/sec. Figure 46 shows the dimensionless velocity distribution near the bed for weak movement and Fig. 47 shows the dimensionless velocity distribution for the general movement conditions.

The average critical boundary shear stresses computed for the above two flow conditions (presented in Tables 10 and 11 in Appendix B) were 1.92×10^{-5} N/cm^2, and 2.49×10^{-5} N/cm^2 respectively. Figures 48 and 49 show the dimensionless critical boundary stress distributions near the bed for these conditions respectively.

The experimental results of the critical values of velocities thus obtained were compared with the data presented by Yang as shown in Fig. 11, p. 47 . It was found that these plots lie in the range of "hydraulically smooth" and "transition regime" conditions of the bed.

Critical values of boundary shear stresses for both "woodchip" and "sand" sediments were calculated using the method described on

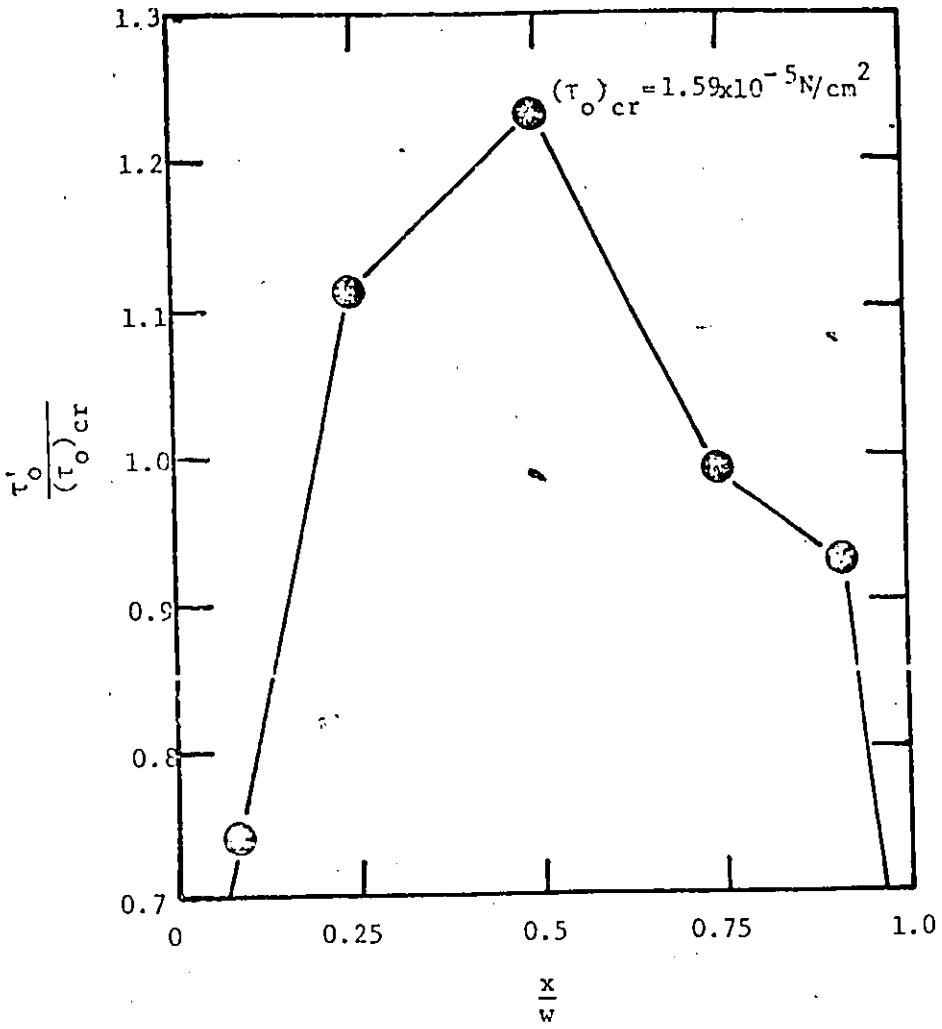

Fig. 44. – Dimensionless boundary shear stress distribution (weak movement) in the case of "woodchip" bed sediment

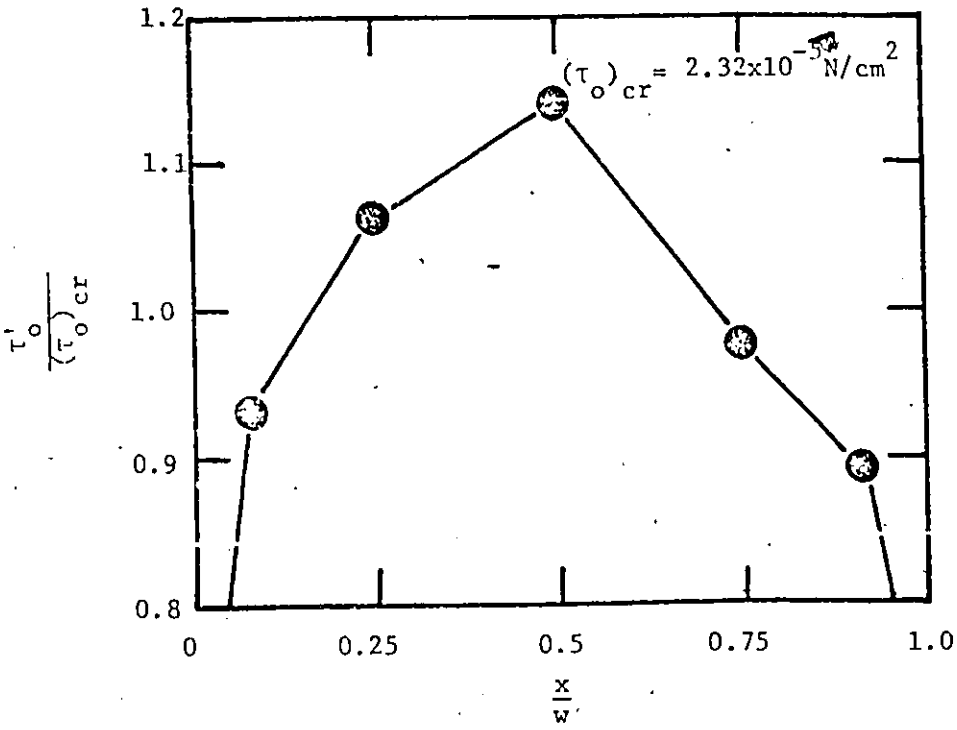

Fig. 45. - Dimensionless boundary shear stress distribution (general movement) in the case of "woodchip" bed sediments.

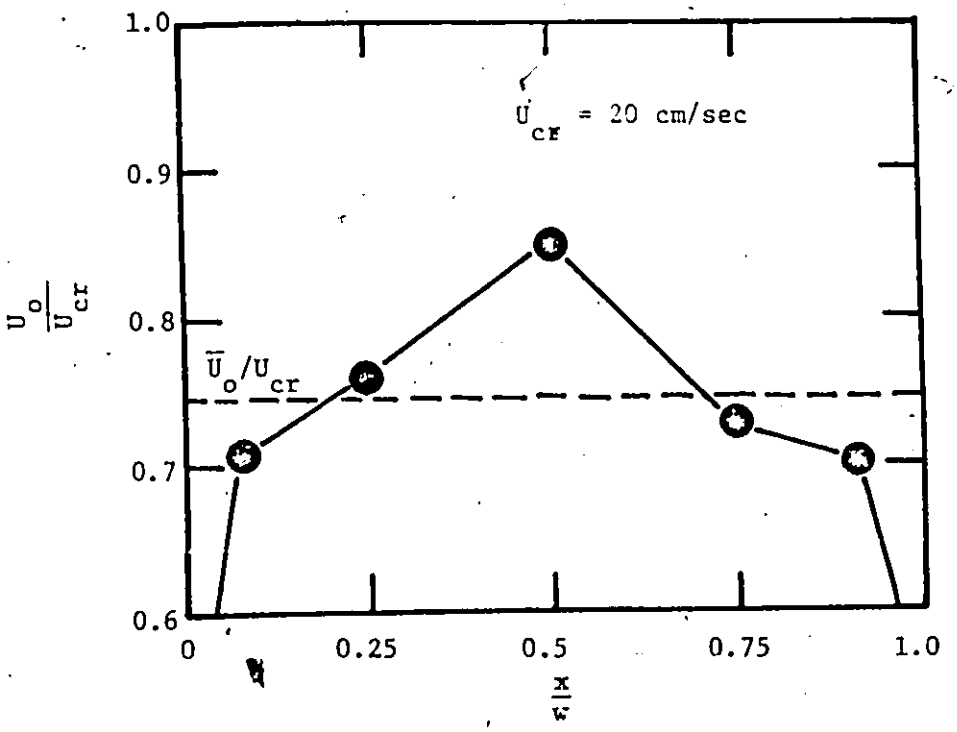

Fig. 46. - Dimensionless velocity distribution near the bed (weak movement) in the case of sand sediment

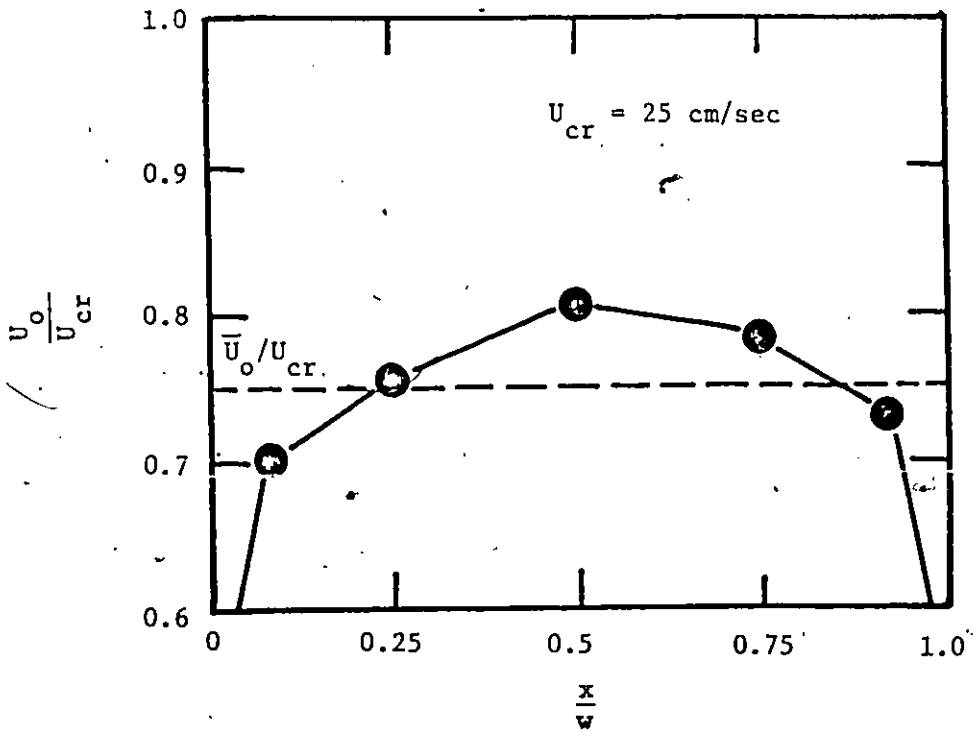

Fig. 47. - Dimensionless velocity distribution near the bed (general movement) in the case of sand sediment

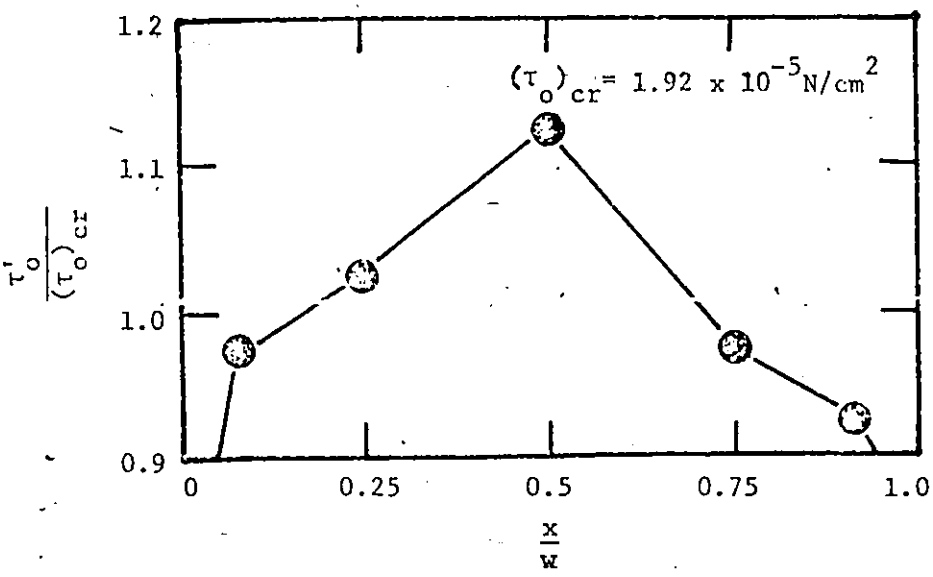

Fig. 48. - Dimensionless boundary shear stress distribution (weak movement) in the case of sand bed sediment

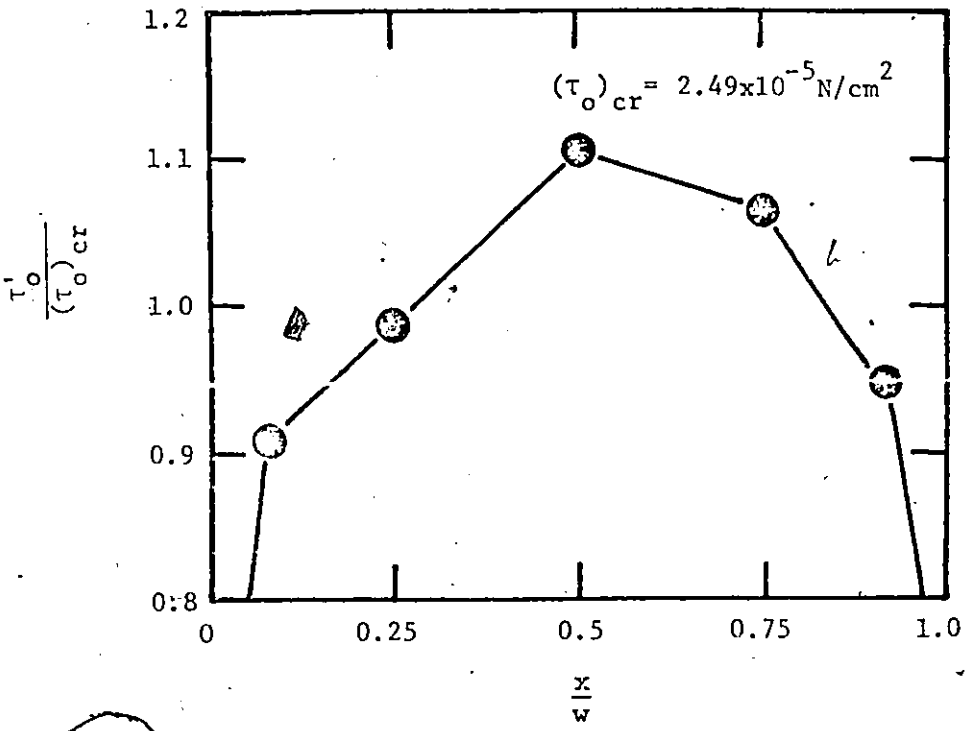

Fig. 49. - Dimensionless boundary shear stress distribution (general movement) in the case of sand bed sediment

page 48. They were found to be 1.66×10^{-5} N/cm^2 and 1.82×10^{-5} N/cm^2 respectively. The experimental results were also plotted on the Shield's diagram (Fig. 12, p.49). As shown these points lie very close to the Shields' curve.

CHAPTER 5

CONCLUSIONS AND RECOMMENDATIONS

5.1 Conclusions

1. Distribution of predominant sediment types along the reach has been obtained in this study. The main channel consists of mainly medium sand (median diameter 280 μm), whereas, near the Ontario bank, the bed material is stiff cohesive clay. On the northern side of Kettle Island in the small Canadian International Paper Company (CIP) channel, the sediment is a complex mixture of fine sand, wood fibres, wood chips and barks. This type of sediment has been classified as "woodchip" sediment, due to the presence of high proportions (up to 100%) of this organic-type material. The median size of the sand component of this particular sediment is 180 μm.

2. Mercury in the Ottawa River is almost completely (>97%) associated with the bed sediments. However, field values vary widely depending on the location and time of the year.

Laboratory studies on the mercury sorption capacity by the bed sediments indicated that the mercury distribution among the various components of the sediment leads to predictions of mercury concentrations which closely resemble observed field values. Sediment components of high organic content, more particularly the wood chips, fibres, barks and very fine clay sized fraction, have associated with them 50 to 100 times the amount of mercury associated with sand particles. The results emphasize the importance of particle type analysis in studies of pollutant transport by bed sediment movement.

3. Cation exchange capacity (CEC) was determined for the different fractions of bed sediments existing in the Ottawa River. In general, it was found that the cation exchange capacity is a function of both size and type of material (mineralogical composition). For the sand fraction, (size ranging from 75 μm to 840 μm), the CEC ranged from 3 to 0.4 meq per 100 grams (dry weight). For the silt sized fraction the CEC ranged from 3 to 22 meq per 100 grams. The cation exchange capacity for the fine fraction (d_{50} less than 38 μm) was found to be higher (i.e., ranging from 12 to 43 meq per 100 grams). In the case of organic materials (wood chips), the exchange capacity was also found to be higher. An exchange capacity ranging from 10 to 54 meq per 100 grams was obtained, depending on the type and size of the materials.

The above information on the range of exchange capacity is useful in estimating the uptake by sediments of ions dissolved in stream water. Stream sediments, having high exchange capacity, are generally expected to remove more ions than those having low exchange capacity. Furthermore, information on exchange capacity is essential in estimating the proportion of industrial waste which may be carried adsorbed on sediment, as compared to that in solution.

4. The laboratory flume studies on interaction between flowing water and bed sediments indicated the importance of understanding, more fully, the complex sediment transport processes in natural water courses in any attempt to assess the exchange rates of pollutants, such as mercury, across the sediment/water interface and mass transport of same along rivers and streams. The following conclusions are based on the results of the flume studies:

a) Mercury, initially introduced to the dynamic system through a small control volume of bed sediment, was transported downstream predominantly by the sediment particles being moved by the water. No rapid desorption of mercury, from bed sediments to the uncontaminated flowing water, was observed. However, mercury concentration in the water increased gradually with time and mass movement of the bed sediment.

b) Movements of sediment particles increased gradually with increasing stream velocity and general movement of the particles was observed throughout the stream bed.

c) Velocity of mercury associated with bed sediment movements was found to be a function of type of sediment as well as mean water velocity. For woodchip sediments, the mercury velocities were 1.7 cm/hr and 36 cm/hr, for mean water velocities of 20 cm/sec and 30 cm/sec, respectively. In the case of sand sediments, the mercury velocities were 0.68 cm/hr and 2.5 cm/hr for mean water velocities of 20 cm/sec and 30 cm/sec, respectively.

d) The mass balance chart, resulting from this investigation, indicates that the component exhibiting the maximum percentage of contamination, under dynamic conditions similar to those in the prototype system, is the bed sediment component. Over 80 percent of mercury originally contained in the bed sediment at the source was transported attached to bed sediment particles being moved downstream.

e) Critical values of velocities and boundary shear stresses also depend on the type of sediment and flow condition. For "woodchip"

sediment, the critical velocities found ranged from 18 cm/sec to 23.33 cm/sec. Corresponding critical boundary shear stresses ranged from 1.59×10^{-5} N/cm^2 to 2.32×10^{-5} N/cm^2. In the case of sand sediment, the critical velocities ranged from 20 cm/sec to 25 cm/sec. Corresponding critical boundary shear stresses ranged from 1.92×10^{-5} N/cm^2 to 2.49×10^{-5} N/cm^2. These values of boundary shear stresses appear to agree quite well with predictions given by the Shields' curve (Fig. 12).

5.2 Recommendations for Further Research

The following studies are recommended as extensions to the present work:

1. Since a major portion of the pollutant (mercury) is attached to the bed sediment in the study section of the Ottawa River, accurate field measurements of the rate of bed sediment movement under different flow conditions should be performed. These measured field values can then be compared with existing bedload formulas developed by various researchers, with a view to developing a modified formula to predict pollutant transport associated with bed load movement.

2. Measurement of velocities near the bed sediment/water interface should be made in the prototype system for a comprehensive range of stream flows. This data is necessary to reproduce the desired boundary layer characteristics in the small-scale laboratory model for further investigations of the interaction between flowing water, bed sediments, and pollutant kinetics.

3. The transport characteristics associated with "wood-chip" and clay type sediments require detailed study.

4. Since turbulence plays a predominant role in the sediment (and pollutant) transport process in rivers, the lack of suitable instrumentation to measure this phenomena has seriously affected major research efforts in this field of research. For example, the use of the hot-film anemometry technique is limited to systems using very clean fluids because of the contamination problem and the

presence of a probe, in the fluid field, inevitably distorts the turbulent structure under investigation.

The recent development of the Doppler anemometry technique should encourage new research on the structure of turbulence near the sediment water interface and its effect on sediment (and pollutant) transport phenomena in rivers and streams.

REFERENCES

1. Armstrong, F.A.J., and Hamilton, A.L., Pathways of Mercury in a Polluted Northwestern Ontario Lake, Singer, P.C. (ed.). Trace Metals and Metal-Organic Interactions in Natural Waters, Ann Arbor Science Publishers Inc., Michigan, 1973.

2. Axelsson, V. and Hakanson, L., The Relation between Mercury Distribution and Sedimentological in Lake Ekoln, Report No. 14, Uppsala University, Sweden, 1972.

3. Beetem, W.A., Janzer, V.J., and Wahlberg, J.S., Use of Cesium-137 in the Determination of Cation Exchange Capacity, U.S. Geological Survey Professional Paper 1140-B, 1962, pp.1-8.

4. Bongers, L.H., and Khattak, M.N., Sand and Gravel overlay for Control of Mercury Sediments, U.S. Environmental Protection Agency Publication, No. 16080, HVA, 1972.

5. Bowles, J.E., Engineering Properties of Soils and their Measurement, McGraw-Hill Book Co., Inc., New York, 1970.

6. Brydon, J.E., and Patry, L.M., Mineralogy of Champlain Sea Sediments and a Rideau Clay Soil Profile, Canadian Journal of Soil Science, 41, 1961, pp.169-181.

7. Chakrabarti, S.K., Discussion of Incipient Motion and Sediment Transport by Chih Ted Yang, Journal of the Hydraulics Division, ASCE, Vol. , No. HY , May, 1974, pp.

8. Colby, B.R., Discharge of Sands and Mean Velocity Relationships in Sand-Bed Streams, U.S. Geological Survey Professional Paper 462-A, Washington, D.C., 1964.

9. Colby, B.R., Practical Computation of Bed-Material Discharge, Journal of the Hydraulics Division, ASCE, Vol. 90, No. HY2, March, 1964, pp.217-246.

10. Cooper, R.H., and Peterson, A.W., Discussion paper, Journal of the Hydraulics Division, ASCE, Vol. 96, No. HY9, Sept., 1970, pp.1880-1886.

11. Cranston, R.E., and Buckley, D.E., Mercury Pathways in a River and Estuary, Environmental Science and Technology, Vol. 6, No. 3, 1972, pp.274-278.

12. Crickmore, M.J., and Lean, G.H., The Measurement of Sand Transport by Means of Radioactive Tracers. Proceedings, Royal Society, London, England, Series A, 226, 1962, pp.402-421.

13. DeGroot, A.J., Contents and Behaviour of Mercury as Compared with Other Heavy Metals in Sediments from the Rivers Rhine and Ems, Institute for Soil Fertility, Haven (Gr.), Netherlands.

14. D'Itri, F.M., (ed.), Environmental Mercury Problem, Institute of Water Research, Michigan State University, E. Lansing, 1971.

15. Einstein, H.A., The Bed-Load Function for Sediment Transportation in Open Channels, U.S. Department of Agriculture, Soil Conservation Service, Technical Bulletin, 1026, Washington, D.C., 1950.

16. Gavis, J., and Ferguson, J.S., The Cycling of Mercury Through the Environment, Water Research, Vol. 6, 1972, pp.989-1008.

17. Gessler, J., Beginning and Ceasing of Sediment Motion, Shen, H.W. (ed.), River Mechanics, Vol. 1, Fort Collins, Colorado.

18. Gilbert, K.G., The Transportation of Debris by Running Water, U.S. Geological Survey Professional Paper 86, 1914.

19. Graf, W.H., Hydraulics of Sediment Transport, McGraw-Hill, New York, 1971.

20. Grdenic, D., and Tunell, G., Mercury, Wedephol. K.H., (ed.), Handbook of Geochemistry, Vol. II/2, 1970.

21. Hart, J.S., (ed.), Distribution and Transport of Persistent Chemicals in Flowing Water Ecosystems. Interim Report No. 1, Ottawa River Project, National Research Council of Canada, Ottawa, 1973.

22. Henderson, F.M., Open Channel Flow, The Macmillan Company, New York, [illegible]6.

23. Herdan, G., Small Particle Statistics, Elsevier Publishing Company, New York, 1966.

24. Hubbell, D.W., and Sayre, W.W., Sand Transport Studies with Radioactive Tracers, Journal of the Hydraulics Division, ASCE, Vol. 90, No. HY3, May, 1964, pp.39-68.

25. Jenne, E.A., Mercury in the Environment, Atmospheric and Fluvial Transport of Mercury, U.S. Geological Survey Professional Paper 713, 1970.

26. Jensen, S., and Jernelov, A., Biological Methylation of Mercury in Aquatic Organisms, Nature, 223, 1969, pp.753-754.

27. Jonassen, I.R., and Boyle, R.W., Geochemistry of Mercury, in Watkin, J.E., (ed.), Mercury in Man's Environment, Royal Society Of Canada, Ottawa, 1971.

28. Kartha, V.C., and Leutheusser, H.J., Distribution of Tractive Force in Open Channels, Journal of the Hydraulics Division, ASCE, Vol. 96, No. HY7, July, 1970, pp.1469-1482.

29. Kennedy, V.C., Mineralogy and Cation Exchange Capacity of Sediments from Selected Streams, U.S. Geological Survey Professional Paper 433-D, 1965.

30. Krenkel, P., Report from International Conference on Environmental Mercury Contamination, Water Research, Vol. 5, 1971, pp.1121-1122.

31. Krenkel, P., Reimers, R.S., and Burrows, W.D., Mechanism of Mercury Transformation in Bottom Sediments, Part I, Final Report, Technical Report No. 31, Vanderbilt University, Nashville, Tenn., 1973.

32. Krenkel, P.A., Burrows, W.D., Shih, E.B., Taimi, K.I., and McMullen, E.D., Mechanism of Mercury Transformation in Bottom Sediments, Part II, Final Report, Technical Report No. 32, Vanderbilt University, Nashville, Tenn., 1973.

33. Krishnamurthy, M., Discussion Paper, Journal of the Hydraulics Division, May 1974.

34. Kudo, A., and Gloyna, E.F., Radioactivity Transport in Water ....., Interaction between Flowing Water and Bed Sediments, Technical Report to U.S. Atomic Energy Commission, Contract AT-(11-1)-490, 1969.

35. Kudo, A., and Gloyna, E.F., Transport of ^{137}Cs, Interaction with Bed Sediments, Water Research, Vol. 5, 1971, pp.71-79.

36. Kudo, A., and Hart, J. Uptake of Inorganic Mercury by Bed Sediments, Journal of Environmental Quality, Vol. 3, No. 3, 1974, pp.273-278.

37. Kudo, A., Mortimer, D.C., and Hart, J.S., Factors Influencing Desorption of Mercury from Bed Sediments, Canadian Journal of Earth Sciences, 1975.

38. Lee, R.A., Investigation of Mercury in Washington State, Dept. of Ecology, State of Washington, Olympia, Jan. 1971.

39. Lofroth, G., Methylmercury, Ecological Research Committee, Bull. No. 4, Swedish Natural Science Research Council, Sweden, 1969.

40. Matida, Y., and Kumada, H., Distribution of Mercury in Water, Bottom Mud and Aquatic Organisms in Japan, Bull. 19, Freshwater Fish Research Lab., Japan, 1969.

41. Mercury in the California Environment, Calif. State Health Dept., Environmental Health and Consumer Protection Program, Berkeley, June 1970 - July 1971.

42. Meyer-Peter, E., Favre, H., and Einstein, A., Neueve Versuchsresultate Uber den Geschiebetrieb, Schweiz, Bauzeitung, Vol. 103, No. 13, 1934.

43. Meyer-Peter, E., and Muller, R., Formulas for Bed-Load Transport, Report on Second Meeting of International Association for Hydraulic Research, Stockholm, 1948, pp.39-64.

44. Miller, D.R., (ed.), Distribution and Transport of Pollutants in Flowing Water Ecosystems, Interim Report No. 2, Ottawa River Project, Division of Biological Sciences, National Research Council of Canada, Ottawa, 1974.

45. Minamata.Disease Study Group, Minamata Disease, Kumamoto University, Kumamoto, Japan, 1969.

46. Morris, H.M., Applied Hydraulics in Engineering, The Ronald Press, Company, New York, 1963.

47. Mortimer, D.C., and Kudo, A., Interaction between Aquatic Plants and Bed Sediments in Mercury Uptake from Flowing Water, Journal of Environmental Quality, 1975.

48. Neill, C.R., A Re-Examination of the Beginning of Movement for Coarse Granular Bed Materials, Hydraulics Research Station, Int. 68, June 1968.

49. Norstrom, R.J. and Peter, D., Chemical Analysis of Field Samples, In J.S. Hart (ed.), Distribution and Transport of Persistent Chemicals in Flowing Water Ecosystems, Interim Report No. 1, Ottawa River Project, National Research Council of Canada, Ottawa, 1973.

50. Norstrom, R.J., and Brownstein, M., Chemical Analysis of Field Samples, In D.R. Miller (ed.), Distribution and Transport of Pollutants in Flowing Water Ecosystems, Interim Report No. 2, Ottawa River Project, National Research Council of Canada, Ottawa, 1974.

51. Oliver, B.G., Heavy Metal Levels of Ottawa and Rideau River Sediments, Environ. Sci. Technol. 9, 1973, pp.135-137.

52. Paintal, A.S., Concept of Critical Shear Stress in Loose Boundary Open Channels, Journal of Hydraulic Research, Vol. 9, 1971.

53. Raudkivi, A.J., Loose Boundary Hydraulics, Pergamon Press, Toronto, New York, 1967.

54. Richardson, E.V., Sediment Properties, in Shen, H.W., (ed.) River Mechanics, Vol. I, Fort Collins, Colorado, 1971.

55. Rust, B.R., and Waslenchuk, D.G., The Distribution and Transport of Bed Sediments and Persistent Pollutants in the Ottawa River, Canada, Proceedings of the International Conference on Transport of Persistent Chemicals in Aquatic Ecosystems, Ottawa, Canada, May 1-3, 1974, p.1-25.

56. Saukov, A.A., and Aidinyan, N. Kh., On the Oxidation of Cinnabar, Akad. Nauk. SSSR, Trudy, Inst. Geol. Nauk, No. 39, Mineral, Geokhim, Ser. No. 8, pp.37-40.

57. Sayre, W.W., Guy, A.P., and Chamberlain, A.R., Uptake and Transport of Radionuclides by Stream Sediments, U.S. Geological Survey Professional Paper 433-A, 1963.

58. Shen, H.W., Wash Load and Bed Load, Shen, H.W. (ed.) River Mechanics, Vol. I, Fort Collins, Colorado, 1971.

59. Shen, H.W., and Cheong, H.F., Dispersion of Contaminated Sediment Bed Load, Journal of the Hydraulics Division, ASCE, Vol. 99, No. HY11, Nov. 1973, pp.1947-1965.

60. Shields, A., Anwendung der Ahnlichkeifsmechanik und Turbulenzforschung auf die Geschiebebewegung, Mitteil, Preuss, Versuchsanst. Wasser, Erd, Schiffsbau, Berlin, No. 26, 1936.

61. Suggs, J.D., Peterson, D.H., and Middlebrook, Jr., J.B., Mercury Pollution Control in Stream and Lake Sediments, U.S. Environmental Protection Agency, Water Pollution Control Research Series 16080, HTD, March 1972.

62. Task Committee on Preparation of Sedimentation Manual, Sediment Transportation Mechanics: Initiation of Motion, Journal of the Hydraulics Division, ASCE, Vol. 92, No. HY2, March 1966, pp.291-314.

63. Task Committee on Preparation of Sedimentation Manual, Sediment Transportation Mechanics: H. Sediment Discharge Formulas, Journal of the Hydraulics Division, ASCE, Vol. 97, No. HY4, April, 1971, pp.523-567.

64. Task Committee on Preparation of Sedimentation Manual, Sediment Transportation Mechanics: Fundamentals of Sediment Transportation, Journal of the Hydraulics Division, ASCE, Vol. 97, No. HY12, Dec., 1971, pp.1979-2019.

65. Thomas, R.L., The Distribution of Mercury in the Sediments of Lake Ontario, Can. J. Earth Sci., 9, 1972, pp.636-651.

66. Turney, W.G., Mercury Pollution: Michigan Action Program, Jour. Water Poll. Control Fed., Vol. 48, No. 7, July, 1971, pp.1427-1438.

67. Vanoni, Vito A., Brooks, N.H., and Kennedy, J.F., Lecture Notes on Sediment Transportation and Channel Stability, W.M. Keck Lab. of Hydraulics and Water Resources, California Institute of Technology, Report No. KH-R-1, 1960.

68. White, C.M., The Equilibrium of Grains on the Bed of an Alluvial Channel, Proceedings of the Royal Society, London, England, Series A, Vol. 174, 1940, pp.332-338.

69. Wood, J., Kennedy, S., and Rosen, C., The synthesis of methylmercury compounds by extracts of methanogenic bacterium, Nature 220, 1968, pp.173-174.

70. Water Quality and its Control in the Ottawa River, Published jointly by the Ontario Water Resource Commission and the Quebec Water Board, Canada, 1971.

71. Yalin, M.S., Mechanics of Sediment Transport, Pergamon Press, 1972.

72. Yang, C.T., and Sayre, W.W., Stochastic Model for Sand Dispersion, Journal of the Hydraulics Division, ASCE, Vol. 97, No. HY2, Feb. 1971, pp.265-288.

73. Yang, C.T., Incipient Motion and Sediment Transport, Journal of the Hydraulics Division, ASCE, Vol. 99, No. HY10, Oct. 1973, pp.1679-1704.

74. Yousef, A.Y., Kudo, A., and Gloyna, E.F., Radioactivity Transport in Water, Summary Report, Tech. Rep. No. 20, U.S. Atomic Energy Commission Contract AT(11-1)-490, 1970.

75. Zeller, H.D., and Finger, J.H., Investigations of Mercury Pollution in the Aquatic Environment of the Southeastern United States, Proc. 10th Annual Environmental and Water Resources Eng. Conf., Vanderbilt University, Nashville, Tenn., June 1971.

APPENDIX A

GRAIN SIZE ANALYSIS

A.1 Sand Sediment

Project Ottawa River Project Job No.

Location of Project Boring No. Sample No.

Description of Soil Depth of Sample

Tested By Date of testing

(ASTM D1140-54)

Soil Sample Size

Nominal diameter of largest particle.	Approximate minimum Wt. of sample, g
No. 10 sieve	200
No. 4 sieve	500
3/4 in.	1500

Wt. of dry sample + container	
Wt. of container	
Wt. of dry sample, W_s	500 g

Sieve analysis and grain shape

Sieve no	Diam (μm)	Wt retained (g)	% retained	% passing
20	>840	0.55	0.11	99.89
30	>590	0.78	0.156	99.734
40	>420	5.45	1.09	98.644
60	>246	332.77	66.50	32.144
80	>177	120.07	24.01	8.134
100	>149	32.93	6.58	1.554
140	>106	6.94	1.39	0.164
200	> 75	0.40	0.08	0.084
270	> 53	0.13	0.026	0.058
400	> 38	0.01	0.002	0.056
Pan	< 38	0.02	0.004	0.054
		500		

% passing = 100 − $\sum$ % retained.

A.2 "Woodchip" sediment

Project Ottawa River Project Job No.

Location of Project Boring No. Sample No.

Description of Soil Depth of Sample

Tested By Date of testing

(ASTM D1140-54)

Soil Sample Size

Nominal diameter of largest particle.	Approximate minimum Wt. of sample, g
No. 10 sieve	200
No. 4 sieve	500
3/4 in.	1500

Wt. of dry sample + container	
Wt. of container	
Wt. of dry sample, W,	500 g

Sieve analysis and grain shape

Sieve no	Diam (μm)	Wt. retained (g)	% retained	% passing
20	>840	1.62	0.32	99.68
30	>590	0.96	0.19	99.49
40	>420	2.33	0.46	99.03
60	>246	38.87	7.77	91.26
80	>177	261.74	52.34	38.92
100	>149	136.50	27.30	11.62
140	>106	48.06	9.61	2.01
200	> 75	6.03	1.20	0.81
270	> 53	2.56	0.51	0.30
400	> 38	0.57	0.11	0.19
Pan	< 38	0.76	0.15	0.04
		500		

% passing = 100 − Σ % retained.

APPENDIX B

COMPUTATIONS OF BOUNDARY SHEAR STRESSES

Table 8. Boundary Shear Stresses at Incipient Movement of "Woodchip" Bed Sediment Particles (weak movement)

Median diameter of sediment particle, d_{50} = 180 μm
Mean water velocity (U_{cr}) = 18 cm/sec
Mean water flow rate = 2.9 ℓ/sec
ν of water at 20°C = 1.0105×10^{-2} cm^2/sec
Outside diameter of the Preston tube, d_o = 1.83 mm
Width of the channel, W = 30.48 cm
Reynolds Number = 147.8×10^2; Froude Number = 0.195

Transverse location of the Preston tube $\frac{x}{w}$	Measured Velocity near the bed U_m cm/sec	$\frac{U_m d_o}{2\nu}$	$\frac{U_*}{U_m}$ from calibration curve, Fig.53	Shear velocity U_* cm/sec	Shear stress τ_o N/cm^2 $\times 10^{-5}$	Average shear velocity $\overline{U}_* = (U_*)_{cr}$ cm/sec	Average shear stress $\overline{\tau}_o' = (\tau_o)_{cr}$ N/cm^2 $\times 10^{-5}$	Grain size Reynolds Number $\frac{(U_*)_{cr} d_{50}}{\nu}$	Dimensionless shear stress $(\tau_*)_{cr} = \frac{(\tau_o)_{cr}}{(\rho_s - \rho) g d_{50}}$
(1)	(2)	(3)	(4)	(5)	(6)	(7)	(8)	(9)	(10)
0.082	9.96	92,63	0.109	1.085	1.18				
0.25	13.70	127.48	0.096	1.315	1.76				
0.5	15.10	140.22	0.092	1.392	1.96	1.255	1.59	2.35	0.055
0.75	12.60	116.71	0.099	1.250	1.57				
0.915	12.20	113.31	0.101	1.232	1.47				

Table 9. - Boundary Shear Stresses at Incipient Movement of "Woodchip" Bed Sediment Particles (general movement)

Median diameter of the sediment particles, d_{50} = 180 μm
Mean water velocity (U_{cr}) = 23.33 cm/sec
Mean water flow rate = 3.4 ℓ/sec
of water at 20°C = 1.0105×10^{-2} cm^2/sec
Outside diameter of the Preston tube, d_o = 1.8 mm
Width of the channel, w = 30.48 cm
Reynolds Number = 191.3×10^2 Froude Number = 0.25

Transverse location of the Preston tube $\frac{x}{w}$ (1)	Measured Velocity near the bed U_m cm/sec (2)	$\frac{U_m d_o}{2\nu}$ (3)	$\frac{U_*}{U_m}$ from calibration curve, Fig. 53 (4)	Shear velocity U_* cm/sec (5)	Shear stress τ_o N/cm² x 10^{-5} (6)	Average shear velocity $\overline{U}_* = (U_*)_{cr}$ cm/sec (7)	Average shear stress $\overline{\tau}_o' = (\tau_o)_{cr}$ N/cm² x 10^{-5} (8)	Grain size Reynolds Number $\frac{(U_*)_{cr} d_{50}}{\nu}$ (9)	Dimensionless shear stress $(\tau_*)_{cr} = \frac{(\tau_o)_{cr}}{(\rho_s - \rho) g d_{50}}$ (10)
0.082	16.7	155.24	0.088	1.47	2.16				
0.250	18.5	171.95	0.085	1.56	2.45				
0.50	19.5	181.30	0.083	1.62	2.65	1.52	2.32	2.84	0.079
0.750	17.6	163.45	0.086	1.52	2.25				
0.915	15.7	145.90	0.091	1.43	2.06				

Table 10. - Boundary Shear Stresses at Incipient Movement of Sand Bed Sediment Particles (weak movement)

Median diameter of sediment particles, d_{50} = 280 μm
Mean water velocity (U_{cr}) = 20 cm/sec
Mean water flow rate = 3.2 ℓ/sec
ν of water at 20°C = 1.0105×10^{-2} cm^2/sec
Outside diameter of the Preston tube, d_o = 1.8 mm
Width of the channel, w = 30.48 cm
Reynolds Number = 164×10^2 Froude No. = 0.216

Transverse location of the Preston tube $\frac{x}{w}$	Measured Velocity near the bed U_m cm/sec	$\frac{U_m d_o}{2\nu}$	$\frac{U_*}{U_m}$ from calibration curve, Fig. 53	Shear velocity U_* cm/sec	Shear stress τ_o $N/cm^2 \times 10^{-5}$	Average shear velocity $\overline{U}_* = (U_*)_{cr}$ cm/sec	Average shear stress $\overline{\tau}_o' = (\tau_o)_{cr}$ $N/cm^2 \times 10^{-5}$	Grain size Reynolds Number $\frac{(U_*)_{cr} d_{50}}{\nu}$	Dimensionless shear stress $(\tau_*)_{cr} = \frac{(\tau_o)_{cr}}{(\rho_s - \rho) g d_{50}}$
(1)	(2)	(3)	(4)	(5)	(6)	(7)	(8)	(9)	(10)
0.082	14.10	130.88	0.095	1.34	1.86				
0.25	15.10	140.22	0.092	1.39	1.96				
0.5	16.95	157.22	0.088	1.48	2.16	1.38	1.92	4.01	0.042
0.75	14.40	133.71	0.094	1.36	1.86				
0.915	14.00	130.31	0.095	1.33	1.76				

Table 11. - Boundary Shear Stresses at Incipient Movement of Sand Bed Sediment Particles (general movement)

Median diameter of the sediment particle, d_{50} = 280 μm
Mean water velocity (U_{cr}) = 25 cm/sec
Mean water flow rate = 3.8 ℓ/sec
ν of water at 20°C = 1.0105×10^{-2} cm^2/sec
Outside diameter of the Preston tube, d_o = 1.8 mm
Width of the channel, w = 30.48 cm
Reynolds Number = 205×10^2 Froude Number = 0.27

Transverse location of the Preston tube $\frac{x}{w}$	Measured Velocity near the bed U_m cm/sec	$\frac{U_m d_o}{2\nu}$	$\frac{U_*}{U_m}$ from calibration curve, Fig. 53	Shear velocity U_* cm/sec	Shear stress τ_o $N/cm^2 \times 10^{-5}$	Average shear velocity $\overline{U}_* = (U_*)_{cr}$ cm/sec	Average shear stress $\overline{\tau}_o' = (\tau_o)_{cr}$ $N/cm^2 \times 10^{-5}$	Grain size Reynolds Number $\frac{(U_*)_{cr} d_{50}}{\nu}$	Dimensionless shear stress $(\tau_*)_{cr} = \frac{(\tau_o)_{cr}}{(\rho_s - \rho) g d_{50}}$
(1)	(2)	(3)	(4)	(5)	(6)	(7)	(8)	(9)	(10)
0.082	17.45	162.32	0.086	1.50	2.25				
0.25	18.80	174.50	0.084	1.58	2.45				
0.5	20.03	188.38	0.082	1.64	2.75	1.58	2.49	4.6	0.055
0.75	19.50	181.30	0.083	1.62	2.65				
0.915	18.15	168.55	0.085	1.54	2.35				

APPENDIX C

CALIBRATIONS

C.1 Calibration of the 90° triangular-notched weir

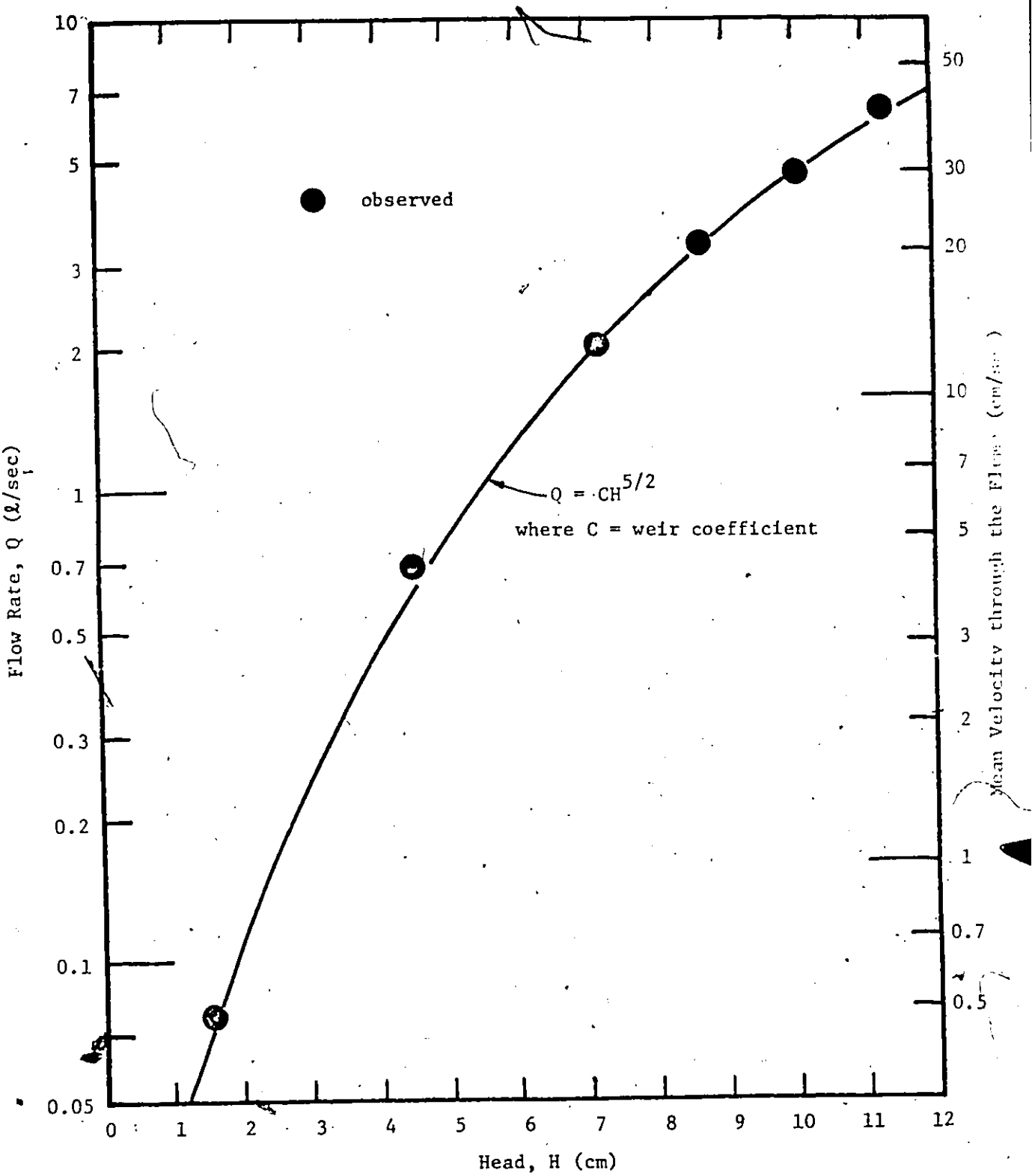

Fig. 50. - Calibration curve of the weir

C.2 Calibration of the Preston tube

Water flowing in a channel exerts a longitudinal shear force on the wetted periphery of the flow cross section which causes the movement of the loose boundary resulting in erosion. Several analytical techniques have been developed for determining the tractive force distribution over the wetted perimeter of a channel cross section. A simple tool is now available in the Preston tube for the experimental determination of wall shear stress (28). Ippen et al (19) were among the first to demonstrate the applicability of the Preston tube to determine the peripheral distribution of local boundary shear in a straight trapezoidal channel.

The Preston technique is based on the experimentally well established inner law of velocity distribution

$$\frac{U_Y}{U_*} = f\left(\frac{U_* Y}{\nu}\right) \qquad C.1$$

in which U_Y = local flow velocity at distance Y from the boundary; $U_* = \sqrt{\frac{\tau_o}{\rho}}$ = shear velocity, and ν = kinematic viscosity.

When the raw velocity data U'_m of a total head probe in the immediate wall zone of a turbulent shear flow are arranged according to Eqn. C.1 they will yield a functional relationship

$$\frac{U'_m}{U_*} = f\left(\frac{U_* Y}{\nu}, \frac{Y}{d_o}, \frac{d_o}{d_i}, \text{tip shape}\right) \qquad C.2$$

in which Y = wall distance of the geometric centre of the probe

d_o = outer diameter of the probe

d_i = inner diameter of the probe

For a given probe geometry (i.e., $\frac{d_o}{d_i}$, tip shape) and fixed wall distance (i.e., $\frac{Y}{d_o}$) any empirical relation of the form of Eqn. C.2 becomes an expression for shear velocity in terms of measured flow velocity. Therefore, total head probes can be used as wall-shear metering devices. For the practical application of this concept according to Preston round tubes with square-cut tip are used, and the wall distance is fixed by placing the probes in wall contact, i.e., by putting $Y = d_o/2$. With this substitution and after some manipulation Eqn. C.2 assumes the form of the calibration equation for Preston tubes (28):

$$\frac{U_*}{U_m} = f\left(\frac{U_m d_o}{2\nu}\right) \qquad C.3$$

A sketch of the pitot tube after Preston for the measurement of boundary shear stress over bed is shown in Fig. 51. This device was manufactured in the laboratory. The two tubes (total head tube and static tube) were connected with piezometer columns attached with the instrument carriage. The difference in head between the two columns (which gives the velocity head = $\frac{U^2}{2g}$) was precisely measured with the help of cathetometer.

For calibration of this tube, a flume (6 m long;12.8cm x 20.4cm) was set horizontally and uniform flow was established. The Preston tube was lowered to the bottom of the channel along its central line. With the probe touching the bottom, the velocity U_m for $Y = \frac{d_o}{2}$ was evaluated. Following this, the velocity distribution along the vertical line of symmetry of the flow cross section was determined at close intervals.

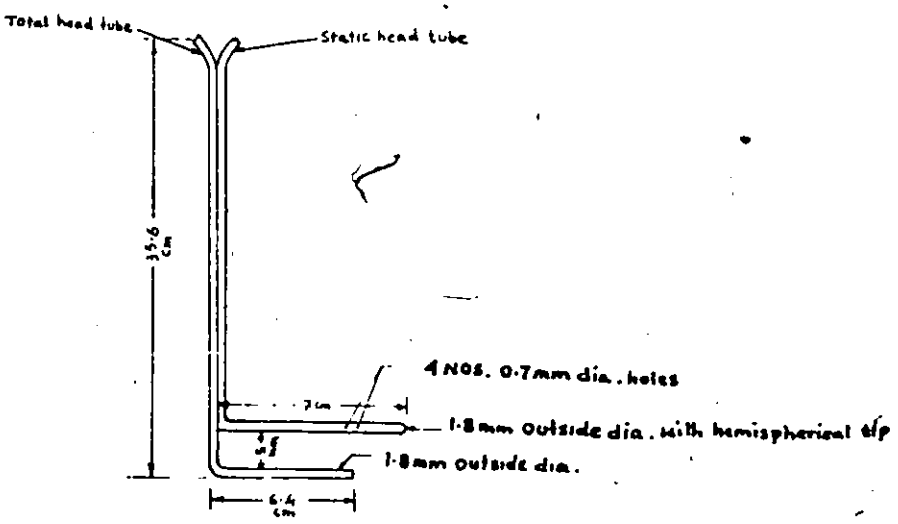

Fig. 51. - Pitot tube after Preston for measurement of boundary shear stress

This procedure was followed for different depths of flow. The temperature of the water was measured for each experiment.

Equation C.1 assumes a logarthmic form given below

$$\frac{U_Y}{U_*} = A \log \frac{U_* Y}{\nu} + B \qquad C.4$$

in which A and B are so called universal constants. These constants have been found to be of the order of magnitude first established by Nikuradse, as A = 5.75 and B = 5.5. By adopting these values Eqn. C.4 was first solved for the apparent shear velocity U_*' for all pairs of values of U_Y versus Y of different velocity profiles.

The computed values of U_*' were then plotted as function of Y (Fig. 52). In all of the plots so prepared in the course of the calibration procedure there occurred a vertical distance Y over which the plotted values of U_*' appeared to be sensibly independent of wall distance. This distance was assumed to correspond to region of applicability of Eqn. C.4 and its quasiconstant value of U_*' was taken to be the correct value of shear velocity U_* (28). Each value of U_* obtained in this manner was appropriately combined with the other parameters in Eqn. C.3 and defined one point of the calibration curve. Table 12 gives the points for the calibration curve. The complete curve is shown in Fig. 53. This curve was used to compute the boundary shear stress over bed sediment as presented in Appendix B.

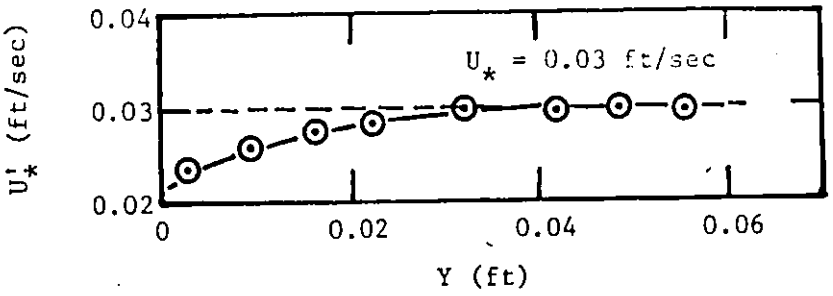

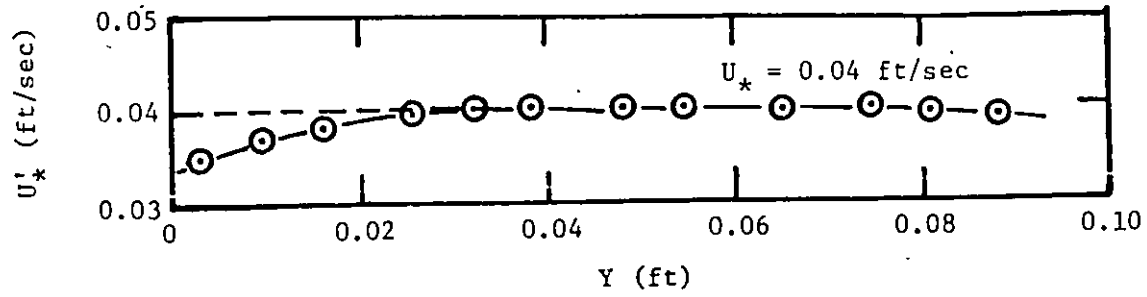

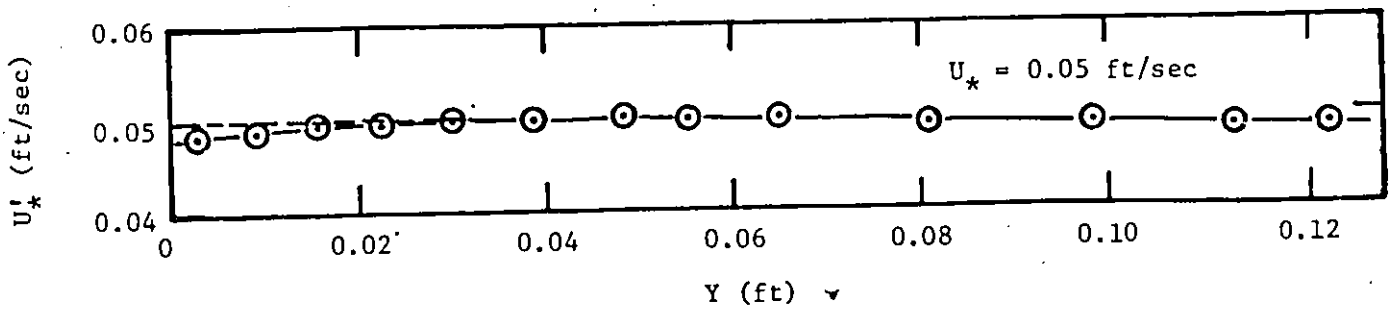

Fig. 52. - (continued)

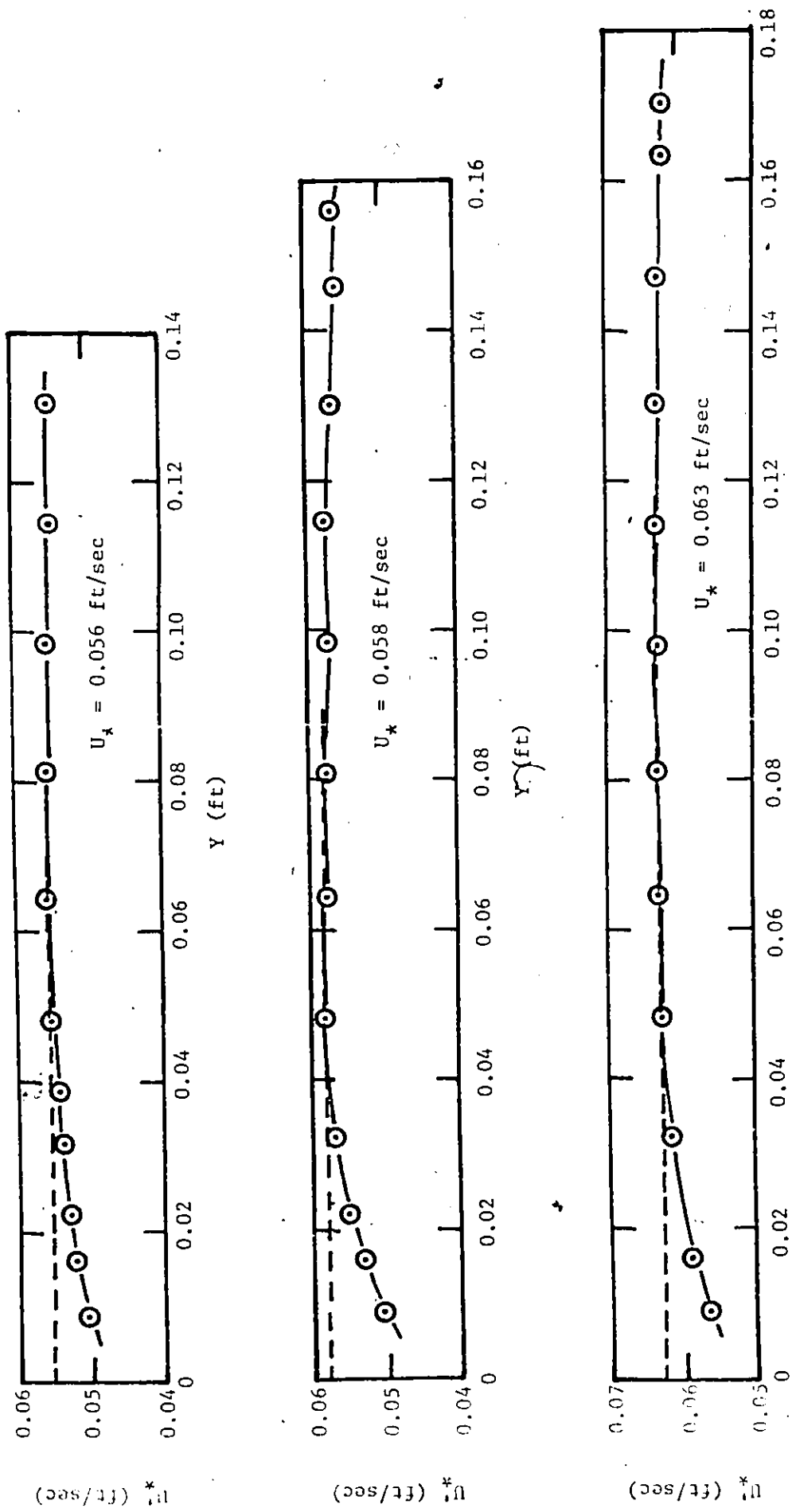

Fig. 52. - Graphical determination of shear velocity

Table 12. - Computations of $\frac{U_*}{U_m}$ and $\frac{U_m d_o}{2\nu}$ for the calibration curve of the Preston tube

Depth of flow D_{cm}	$\frac{U_*}{U_m}$	$\frac{U_m d_o}{2\nu}$
2.35	0.122	68.6
3.30	0.101	112.0
4.50	0.086	165.4
4.95	0.083	189.0
5.60	0.080	205.5
6.10	0.078	228.0

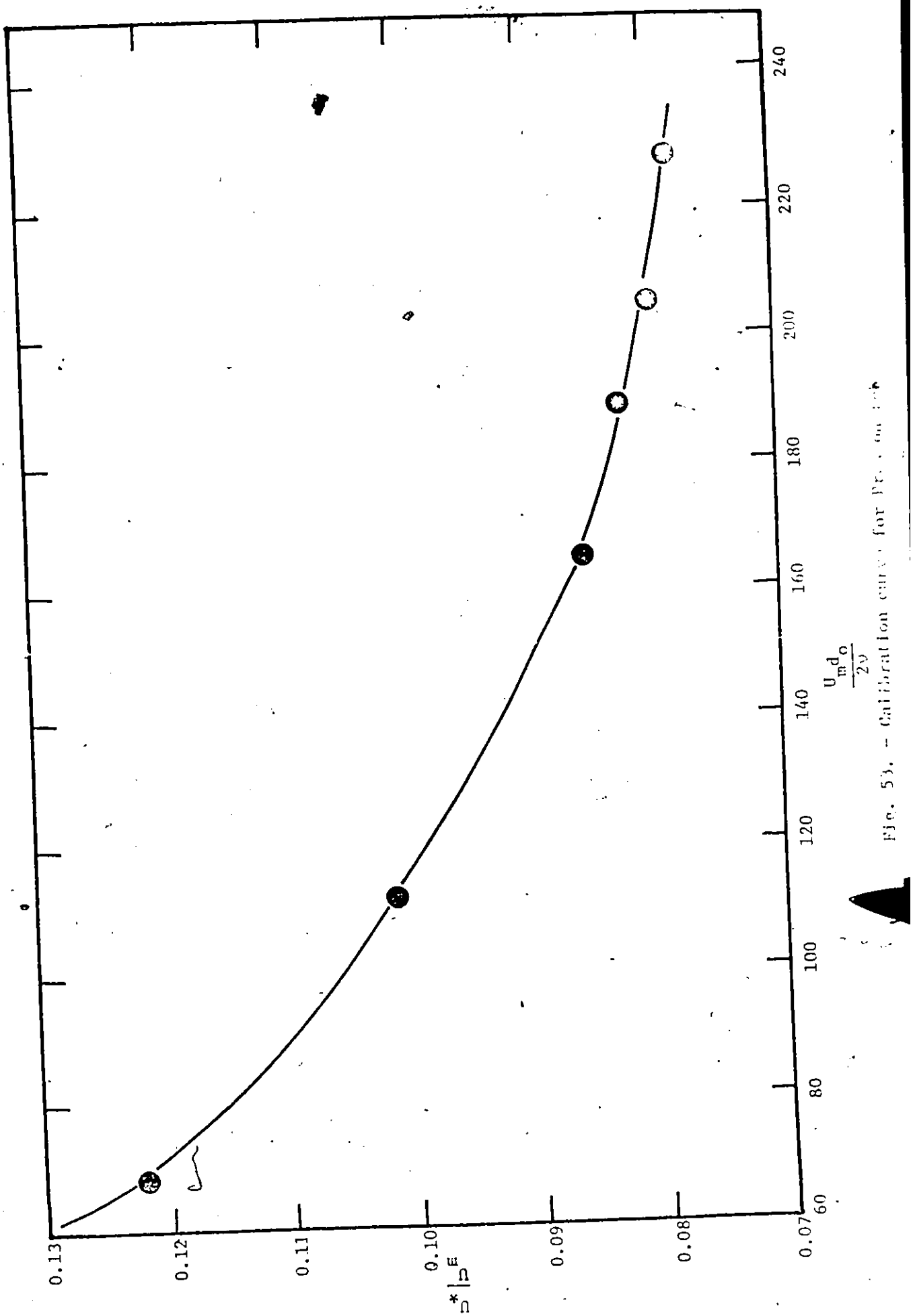

Fig. 53. - Calibration curve for Pr = 0.71

C.3 Velocity distribution across the test section of the laboratory model

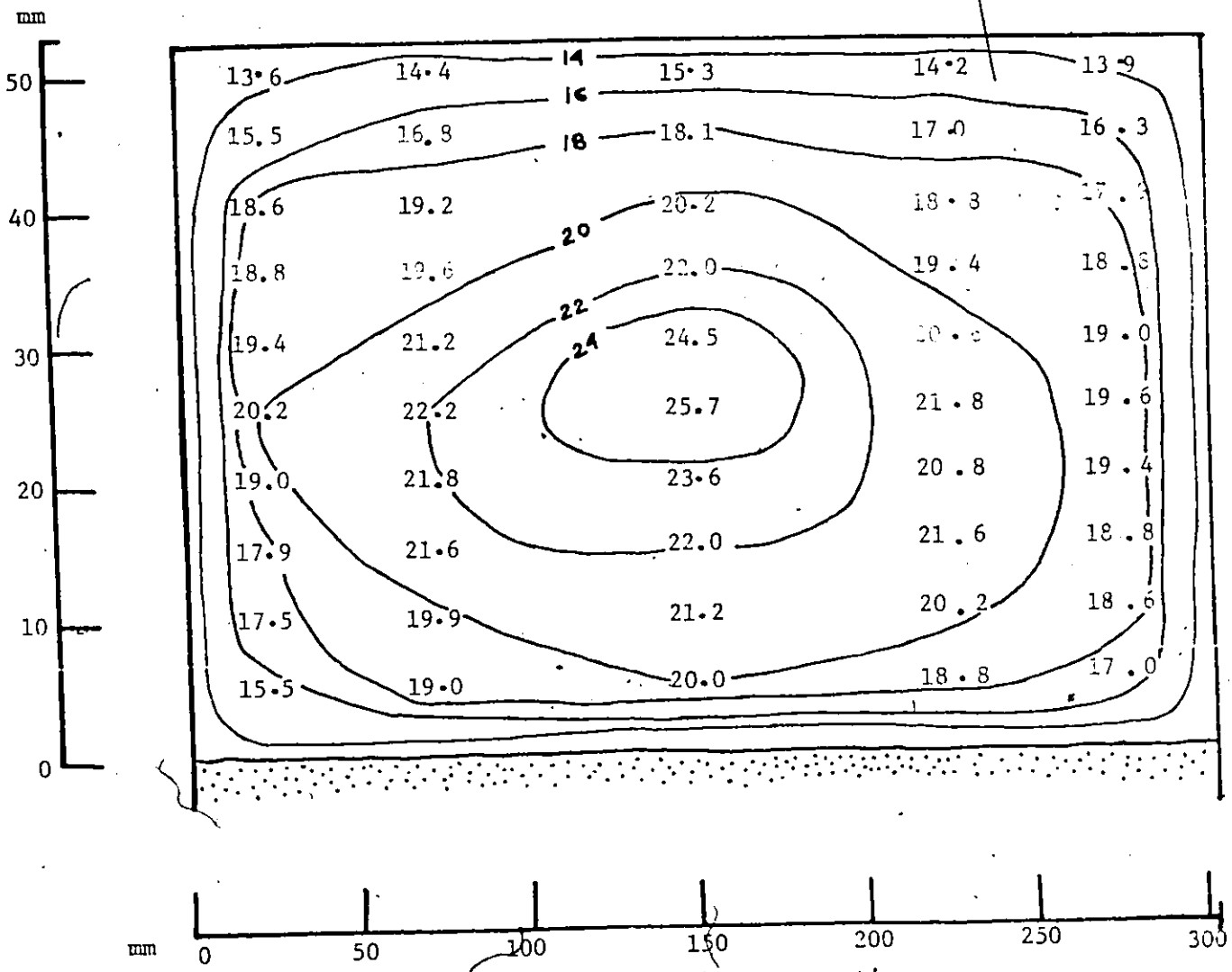

Cross-section of the test section

Mean water velocity = 20 cm/sec

Mean flow rate = 3.2 l/sec

Reynolds Number = 164×10^2

Froude Number = 0.216

Fig. 54. - (continued)

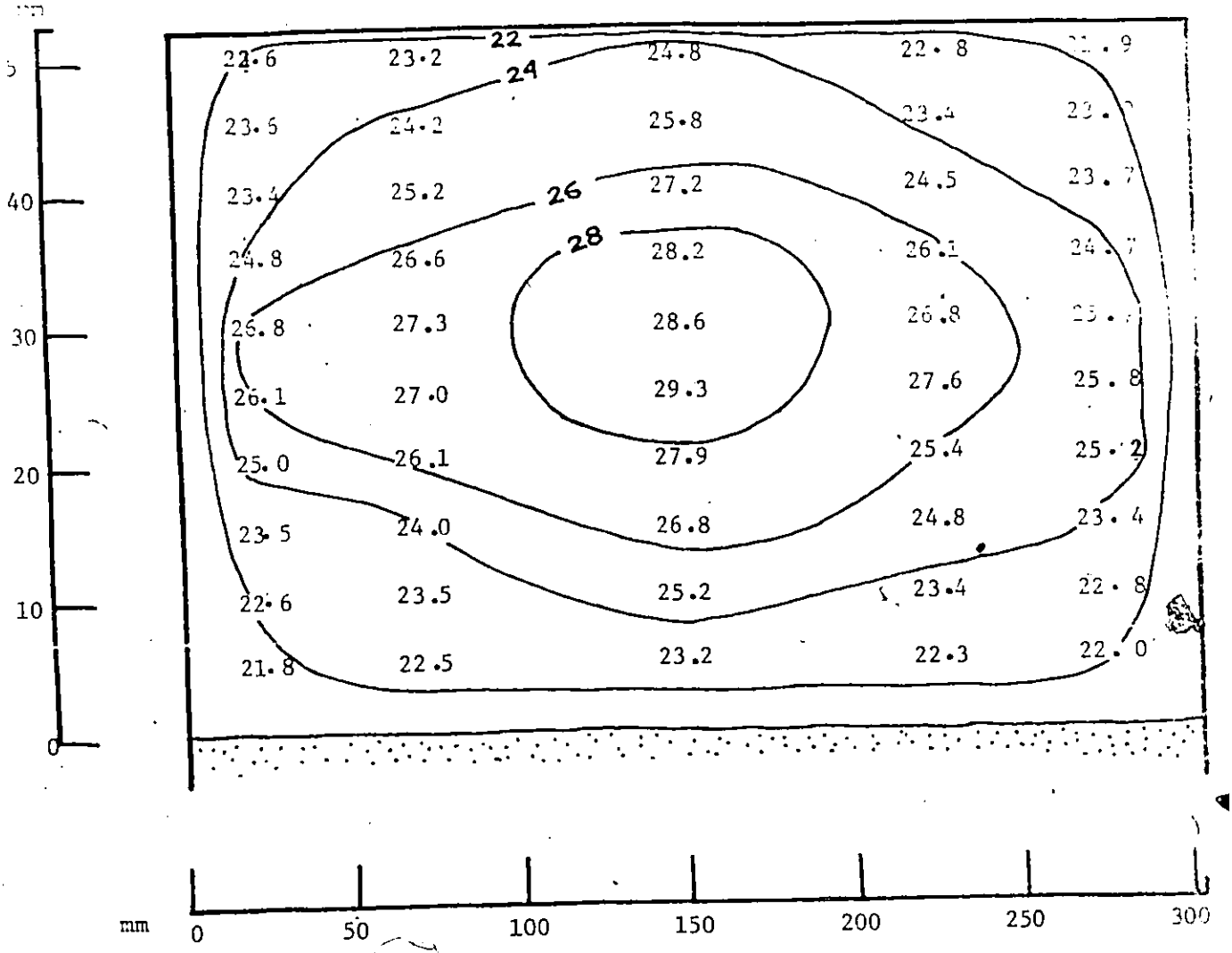

Cross-section of the test section

Mean water velocity = 25 cm/sec
Mean flow rate = 3.8 l/sec
Reynolds Number = 205×10^2
Froude Number = 0.27

Fig. 54. - (continued)

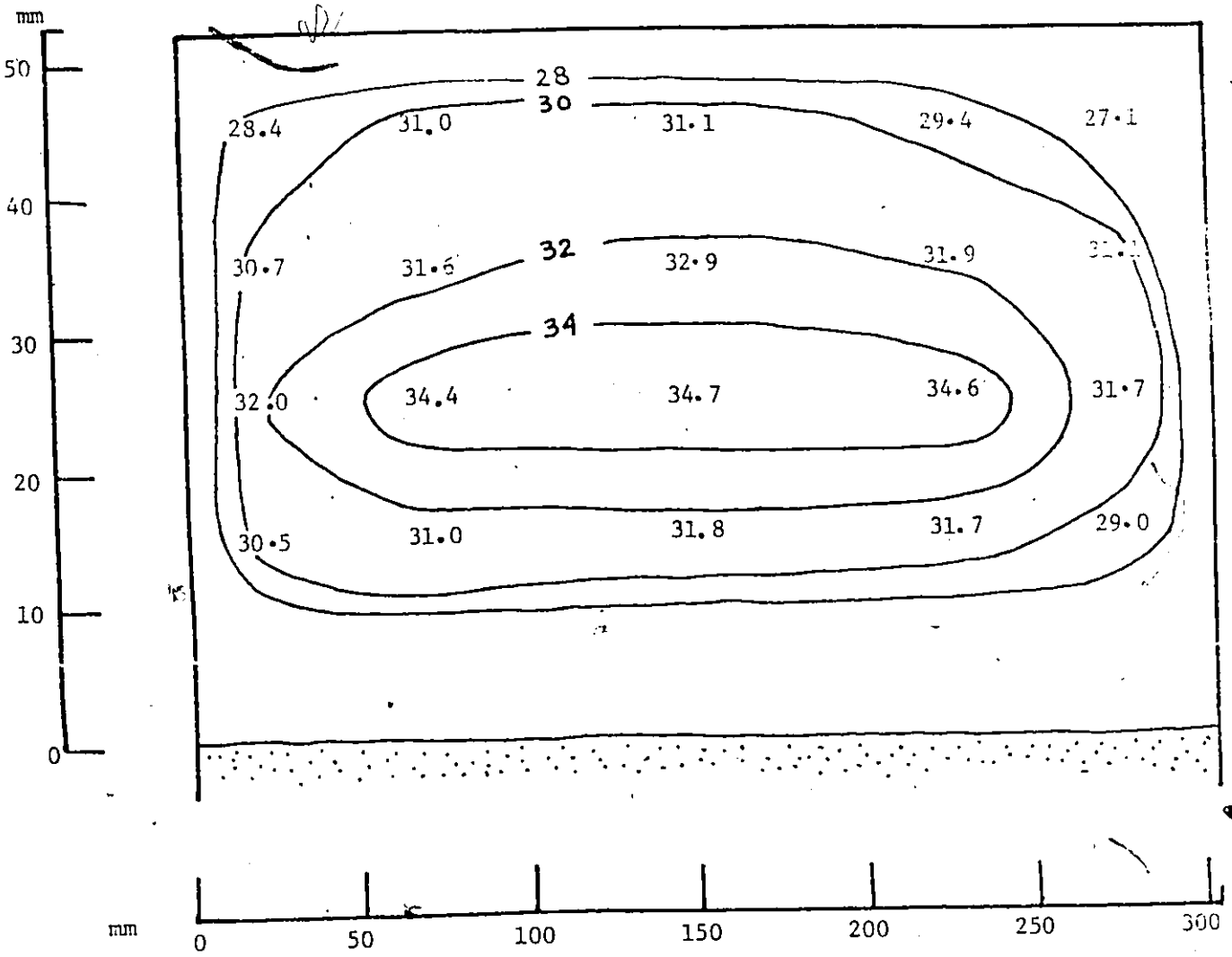

Cross-section of the test section

Mean water velocity = 30 cm/sec
Mean flow rate = 4.7 l/sec
Reynolds Number = 246×10^2
Froude Number = 0.325

Fig. 54. - Velocity distribution across the test section for different flow conditions